ELSEVIER

Coordination Chemistry Reviews
219–221 (2001) 311–378

COORDINATION CHEMISTRY REVIEWS

www.elsevier.com/locate/ccr

η^1-Indenyl derivatives of transition metal and main group elements: synthesis, characterization and molecular dynamics

Mark Stradiotto [a,*1], Michael J. McGlinchey [b,*2]

[a] *Department of Chemistry, Dalhousie University, Halifax, Nova Scotia, Canada B3H 4J3*
[b] *Department of Chemistry, McMaster University, Hamilton, Ont., Canada L8S 4M1*

Received 14 July 2000; accepted 15 November 2000

This paper is dedicated to Barry Lever on the occasion of his 65th birthday, in recognition of his outstanding contributions not only as a scientist, but also as a promoter of inorganic chemistry in Canada

Contents

[1] * Corresponding author. Tel.: + 1-902-494-3305; fax: + 1-902-494-1310; e-mail: mark.stradiotto@dal.ca (M. Stradiotto).
[2] * Corresponding author. Tel.: + 1-905-5259140, ext. 27318; fax: + 1-905-5222509; e-mail: mcglinc@mcmaster.ca (M.J. McGlinchey).

PII: S0010-8545(01)00339-3

Abstract

Transition metal and main group compounds bearing η^1-indenyl ligands have figured importantly since the beginnings of organometallic chemistry, and continue to attract considerable attention. The novel reactivity of the transition metal derivatives and the utility of the main group species as ligands in the development of chiral metallocene pre-catalysts have led to a renaissance in this field of study. The dynamic behavior of these η^1-indenyl complexes has also been examined: the preponderance of evidence points to a circumambulatory process involving sequential [1,5]-elementotropic shifts that proceed via short-lived isoindene intermediates.

Keywords: Indene; Indenyl; Fluxionality; Dynamics; Main group; Transition metal

1. Introduction

The indenyl (C_9H_7) molecular framework served a crucial role in the early development of organometallic chemistry [1], and continues to figure prominently in this and other fields of chemical research. Though the indenyl ligand can be simplistically envisioned as a 'benzannulated' relative of the cyclopentadienyl (C_5H_5) moiety, transition metal complexes derived from the former commonly exhibit reactivity which differs significantly from metal derivatives of the latter. These reactivity differences can often be ascribed to the numerous stable binding configurations which are accessible in indenyl metal chemistry [2]. Notably, indene (C_9H_8) and its derivatives readily serve as six-electron donors via hexahapto (η^6) complexation [3] involving the arene ring; pentahapto (η^5-C_9H_7) coordination [4] to the C_5 ring, analogous to the vast number of complexes derived from the cyclopentadienyl ligand, is also commonly observed. Less common are metal species containing η^3-C_9H_7 ligands [5], as are η^2-compounds in which the unsaturated portion of the C_5 ring serves as an olefinic π-donor to the metal center [6].

The heightened ability of polyhapto indenyl metal complexes, in comparison to their cyclopentadienyl counterparts [7], to undergo modification of the ligand-to-metal connectivity in response to electronic changes at the metal center is perhaps best illuminated by the indenyl 'ring slippage' phenomenon examined by Basolo and co-workers [8,9]. These researchers noted that the rate of associative substitution reactions at transition metal centers in η^5-indenyl complexes are up to 10^8 times more rapid than in analogous cyclopentadienyl systems. Basolo deemed this phenomenon the 'kinetic indenyl ligand effect' [8], in which the intermediate η^3-coordination mode is uniquely stabilized in the indenyl system via aromatization of the C_6 ring.

An interesting variation on the indenyl ligand slip process can be envisioned if, instead of expelling a two-electron donor to return to the η^5-C_9H_7 binding configuration, the intermediate η^3-complex coordinates a second two-electron donor. Such an occurrence could lead to the generation of a metal complex comprising an η^1-C_9H_7 ligand (Scheme 1). Indeed, though generally overlooked in

surveys of indenyl transition metal chemistry, examples of such η^1-C_9H_7 species are numerous. Related η^1-indenyl (or σ-C_9H_7) main group compounds are also plentiful, and derivatives comprising Groups 13, 14 and/or 15 elements have gained recent notoriety, owing to their utility as ligands in the preparation of chiral *ansa*-metallocene precatalysts [10].

Despite the fact that η^1-indenyl complexes have been known for 50 years [11], a comprehensive survey of this class of molecules has yet to be published. Herein we provide a current summary of transition metal and main group η^1-indenyl compounds of Groups 4 through 13, and the heavier element derivatives of Groups 14 and 15; particular emphasis is given to molecular systems that exhibit dynamic behavior on the NMR time-scale. This review endeavors to cover the academic literature appearing from 1951 through April, 2000.

2. Transition metal η^1-indenyl compounds

2.1. Groups 4, 5 and 6

A series of novel η^1-indenyl compounds comprising Group 4 elements has been prepared by Alt and co-workers. Starting from the appropriate metal dichloride, the tris(indenyl) complexes, **1** and **2**, and the mono- and bis-indenyl metallocenes, **7** and **8**, were prepared via addition of indenyllithium [12]. The dynamic or 'stereochemically non-rigid' [13] nature of the tris(indenyl) compounds is evident upon examination of their temperature-dependent ^{1}H- and ^{13}C-NMR spectra. Under ambient conditions, NMR spectral data obtained from samples of these complexes reveal effective C_{3v} geometries in solution; the authors attributed these spectral features to a static η^5-η^5-η^5 structural formulation (formally a 20-electron configuration at the metal), as depicted for **1** and **2** in Scheme 2. At reduced temperatures (-100°C for **1**; -40°C for **2**) the acquired NMR spectra coincide with structures possessing effective C_3 molecular symmetries, in which all three indenyl ring environments are again equivalent; for **1**, variable-temperature NMR data yield $\Delta G^{\ddagger}$ ca. 14.4 kcal mol^{-1}. Alt and co-workers rationalized the equilibra-

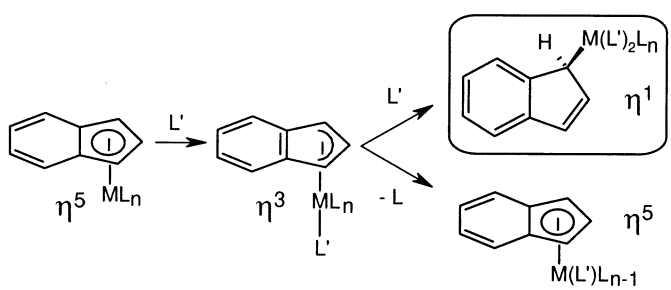

Scheme 1. Ligand 'slip' rearrangements involving an η^5-indenyl transition metal complex, giving rise to η^3 and η^1 species in which the aromatic character of the C_6 ring is recovered.

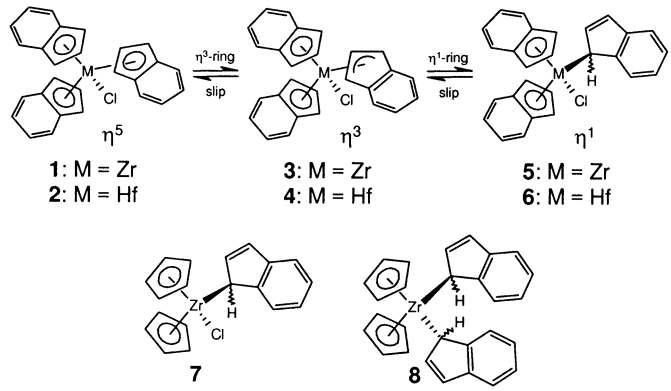

Scheme 2. Some η^1-indenyl derivatives of the heavier Group 4 elements.

tion of the three indenyl rings in these zirconium and hafnium systems in terms of a rapid $\eta^5 \rightarrow \eta^3 \rightarrow \eta^1$ ligand interconversion process (via the intermediates **3**–**6**, Scheme 2), though no specific mechanistic details were provided. Indirect support for the viability of such η^1-indenyl species was gained through the X-ray crystallographic characterization of the hafnium derivative, **6**, which adopts an η^5-η^5-η^1 geometry in the crystal. However, based on these crystallographic data it is conceivable that the instantaneous structure in solution does not correspond to **1** and **2** as the authors suggest, but rather to that of the η^5-η^5-η^1 configuration possessed by **5** and **6**. Moreover, it is possible that the 270 MHz ^{1}H-NMR spectrum acquired at -100°C is not the limiting spectrum. Under these circumstances, one might therefore propose that rapid haptotropic shifts in these latter molecular species could initially exchange η^5 and η^1 sites, while at higher temperatures [1,5]-metallotropic shifts may become sufficiently rapid so as to equilibrate the two halves of the indenyl framework on the NMR time-scale (leading to effective C_{3v} symmetry).

In 1998, Alt and co-workers [14] reported the synthesis and crystallographic characterization of **9**, a rare example of an η^1-1*H*-inden-2-yl transition metal complex. The following year, Green and Popham [15] detailed the synthesis of the related hafnium species, **10** (Scheme 3). The latter molecule was unexpectedly generated in ca. 20% yield from an equimolar mixture of $Li_2[(C_5H_4)C(CH_2)_5(C_9H_6)]\cdot 0.8Et_2O$ and $[Hf(\eta^1\text{-}C_5H_5)Cl_3]\cdot 2THF$.

The singular Group 5 η^1-indenyl complex, **11**, was reported by Rothwell and co-workers [16] in 1999. These researchers found that treatment of $Ta(NMe_2)_5$ with one equivalent of 2-(inden-3-yl)-4,6-di-*tert*-butylphenol at elevated temperatures lead to the formation of **11**, with concomitant loss of two equivalents of dimethylamine (Scheme 4). Data obtained from single crystal X-ray diffraction experiments involving **11** reveal a trigonal bipyramidal geometry at the metal center, in which tantalum is bonded in an η^1-fashion to the indenyl ligand. Moreover, variable-temperature NMR spectroscopic data obtained for **11** reveal the operation of a dynamic process involving the amine groups, that is slow on the NMR time-scale below ambient temperature.

Group 6 η^1-indenyl complexes are also relatively scarce. The two known examples, **12** and **13**, were generated by Alt and co-workers [17] via the photochemical extrusion of methane from η^5-$(C_5H_4CMe_2C_9H_7)M(CO)_3Me$ precursors (M = Mo and W, respectively; Scheme 5). These complexes can be compared to the Group 4 compounds, **9** and **10**, and represent two further examples of η^1-1*H*-inden-2-yl transition metal derivatives. The structure of the molybdenum compound, **12**, was confirmed by single crystal X-ray diffraction studies.

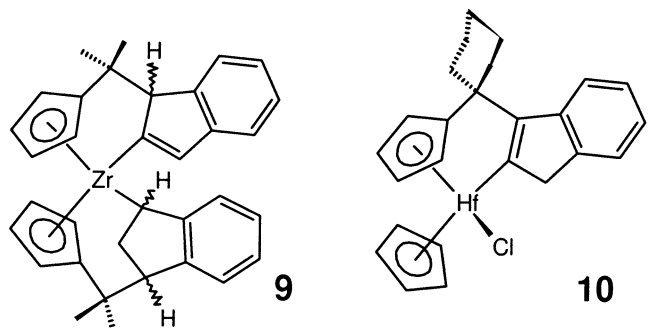

Scheme 3. Novel η^1-indenyl derivatives of the heavier Group 4 elements, in which bonding occurs at the vinylic C(2) position.

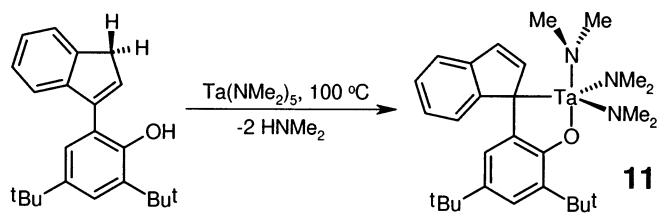

Scheme 4. Generation of a Group 5 η^1-indenyl complex.

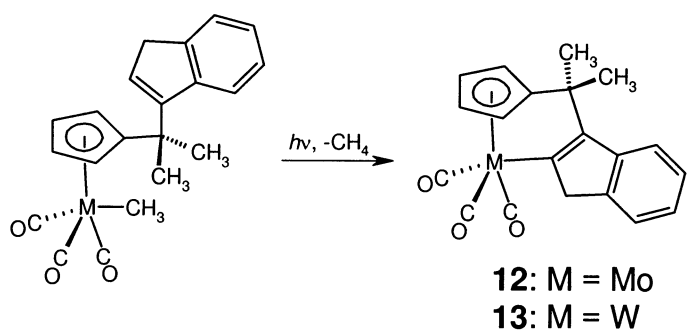

Scheme 5. Photochemically generated C(2)-bonded Group 6 η^1-indenyl complexes.

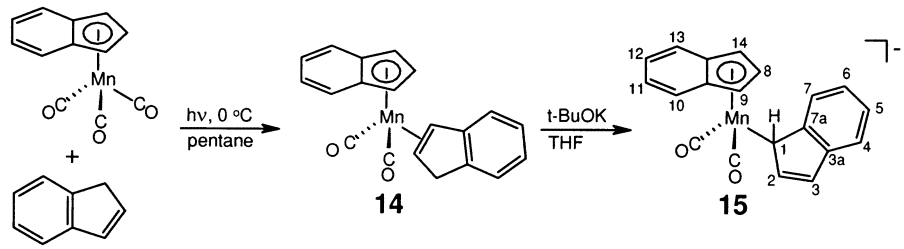

Scheme 6. The generation of an η^2-indene compound (**14**) and its conversion into the η^1-indenylmanganese complex (**15**).

2.2. Group 7

In 1993, Ustynyuk and co-workers [18] reported the in situ generation of the anionic η^1-indenylmanganese complex, **15** (Scheme 6). Photolysis of $(\eta^5\text{-}C_9H_7)Mn(CO)_3$ in the presence of indene yielded the η^2-indene intermediate, **14**, which was subsequently converted to **15** upon treatment with base at -60°C. This latter transformation was accompanied by the disappearance of the ν(CO) bands associated with **14** (1900 and 1975 cm^{-1}) and the development of new peaks attributable to **15** (1800 and 1880 cm^{-1}). The presence of both η^1- and η^5-coordinated indenyl ligands in **15** was ascertained by ^{1}H-NMR; particularly diagnostic was AMX spin pattern (allyl C–*H* at δ 2.45; vinyl C-*H*'s at δ 6.32 and δ 5.98), which is characteristic of the protons in the five-membered ring of η^1-indenyl compounds. Upon warming to -40°C, the H(1) and H(3) resonances in the η^1-indenyl unit of **15** broaden, as do the H(9)/H(14) and H(10)/H(13) pairs. Spin saturation transfer experiments conducted at this temperature, whereby the H(3) resonance was irradiated, resulted in the disappearance of the H(1) signal, suggesting the operation of a chemical exchange process involving these sites. At -20°C, the H(4)/H(7) and H(9)/H(14) pairs of resonances collapse, and the H(1) and H(3) signals are broadened significantly. Between -20 and 25°C, additional ^{1}H-NMR spectral changes ensue, which are rationalized by these authors in terms of an inner-sphere rearrangement process, in which the η^1- and η^5-indenyl ligands in **15** exchange structural positions. However, this process was found to be slow on the NMR time-scale at 25°C, since irradiation of the ^{1}H-NMR resonances attributable to H(4)/H(7) did not result in a substantial decrease in the intensity of the H(10)/H(13) signals. Attempts to study the molecular dynamics of **15** at higher temperatures were thwarted due to the low thermal stability of this complex.

The successful conversion of η^5-C_9H_7 complexes into isolable η^1-C_9H_7 species, via sequential ligand addition in an $\eta^5 \rightarrow \eta^3 \rightarrow \eta^1$ process, was first reported by Casey and O'Connor [19] in 1985 (Scheme 7). In attempting to prepare and examine the behavior of η^3-indenyl compounds, these workers noted that the addition of either trimethylphosphine or tri(*n*-butyl)phosphine to $(\eta^5\text{-}C_9H_7)Re(CO)_3$ (**16**), instead resulted in the rapid generation of the double-addition, η^1-indenyl complexes, **17** and **18**, respectively. In both cases only the facial isomer

was generated, an assertion that was supported by comparison of spectroscopic data obtained from these samples with data acquired for *fac*-(η^1-C_5H_5)$Re(CO)_3(PMe_3)_2$, whose structure has been established by X-ray crystallography [20].

The aforementioned rhenium complexes are of considerable significance, as they represent the first bona fide examples of dynamic transition metal η^1-indenyl species to be identified; their stereochemically non-rigid character was detected by use of variable-temperature NMR techniques. In the case of **17**, the low-temperature limiting ^{1}H-NMR spectrum (-68°C) is consistent with the 'instantaneous' structure depicted in Scheme 7, and is characterized by the appearance of signals attributable to the diastereotopic trimethylphosphine ligands and an η^1-indenyl framework. As the sample is warmed, the pairs of symmetry-related indenyl ring signals merge, and at higher temperatures the diastereotopic phosphorus methyl signals similarly coalesce to a virtually coupled triplet (consistent with a molecule possessing C_s symmetry on the NMR time-scale) above 40°C. Comparison of these experimentally obtained spectroscopic data with simulated NMR spectra yielded $\Delta G^{\ddagger}$ ca. 12.0 ± 0.1 kcal mol^{-1} for this dynamic process, a value which is significantly larger than that determined for the related cyclopentadienyl compound, (η^1-C_5H_5)$Re(CO)_3(PMe_3)_2$ ($\Delta G^{\ddagger} < 7$ kcal mol^{-1}) [19,20]. The thermal stability of these η^1-compounds was also brought to light during the variable-temperature ^{1}H-NMR analysis of **17**, as the formation of neither dissociation nor substitution products was found, even after continuous heating at 65°C for over an hour.

The virtual coupling involving the PMe_3 ligands of **17** in the fast exchange regime proved to be an important result, as it verified the non-dissociative nature of the dynamic process. Moreover, in the absence of restricted rotation about the indenyl–Re bond in the η^1-configuration at reduced temperatures, the exchanging phosphine methyl resonances confirmed the facial geometrical assignment, suggesting that the rearrangement proceeds with retention of configuration at the rhenium

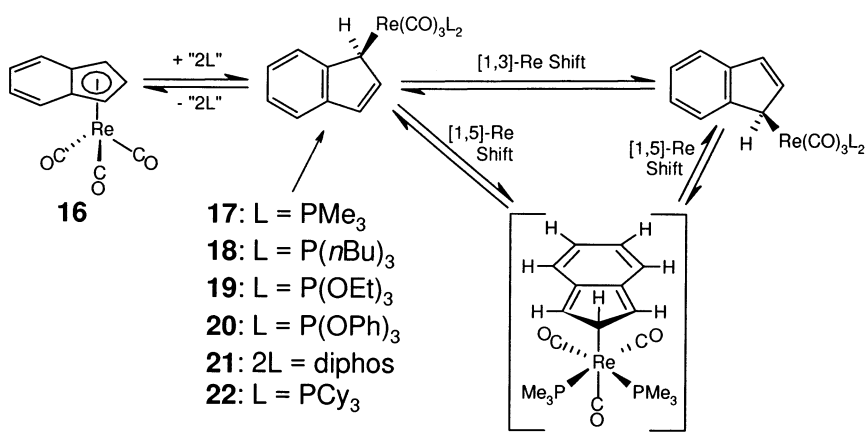

Scheme 7. The synthesis and molecular rearrangements of (η^1-C_9H_7)$Re(CO)_3L_2$ complexes.

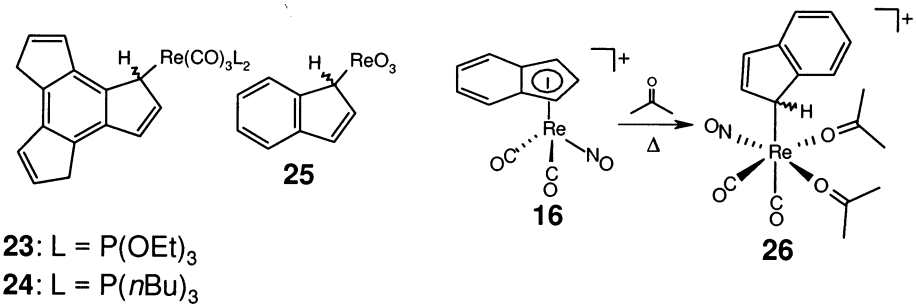

Scheme 8. A selection of rhenium-based η^1-indenyl compounds, including novel η^1-trindenyl species, an oxorhenium compound and the formation of a cationic complex containing a nitrosylrhenium center.

center. Casey and O'Connor skillfully recognized that the heightened barrier associated with molecular rearrangements in **17**, in comparison to the corresponding η^1-cyclopentadienyl analogue, is entirely consistent with the operation a '1,2 shift' mechanism. Using the orbital symmetry formalism of Woodward and Hoffmann [21,22], these transitions are conveniently reformulated as symmetry-allowed [1,5]-suprafacial sigmatropic shifts [23,24]. However, based on the apparently static nature (see Section 2.3) of the previously examined iron complex (η^5-C_5H_5)Fe(CO)$_2$(η^1-C_9H_7) (**31**) [25], Casey and O'Connor suggested that the required intermediacy of isoindenes in a '1,2' (= [1,5]) shift rearrangement pathway may be prohibitive, and proposed that 'the observed fluxionality… of **17**… may be due to a direct 1,3 shift' [19].

Following the pioneering work of Casey and O'Connor, a detailed kinetic study was published by Bang, Lynch and Basolo, in which reactions of **16** with a series of phosphines and phosphites were examined as a function of temperature and reactant concentration [26]. In addition to detailing the preparation and characterization of four new η^1-indenyl rhenium compounds (**19**–**22**), Basolo and co-workers identified the operation of both phosphine addition and carbonyl displacement reaction pathways, similar to that depicted in Scheme 1. For reactions involving triethyl phosphite, reduced temperatures and high ligand concentrations favored the formation of the η^1-C_9H_7 complex, **19** in contrast, under conditions of high temperature and low ligand concentration, the displacement product, (η^5-C_9H_7)Re(CO)$_2$P(OEt)$_3$, was preferentially formed. These workers note that the nature of the entering phosphine plays a major role in partitioning between η^1 and η^5 products, with small and strongly basic nucleophiles favoring the formation of η^1-indenyl complexes. An additional facet of this work involved a kinetic study of the related compound, (η^5-trindenyl)Re(CO)$_3$. When reacted with triethyl phosphite at 80°C, the initially formed η^1-complex (**23**), is converted rapidly to the carbonyl displacement product, (η^5-trindenyl)Re(CO)$_2$P(OEt)$_3$ (Scheme 8). However, when the reaction was carried out at a lower temperature (40°C), the stepwise nature of the process became evident, since spectral changes corresponding to an $\eta^5 \rightarrow \eta^3 \rightarrow \eta^1$ transformation were observed. The tributylphosphine complex (**24**), was also prepared and studied by these workers [26].

Herrmann and co-workers [27] have demonstrated that tetrahedrally coordinated η^1-indenyl rhenium complexes are preparable. The moisture and temperature-sensitive molecule, $(\eta^1\text{-}C_9H_7)ReO_3$ (**25**), synthesized from Re_2O_7 and $(\eta^1\text{-}C_9H_7)Sn(n\text{-}Bu)_3$, was deemed stereochemically non-rigid based on data obtained from a variable-temperature spectroscopic study. The ^{1}H-NMR spectrum of **25** acquired at -50°C is in keeping with an η^1-C_9H_7 structural formulation. Upon warming the sample to 0°C, the H(1) and H(3) signals broaden significantly, and the aromatic protons approach coalescence. Presumably, the thermal instability of **25** (decomposition temperature ca. -30°C) prevented the authors from acquiring sufficiently reliable spectroscopic data so as to allow for the accurate determination of the free energy associated with this rearrangement process.

In 1993, Zhou et al. [28] reported the generation of a cationic η^1-indenyl complex of rhenium. Starting from the tricarbonylrhenium compound, **16**, treatment with $NOBF_4$ in dichloromethane gave rise to what was the desired cationic π-complex, $[(\eta^5\text{-}C_9H_7)Re(CO)_2NO]^+BF_4^-$ (Scheme 8). However, when this product was dissolved in deuterated acetone to allow for an ambient-temperature NMR study, the observation of characteristic η^1-C_9H_7 resonances, including readily discernible Re*CH* ^{1}H-NMR signals, clearly revealed the formation of several η^1-complexes; similar results were also obtained when acetonitrile was employed as the solvent. Ambient temperature ^{1}H- and ^{13}C-NMR spectral data acquired after heating the sample at 57°C (0.5 h) verified the conversion of this mixture to a single product ($>$ 95%), which was assigned as the facial-coordinated isomer, **26**. Unfortunately, attempts to isolate **26** were unsuccessful, and no comment is made about the operation of dynamic processes in this interesting molecule.

As an extension of the work of Casey and O'Connor, who studied reactions involving $(\eta^5\text{-}C_9H_7)Re(CO)_3$ (**16**) with neutral, two-electron donor ligands, Richmond and Lee [29] examined the reactivity of this molecule with anionic reagents. Under ambient conditions, treatment of **16** with a hydride source was found to rapidly produce lithium indenide and the tetranuclear cluster, $[H_6Re_4(CO)_{12}]^{2-}$ (Scheme 9). In rationalizing the formation of these products, Richmond proposed a mechanistic pathway involving η^3-C_9H_7 and η^1-C_9H_7 anionic intermediates (**27** and **28**, respectively), which are ultimately converted to the observed 'η^0' product (lithium indenide) and the tetrarhenium complex; neither of the purported intermediates was observed spectroscopically. Overall, the proposed reaction sequence

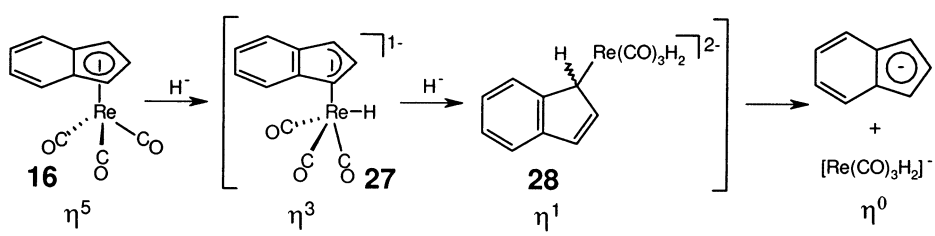

Scheme 9. The successive transformation of the η^5-compound (**16**) into the 'η^0' compound, lithium indenide, via the η^3 and η^1 intermediates (**27** and **28**).

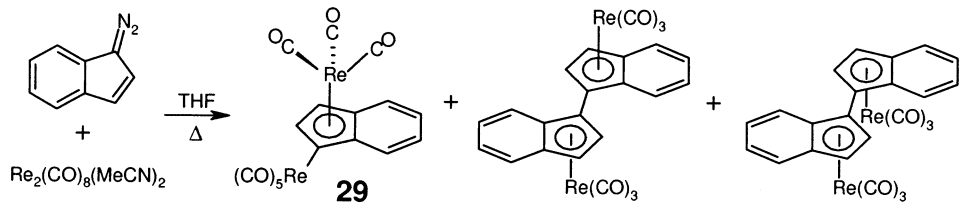

Scheme 10. Generation of the mixed η^5/η^1-dinuclear rhenium complex (**29**).

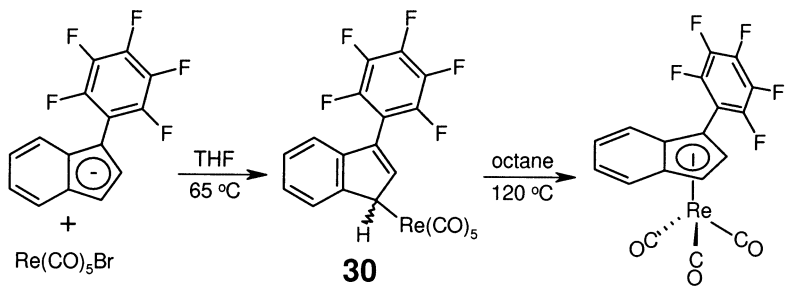

Scheme 11. Formation of the η^1-indenyl complex (**30**) and its conversion to the corresponding η^5-indenyl compound.

represents an interesting example of an $\eta^5 \rightarrow \eta^3 \rightarrow \eta^1 \rightarrow \eta^0$ ring-slippage transformation process.

Arce et al. [30] have reported on the preparation of binuclear rhenium derivatives of indene. Treatment of $Re_2(CO)_8(MeCN)_2$ with diazoindene generates a mixture of three dirhenium complexes, viz. the crystallographically characterized η^1/η^5 species (**29**) and the *meso*- and *rac*-isomers depicted in Scheme 10.

In 2000, Deck and Fronczek [31] reported on the synthesis and characterization of pentafluorophenyl-functionalized indenylrhenium complexes. Treatment of $Re(CO)_5Br$ with the indenide anion derived from 3-$(C_6F_5)C_9H_7$ at 65°C afforded the crystallographically characterized η^1-indenyl complex (**30**) in 57% yield (Scheme 11). Conversion of this species to the corresponding pentahapto compound (via thermolytic decarbonylation) required more forcing conditions (120°C). Interestingly, the analogous reaction conducted at 65°C employing the diarylated indenyl precursor, 1,3-$(C_6F_5)_2C_9H_6$, led directly to the formation of the corresponding η^5-tricarbonylrhenium complex, perhaps attributable to steric crowding at the sp^3 carbon.

2.3. Group 8

Pioneering studies by Cotton [32] involving η^1-indenyliron compounds figured prominently in the evolution of fluxionality concepts in organometallic chemistry. In what is now widely recognized as a pioneering study, Cotton and co-workers [33]

not only correlated the limiting low-temperature ^{1}H-NMR spectrum with the solid state structure of $(\eta^5\text{-}C_5H_5)Fe(CO)_2(\eta^1\text{-}C_5H_5)$, but also characterized the circumambulatory rearrangement ('ring-whizzing') pathway as proceeding via sequential 1,2- (=[1,5]) (rather than 1,3) shifts. Important supporting evidence for the proposed [1,5]-iron shift mechanism in this η^1-C_5H_5 derivative was obtained by Cotton and co-workers through a study of the corresponding indenyl system, $(\eta^5\text{-}C_5H_5)Fe(CO)_2(\eta^1\text{-}C_9H_7)$ (**31**), for which it is anticipated that [1,5]-iron shifts would be suppressed because of the required intermediacy of the high-energy isoindene, **31**-*iso* (Scheme 12) [25]. The apparently static nature of **31**, an assumption based on the lack of ^{1}H-NMR line-broadening up to temperatures at which sample decomposition is rapid, provided indirect support for the operation of a [1,5]-iron shift mechanism involving $(\eta^5\text{-}C_5H_5)Fe(CO)_2(\eta^1\text{-}C_5H_5)$. Until recently, the 'non-fluxional' [32] nature of **31** has underpinned our conceptual understanding of molecular rearrangements involving η^1-indenyl transition metal complexes.

In 1997, Stradiotto et al. [34] reinvestigated the molecular dynamics of $(\eta^5\text{-}C_5H_5)Fe(CO)_2(\eta^1\text{-}C_9H_7)$ (**31**). By use of slow exchange regime dynamic NMR techniques (including 2D-EXSY [35]), which are effective in probing chemical exchange processes that are slow on the NMR line-broadening time-scale, these workers unambiguously demonstrated that **31** is, in fact, stereochemically non-rigid. The barrier to [1,5]-iron shifts in **31** ($\Delta G^{\ddagger}$ ca. 20 kcal mol^{-1}) was determined based on kinetic data obtained using single selective inversion ^{1}H-NMR methods [36,37]; this value is in keeping both with the 10.7 kcal mol^{-1} migration barrier associated with $(\eta^5\text{-}C_5H_5)Fe(CO)_2(\eta^1\text{-}C_5H_5)$ [38–40], and the energetic cost (ca. 8.5 kcal mol^{-1}) of transforming an indenyl complex into the corresponding isoindenyl species, as predicted by Cotton and coworkers [25,33].

The detection of quasi-fluxional behavior involving **31** provides mechanistic insight into the reactivity of this compound. In 1996, Kerber et al. [41] noted that the addition of either tetracyanoethylene (TCNE) or maleic anhydride to solutions of **31** results in the formation of the cycloadducts, **32** and **33**, respectively (Scheme 13). In light of the assumed static nature of **31**, the authors chose to preclude the involvement of the corresponding isoindene (**31-*iso***), and the formation of **32** and

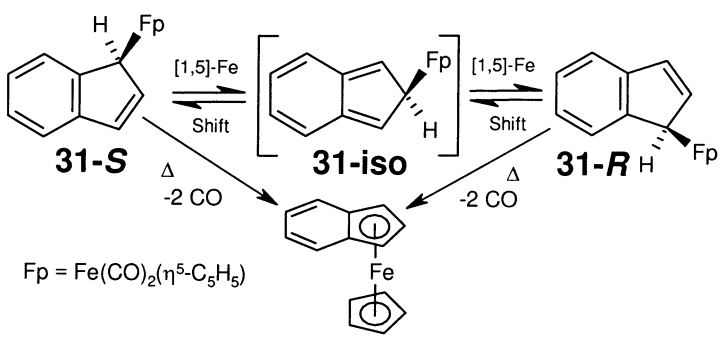

Scheme 12. [1,5]-Suprafacial shifts in the η^1-indenyl system (**31**) showing the formation of the isoindene (**31**-*iso*) and benzoferrocene.

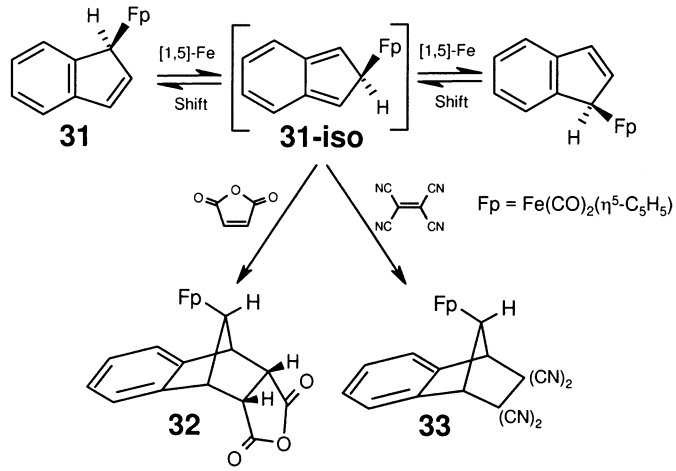

Scheme 13. Cycloaddition chemistry involving $(\eta^5\text{-}C_5H_5)Fe(CO)_2(\eta^1\text{-}C_9H_7)$ (**31**).

33 was rationalized in terms of a [3 + 2] mechanism. However, with the dynamic character of **31** revealed, it is also possible to envision the generation of these cycloadducts in a Diels–Alder ([4 + 2]) process, via the isoindene, **31**-*iso*. Although conclusive kinetic data are still lacking, indirect support for the attack of TCNE on **31**-*iso* in a [4 + 2] mechanism comes from the anti-disposition of the iron and dienophilic fragments, which is evident in the crystal structure of **32** [34]. Larrabee and Dowden [42] and Ashe [43] independently reported the use of suitably reactive dienophiles as isoindene trapping agents in 1970 (Section 3.2).

In 1986, Belmont and Wrighton [44] reported the stepwise photochemical decarbonylation of **31**, and the related bis(indenyl) complex, $(\eta^5\text{-}C_9H_7)Fe(CO)_2(\eta^1\text{-}C_9H_7)$, **35**. Irradiation with near-UV light at reduced temperatures allowed for the infrared detection of the corresponding monocarbonyl intermediates, **34** and **36**, in which a formerly η^1-bonded indenyl ring has slipped to an η^3-configuration. These monocarbonyl species were found to be thermally and photochemically labile, readily yielding the corresponding metallocene sandwich complexes, as shown in Scheme 14.

In a more recent publication, Waldbaum and Kerber [45] reported the isolation and characterization of **39** and **40**, two interesting η^1-indenyliron derivatives of 2,2′-biindene (Scheme 15). In an effort to prepare the diiron species, **38**, 2,2′-biindene was treated with two equivalents of base, followed by two equivalents of $(\eta^5\text{-}C_5H_5)Fe(CO)_2Br$; chromatographic separation of the reaction products revealed the unexpected formation of **39** and **40** (42 and 6% yield, respectively), in the absence of **38**. The identity of **39** was formulated based on ^{1}H- and ^{13}C-NMR spectroscopic data, mass spectrometry and elemental analysis, while the structure of **40** was proposed based on data obtained from ^{1}H-NMR and infrared spectroscopic experiments. Waldbaum and Kerber tentatively propose that these two η^1-indenyliron products are derived from the unobserved anionic intermediate, **37**;

simple protonation of this anion leads directly to **40**. In the case of **39**, the authors suggest that oxidation of **37** (or homolytic scission of an Fe–C(1)indenyl bond in the purported intermediate, **38**) could lead to the formation of an indenyl radical

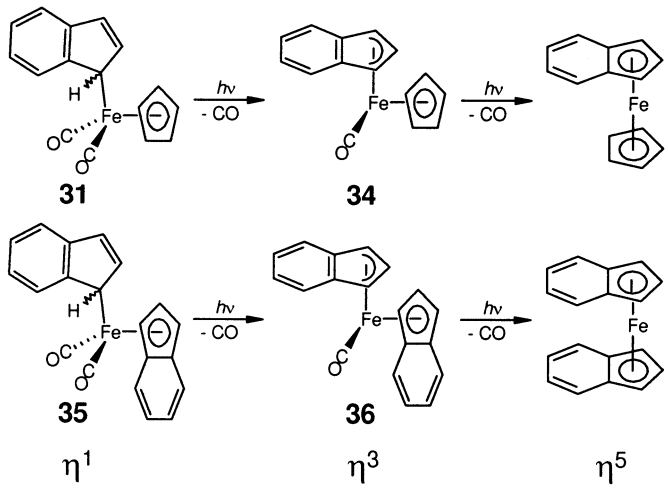

Scheme 14. Photochemically promoted decarbonylation reactions involving the η^1-indenyliron complexes (**31** and **35**).

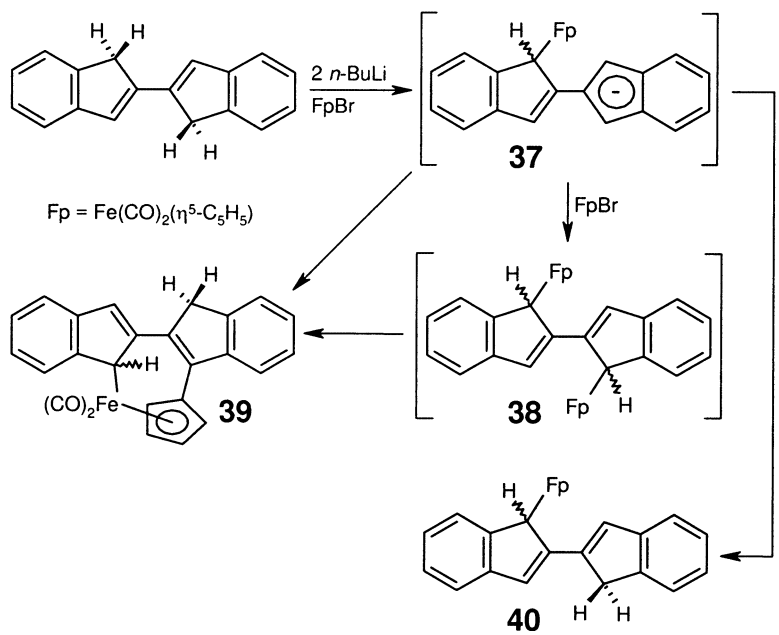

Scheme 15. Proposed pathway leading to **39** and **40**, η^1-indenyliron derivatives of 2,2′-biindenyl.

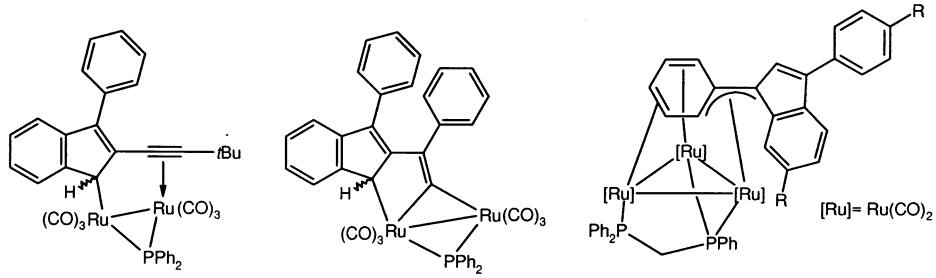

Scheme 16. Rare examples of η^1-indenyl compounds of ruthenium.

which, upon attack at the coordinated η^5-C_5H_5 ligand followed by loss of a hydrogen atom, would lead to **39**.

Two intriguing examples of η^1-indenyl ruthenium compounds, **41** and **42**, have been published by Carty and co-workers [46] (Scheme 16). These crystallographically characterized complexes were generated in an unconventional manner, from reactions involving butadiynyl–$Ru_2(CO)_6$ complexes and the carbene derived from Ph_2CN_2. The authors rationalize the stability of these dinuclear η^1-complexes as arising due to the presence of an unsaturated fragment at the C(2) position, which allows for intramolecular coordination to the second ruthenium center. Somewhat related to the aforementioned compounds are the trinuclear species, **43** and **44**, reported by Bruce et al. [47] in 1999. Unlike **41** and **42**, the crystallographically characterized complex, **43**, contains a ruthenium center which is bonded in a delocalized η^3-benzylic fashion to the indenyl C(1) carbon and two carbons on an adjacent pendant phenyl unit.

2.4. Group 9

Group 9 η^1-indenyl complexes were first observed spectroscopically by Green and co-workers [48] in 1977. In examining the reactivity of (η^5-C_9H_7)$Rh(C_2H_4)_2$, these researchers noted that while treatment with two equivalents of *tert*-butyl isonitrile rapidly displaces ethylene to form **45**, the addition of excess *tert*-butyl isocyanide generates the η^1-indenyl complex, **46** (Scheme 17). The formation of **46** was proposed based upon infrared spectroscopic data.

In 1989, Merola and Kacmarcik [49] reported the conversion of the η^5 iridium complex, **47**, to the crystallographically characterized 'η^{0}' species, **50** (Scheme 18). In studying the reactivity of **47** with nucleophiles, these workers observed that treatment with excess carbon monoxide displaces the 1,5-cyclooctadiene (COD) ligand, giving rise to the pentahapto species, (η^5-C_9H_7)$Ir(CO)_2$. In contrast, the addition of excess PMe_3 to **47** unexpectedly resulted in the quantitative formation of **50**, in which the indenyl fragment has formally been transferred from the iridium center to the COD moiety. Merola and Kacmarcik propose an $\eta^5 \rightarrow \eta^3 \rightarrow \eta^1 \rightarrow \eta^0$

ring-slippage process leading to the formation of **50**, which parallels the mechanistic rationale put forth by Lee and Richmond [29] for the reaction involving (η^5-C_9H_7)Re(CO)$_3$ and hydride (Scheme 9).

In the same year, Crabtree and co-workers [50] reported the formation of isolable η^1-indenyl compounds, derived from reactions of $[(\eta^5\text{-}C_9H_7)Ir(R)(PPh_3)_2]^+$ (R = H, Me) with donor ligands (Scheme 19). Addition of *tert*-butyl isonitrile to the aforementioned hydride precursor at -73°C generates an η^3-intermediate, while above this temperature, low-yield conversion to the η^1-complex (**51**) is detected by NMR spectroscopy ($< 20\%$). As the sample is warmed further, signals attributable

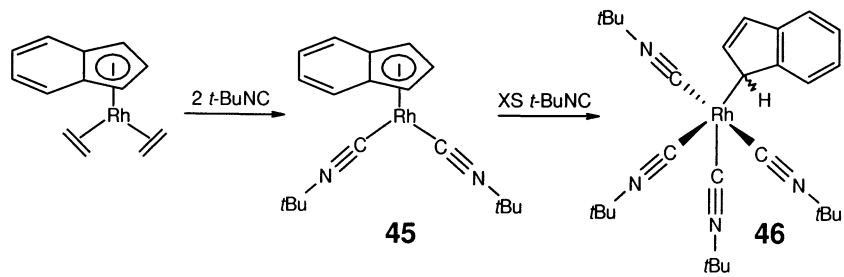

Scheme 17. Generation of the first spectroscopically detected η^1-indenyl complex of rhodium.

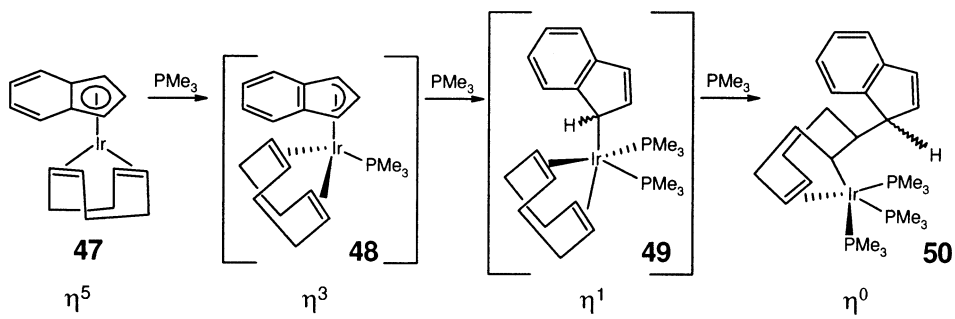

Scheme 18. The proposed stepwise η^5 to η^0 transformation of the iridium complex (**47**).

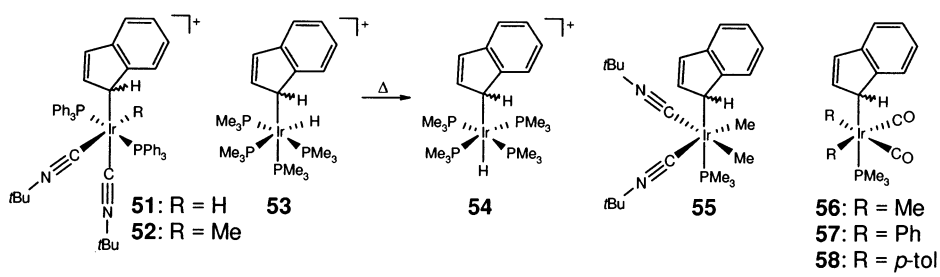

Scheme 19. Some selected examples of η^1-indenyl iridium compounds bearing hydride and alkyl substituents.

to free indene are observed, coinciding with an $\eta^5 \rightarrow \eta^3 \rightarrow \eta^1 \rightarrow \eta^0$ ring-slippage process. Comparable reactivity is found for the cationic methyl complex, $[(\eta^5\text{-}C_9H_7)Ir(Me)(PPh_3)_2]^+$, with the exception that the η^1 complex (**52**) is formed preferentially and can be isolated in ca. 90% yield. The *cis* orientation of the 'R' (H, Me) and indenyl ligands in **51** and **52** was inferred by comparison with structurally characterized analogues. Interesting results were also obtained when $[(\eta^5\text{-}C_9H_7)Ir(H)(PPh_3)_2]^+$ was allowed to react with trimethylphosphine in dichloromethane under ambient conditions. During the early stages of the reaction (2–12 h), the authors noted the formation of **53**, in which the hydride and indenyl ligands are *cis* to one another; after 24 h, this kinetic product is transformed into the thermodynamic *trans*-disposed product (**54**), which was isolated as an analytically pure solid in 86% yield. The structures of these products were readily assigned based on the magnitude and multiplicity of the coupling (J_{PH}) between the Ir–*H* proton and the phosphine ligands. It is interesting to note that, in contrast to the behavior of **51**, the hydrides **53** and **54** show no tendency to eliminate indene.

The library of isolable η^1-indenyl complexes of iridium was extended by Foo and Bergman [51] in 1992. Starting from $(\eta^5\text{-}C_9H_7)IrMe_2(PMe_3)$, the indenyl complex, **55**, was generated rapidly via addition of excess *tert*-butyl isonitrile, and subsequently isolated in 97% yield as a white analytically pure solid. The dialkyl derivatives, $(\eta^5\text{-}C_9H_7)Ir(R)_2(PMe_3)$ (R = Me, Ph, *p*-tol), were similarly converted in high yield to the corresponding $(\eta^1\text{-}C_9H_7)Ir(R)_2(PMe_3)(CO)_2$ compounds, **56**–**58**, upon exposure to excess carbon monoxide. The relative orientation of the ligands in compounds **55**–**58** was determined based on IR and NMR spectroscopic data. Especially informative was the diastereotopic nature of the isonitrile and methyl ligands in **55**, and the alkyl and carbonyl moieties in compounds **56**–**58**. The generation of diastereomeric mixtures of η^1-indenyl complexes was observed when asymmetrical precursors $(\eta^5\text{-}C_9H_7)Ir(R)(R')(PMe_3)$ ($R \neq R'$; R and R′ include Me, Ph, *p*-tol, H) were exposed to carbon monoxide. In the case of these hydrido-alkyl η^1-indenyl products, Foo and Bergman found that the addition of excess carbon monoxide at ambient temperature eventually results in the reductive elimination of R–H.

Ceccon and co-workers have published a series of papers pertaining to the synthesis and spectroscopic behavior of η^3 and η^1-indenyl complexes of rhodium and iridium. Following the work of Merola and Kacmarcik [49] in 1989, Ceccon and co-workers [52] reexamined carefully the reactivity of $(\eta^5\text{-}C_9H_7)Ir(COD)$ (**47**) with carbon monoxide, in the hopes of observing one or more of the intermediates along the associative substitution reaction pathway. In agreement with the findings of Merola and Kacmarcik, Ceccon et al. noted that under ambient conditions, solutions of **47** are converted rapidly to $(\eta^5\text{-}C_9H_7)Ir(CO)_2$, when treated with excess carbon monoxide (Scheme 20). However, when the reaction temperature was kept below -30°C, these workers observed the quantitative formation of the η^1-indenyl complex, **59**; this dicarbonyl species is directly comparable to the trimethylphosphine intermediate, **49**, proposed by Merola and co-workers. The presence of an η^1-bonded indenyl ligand in **59** is supported by the apparent magnetic non-equivalence of the carbonyl ligands and the appearance of characteristic indenyl ^{1}H-NMR

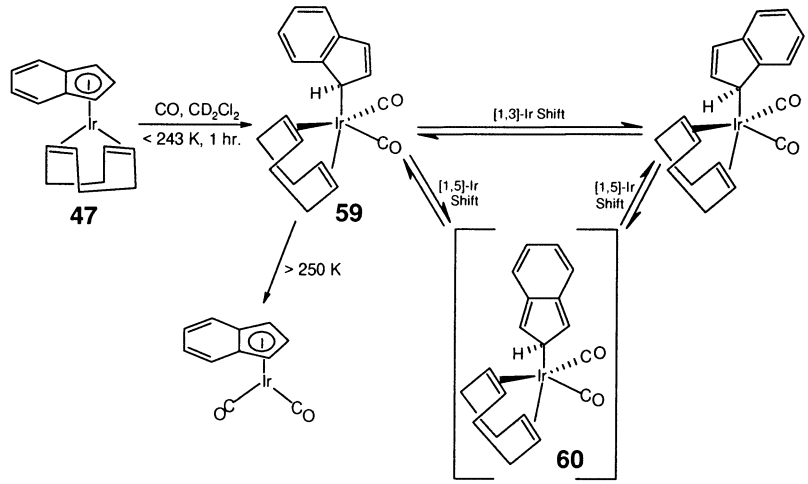

Scheme 20. Synthesis, decomposition and possible molecular rearrangement pathways involving the dynamic iridium compound (**59**).

resonances. The COD ligand also produces two well-resolved signals in the ^{1}H-NMR spectrum of **59** at -40°C, owing to the diastereotopicity induced by the chiral η^1-indenyl ligand. As the temperature is lowered, rotation of the COD ligand is slowed on the NMR time-scale, giving rise to four distinct resonances at -100°C. Furthermore, on raising the temperature to ca. 0°C, broadening of the indenyl H(1) and H(3) signals and related pairs of C_6 indenyl ring proton signals is evident. Unfortunately, attempts to monitor this dynamic process at higher temperatures were prevented by the competitive decomposition of **59** to yield (η^5-C_9H_7)Ir(CO)$_2$. In the absence of kinetic data, the authors qualitatively rationalized these NMR spectral changes in terms of 'a rapid 1,3-exchange through an η^3-species in which COD is monodentate and the Ir maintains its 18-electron shell' [52]. Given the non-rigid nature of the aforementioned rhenium [19,27] and iron [34] η^1-indenyl complexes, which lack similar neutral multidentate ancillary ligands required in such a mechanistic scenario, a rearrangement pathway for **59** involving [1,5]-iridium shifts (via the isoindene, **60**) remains equally viable (Scheme 20).

In 1996, Ceccon and co-workers [53] examined the kinetics and mechanistic aspects of carbonyl substitution at rhodium in a bimetallic system. These studies involved the addition of either COD or norbornadiene (NBD) to the *anti*-coordinated chromium–rhodium complex, **61** (Scheme 21), and were monitored by use of UV–vis spectroscopy. The rate of carbonyl substitution in **61** was found to be ca. 2000 times more rapid than in (η^5-C_9H_7)Rh(CO)$_2$, inspiring the authors to refer to this phenomenon as the 'extra-indenyl effect'. Based on the kinetic data obtained in these experiments, Ceccon et al. postulated that the rate-determining step involves addition of the bidentate olefin to the bimetallic pentacarbonyl complex, generating an η^1-intermediate (**62** in the case of COD addition). The observed substitution product, **63**, is then generated via rapid loss of two molecules of carbon monoxide.

Although no low-hapticity species were spectroscopically detected in these studies, evidence for the existence of intermediates analogous to **62** was provided in a subsequent publication, in which related iridium complexes were examined.

In 1998, Cecchetto et al. [54] logically extended the aforementioned studies to include *anti*-coordinated iridium-based bimetallic complexes (Scheme 22). The reaction of **64** with an excess of carbon monoxide at reduced temperature (− 70°C) led to the quantitative formation of the η^1-indenyl complex, **65**; this latter compound is directly comparable to the iridium complex, **59**, and the proposed rhodium bimetallic intermediate, **62**. However, unlike these species, **65** is cleanly converted (above 0°C) to the bimetallic heptacarbonyl η^1-complex, **66**. The preferential formation of this latter compound is in striking contrast to the facile transformation of **59** into the η^5-complex, $(\eta^5\text{-}C_9H_7)Ir(CO)_2$; the conversion of **66** into the chromium-complexed analogue of $(\eta^5\text{-}C_9H_7)Ir(CO)_2$ requires more forcing conditions. Indeed, the bimetallic η^1-indenyl complex, **66**, is remarkably stable,

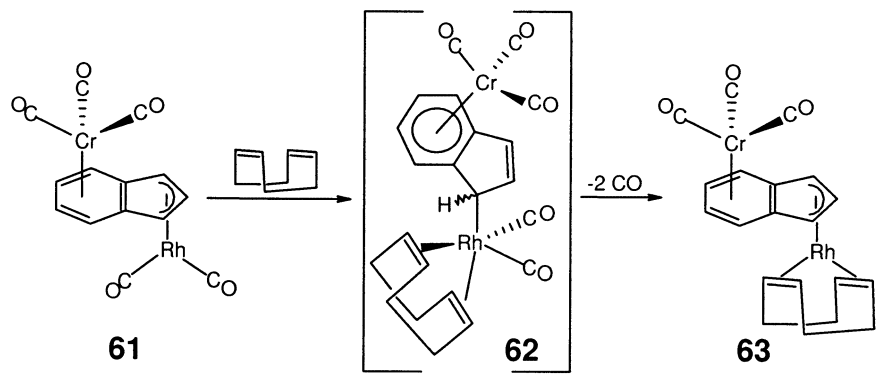

Scheme 21. Conversion of the bimetallic pentacarbonyl complex (**61**) into **63**, by way of carbonyl displacement.

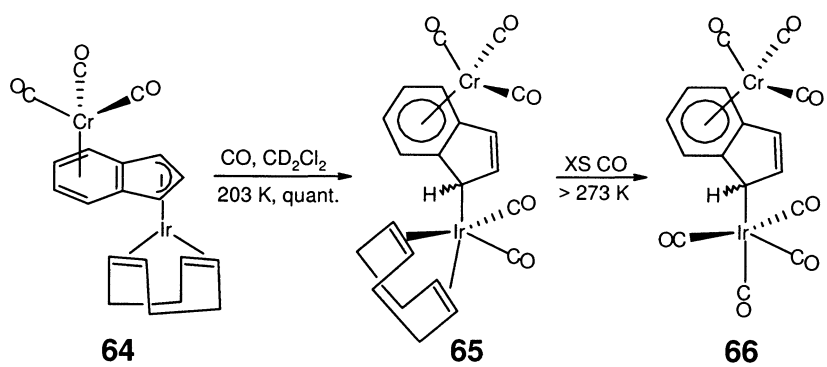

Scheme 22. Addition of carbon monoxide to the bimetallic complex (**64**) producing **65** and ultimately the heptacarbonyl complex (**66**).

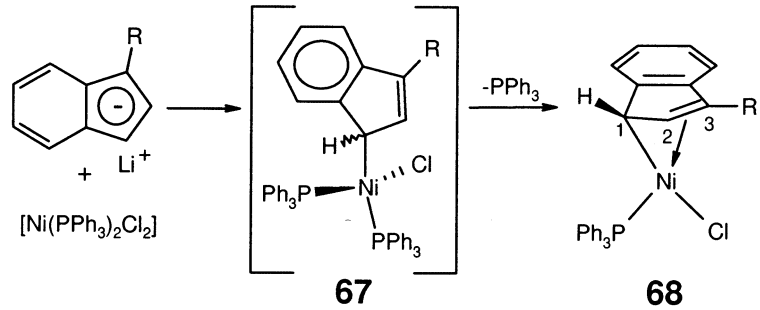

Scheme 23. Proposed synthetic pathway to 'η^1:η^{2}' indenyl nickel complexes (**68**) (R = H or Me), via the η^1-intermediate (**67**).

persisting in solution up to 40°C. Analogous experiments carried out using tricarbonylchromium-complexed $(\eta^5\text{-}C_9H_7)Ir(COE)_2$ (COE = cyclooctene) also yielded **66**, presumably via an undetected pentacarbonyl intermediate similar to **65**.

Ceccon and co-workers readily monitored the chemical reactions described above by use of IR and ^{1}H-NMR spectroscopy; because of the low solubility of the products, no ^{13}C-NMR spectral data were acquired. The conversion of **64** into the η^1-complex, **65**, was identified by the appearance of two IR bands attributable to an $Ir(CO)_2$ fragment, and the development of ^{1}H-NMR signals indicative of an η^1-indenyl compound. The subsequent generation of **66** was accompanied by a decrease in the intensity of the aforementioned IR absorptions, and the concomitant growing in of three new signals characteristic of an $Ir(CO)_4$ unit. The formation of **66** was also evinced by the considerable shift of the H(1) signal to higher frequency ($\Delta\delta$ ca. 1.5 ppm), an observation which is consonant with the replacement of olefinic ligands in **65** with carbonyl groups in **66**.

The molecular dynamics of **66** were qualitatively probed by Ceccon and co-workers through the acquisition of ^{1}H-NMR spectra between -40 and 25°C, though no quantitative rate data were provided. Slow warming of a dichloromethane solution containing **66** over this temperature range was accompanied by the collapse of the H(1) and H(3) signals, and the transformation of the H(2) signal from a doublet of doublets into a triplet. Similar spectral changes were observed for the signals associated with the indenyl C_6 unit. These workers interpreted the spectral changes in terms of direct [1,3]-shifts of the $Ir(CO)_4$ group, citing the similarity in dynamic behavior between **66** and the monometallic iridium complex, **59**. Alternatively, the overall transition of the iridium fragment from C(1) to C(3) in **66** may proceed via sequential [1,5]-iridium shifts, as depicted for **59** in Scheme 20.

2.5. Groups 10, 11 and 12

Zargarian and co-workers [55,56] have studied the chemistry of related nickel complexes. Using the synthetic methodology depicted in Scheme 23, η^1-indenyl species such as **68** (R = H, Me) and the corresponding methylnickel compounds

have been prepared and characterized. Starting from the indenyl anion derived from an appropriately substituted indene precursor, these authors propose that reaction with $(PPh_3)_2NiCl_2$ generates **68**, via the η^1-indenyl intermediate, **67**. Vestiges of the η^1-coordination proposed in **67** are retained in **68**, as evidenced by crystallographic data obtained for the parent compound (R = H), which reveal asymmetrical bonding in the solid state (Ni–C(1) ca. 2.04 Å; Ni–C(3) ca. 2.09 Å); ^{1}H-NMR ($\Delta\delta_{H(1)-H(3)} > 2.9$ ppm) and ^{13}C-NMR ($\Delta\delta_{C(1)-C(3)} > 20$ ppm) data suggest that such a bonding configuration also exists in solution.

In 1998, Poveda and co-workers [57] reported the in situ generation and NMR spectroscopic characterization of an η^1-indenyl complex of palladium. Treatment of the η^3-indenyl precursor, **69**, with two equivalents of *tert*-butyl isonitrile at -50°C leads cleanly to the η^1-indenylpalladium compound, **70** (Scheme 24). In addition to observing ^{1}H-NMR resonances characteristic of the η^1-C_9H_7 architecture, Poveda and coworkers note a doublet at 48.15 ppm ($^2J_{CP} = 69$ Hz) in the ^{13}C-NMR spectrum of **70**. They assign this diagnostic resonance to the Pd–*C*(1) carbon on the indenyl unit, and propose a *trans*-orientation of the phosphine and indenyl fragments in **70**, based on the magnitude of the ^{13}C–^{31}P coupling constant. Upon warming to 0°C, the η^1-indenyl species, **70**, takes up a second equivalent of isonitrile and is transformed into the palladated fulvene, **71**.

The preparation of η^1-indenyl derivatives of platinum was examined by O'Hare [58] in 1987. Treatment of $Pt(COD)Cl_2$ with either 1.0 or 2.5 equivalent(s) of sodium indenide in tetrahydrofuran at room temperature produced compounds **72** and **73**, respectively, which were isolated as crystalline solids in ca. 70% yield (Scheme 25). The chloro compound, **72**, was found to exhibit remarkable stability in polar solvents, showing little tendency to isomerize to the corresponding η^5-indenyl compound, in contrast to its η^1-C_5H_5 and η^1-C_5Me_5 counterparts. Although the bis(η^1-indenyl) compound, **73**, proved to be considerably less stable in solution, the ^{1}H- and ^{13}C-NMR data obtained for this compound were of sufficient quality so as to allow for the assignment of a 1:1 mixture of *meso*- and *rac*-diastereomers, arising from the stereogenicity of the indenyl groups. O'Hare was also able to demonstrate that the formation of the cationic complex, **74**, could be realized via treatment of either **72** with $AgBF_4$, or **73** with HBF_4.

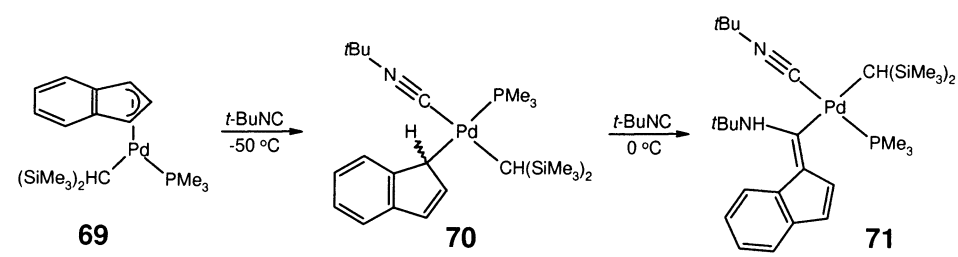

Scheme 24. Transformation of the η^3-indenyl complex (**69**) into the η^1-indenylpalladium species (**70**) and ultimately the metallafulvene (**71**).

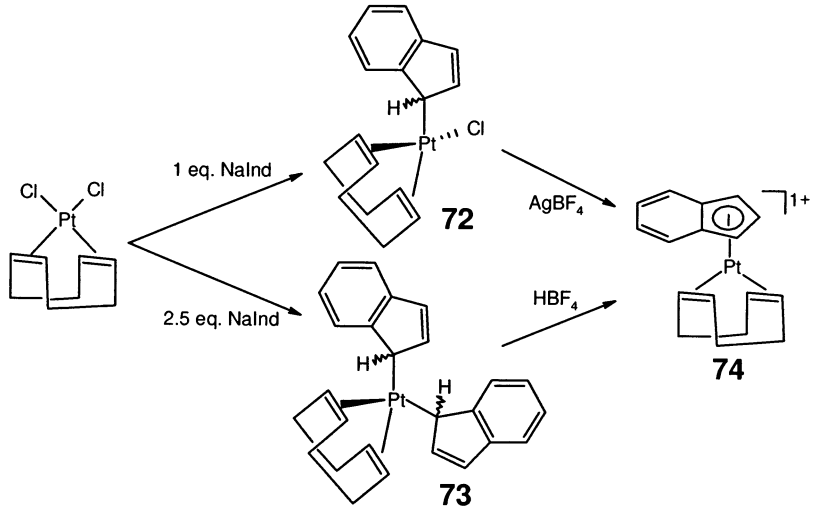

Scheme 25. The preparation of mono(η^1-indenyl) (**72**) and bis(η^1-indenyl) (**73**) complexes of platinum, and their conversion to the cationic η^5-complex (**74**).

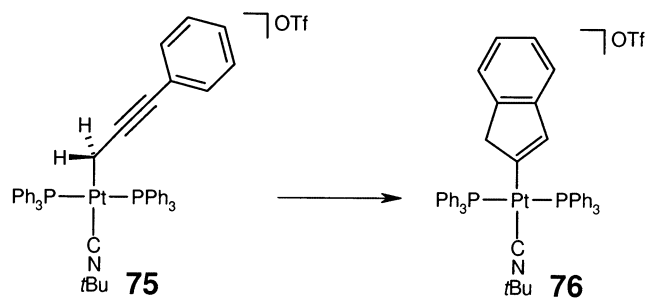

Scheme 26. Spontaneous rearrangement of **75**, resulting in the generation of a novel η^1-indenyl complex of platinum (**76**).

In 1999, Ackermann et al. [59] reported the generation and subsequent characterization of the square planar η^1-1*H*-inden-2-yl platinum complex, **76** (Scheme 26). These researchers noted that when solutions of the η^1-propargyl precursor, **75**, are allowed to stand for periods of time ranging from a few hours to several days at ambient temperature, an interesting rearrangement occurs, giving rise to **76** as an off-white solid in 76% yield. The structure of **76** was elucidated by use of NMR spectroscopic and X-ray crystallographic techniques.

A report pertaining to the synthesis of an indenylcopper complex was published in 1971 by Segusa et al. [60]. From a mixture of indene, Cu_2O and *tert*-butyl isonitrile was isolated **77**, as a heat- and moisture-sensitive compound, in 30% yield (Scheme 27). The ^{1}H-NMR spectrum of this product at room temperature exhibited an $A_2B_2X_2Y$ signal pattern, which was tentatively rationalized by the authors as

arising due to the rapid interconversion of the carbon–metal bond between the C(1) and C(3) positions in an η^1-species, as depicted in Scheme 27. Support for this η^1-bonding proposal, rather than one involving a multihapto-indenyl configuration, was based primarily on a comparison of the NMR spectral data acquired for **77** with those obtained for **78** (vide infra). Unfortunately, low-temperature NMR spectroscopic data for **77**, which may provide further insight into the instantaneous structure of this compound, were not provided in this report.

Consistent with the trend toward a localized, covalent η^1-indenyl bonding configuration in diindenylzinc suggested by Boersma and co-workers [61], are the findings of Cotton and Marks [62]. These latter workers reported in 1969 that the addition of mercuric chloride to a solution of lithium indenide at reduced temperature affords bis(η^1-indenyl)mercury, **78**, as a colorless solid in 12% yield after purification. In this report were presented ^{1}H-NMR spectroscopic data, acquired between -41 and 68°C, for this compound. The spectrum of **78** at the low temperature limit is entirely consistent with a bis(η^1-indenyl) structural formulation, as presented in Scheme 28; monohapto structures have also been proposed by Kitching and coworkers [63,64] for (η^1-C_9H_7)HgCl (**79**) and (η^1-C_9H_6Me)HgCl (**80**). Curiously, although Cotton and Marks were perceptive in recognizing that **78** should exist as a mixture of *rac*- and *meso*-isomers, they found no indication of such an isomeric mixture in the low-temperature limiting spectrum of **78**. Upon warming, several reversible spectral changes ensued, including the broadening, collapse, coalescence and sharpening of the signals assigned to the H(1) and H(3) protons. The concentration independence of these spectral changes allowed for the exclusion of second-order intermolecular phenomena, and led the authors to propose the operation of one or more temperature-dependent intramolecular exchange process(es), which permute the H(1) and H(3) indenyl ring environments in **78**. Careful analysis of these ^{1}H-NMR data allowed for a determination of the activation energy ($E_a = 12.9 \pm 0.6$ kcal mol^{-1}) for this system. Further insight into a possible rearrangement mechanism for **78** was provided in 1975, when Cotton et al. [65] published a variable-temperature ^{13}C-NMR examination of **78**, and related

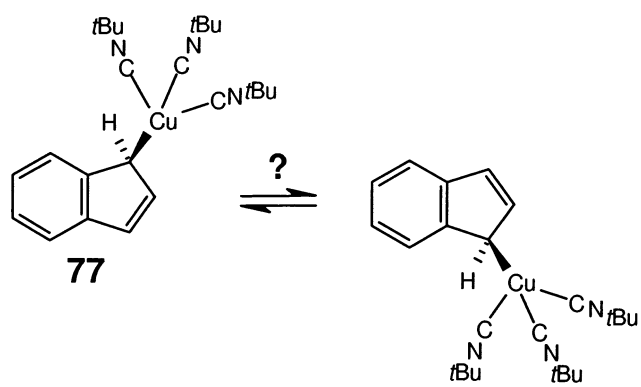

Scheme 27. The η^1-indenyl copper system (**77**).

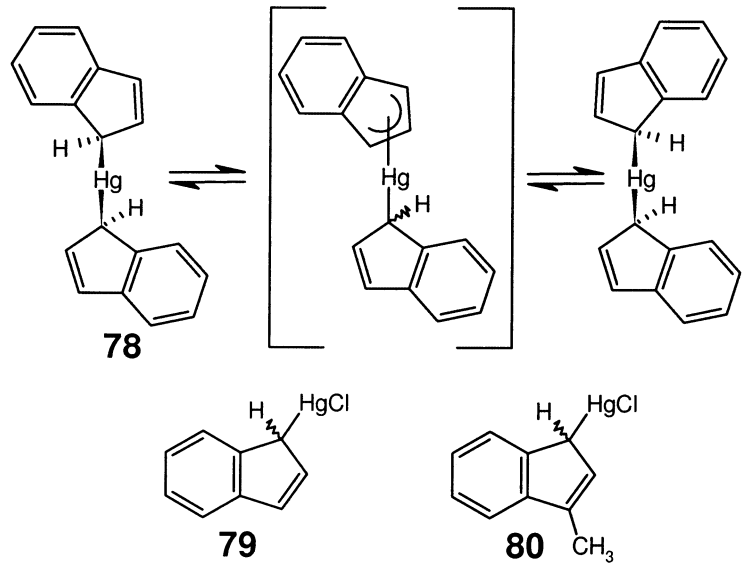

Scheme 28. The bis(η^1-indenyl)mercury compound (**78**) and the mono(η^1-indenyl) species (**79** and **80**).

η^1-cyclopentadienyl compounds, including (η^1-C_5H_5)HgCl. Data obtained in the course of these studies clearly point to the operation of a [1,5]-mercury shift mechanism involving (η^1-C_5H_5)HgCl ($E_a = 7.7 \pm 0.7$ kcal mol^{-1}); by analogy, a [1,5]-mercury shift process for **78** is plausible.

3. Main group η^1-indenyl compounds

3.1. Group 13

The earliest examples of indenylboranes were provided by Mikhailov et al. [66]. In 1972, these researchers reported that treatment of indenyllithium with chlorodimethoxyborane at reduced temperatures produced the indenylborane, **81**, which was subsequently isolated in 33% yield by distillation. The connectivity in **81** was identified based primarily on ^{1}H- and ^{11}B-NMR data, which revealed the allylic structure shown in Scheme 29. Despite the moisture sensitive nature of **81**, this compound was shown to be thermally stable up to ca. 120°C.

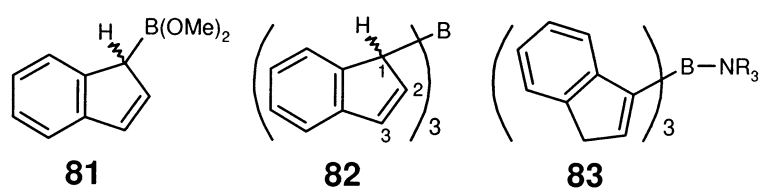

Scheme 29. Early examples of indenylboranes.

In a subsequent publication, Mikhailov et al. [67] presented the synthesis and characterization of the tris(indenyl)borane (**82**). Prepared from indenyllithium and BF_3, the spectroscopic features of this novel compound between 20 and 120°C were found to depend reversibly on temperature. Below 20°C, the ^{1}H-NMR spectrum of **82** is comprised of signals attributable to a tris(η^1-indenyl) system; as the sample is warmed, the H(1) (ca. 2.8 ppm) and H(3) (ca. 6.8 ppm) signals slowly broaden, with full collapse observed near 104°C. Contemporaneously, the H(2) signal (ca. 5.9 ppm) is transformed from a doublet of doublets into a triplet. Evaluation of these temperature-dependent NMR data using the Arrhenius methodology allowed for an estimation of the activation energy for this dynamic process ($E_a = 13 \pm 1$ kcal mol^{-1}). Although the spectral assignments and data analysis provided by the authors appear to be in order, their description of the dynamic behavior of **82** is somewhat confusing. In this report, these workers refer to an 'allylic rearrangement' process involving **82**, which appears to coincide with an overall C(1) to C(3) transfer of the boron fragment; the NMR spectroscopic data provided are in agreement with such a process. However, the authors also state that 'if the signal at 6.83 ppm had belonged to the …H(2)… proton, then a 1,2-shift would have occurred, and not [an] allyl rearrangement'. It is unclear what chemical exchange process involving the migration of the boron fragment alone could result in the permutation of the H(1) and H(2) sites in **82**. Moreover, Mikhailov et al. failed to recognize the potential for diastereoisomerism in **82**. This compound could, in principle, exist as a mixture of four isomers due to the stereogenic indenyl C(1) center. The generation of such isomeric mixtures is not a concern in the case of achiral tris(indenyl)borane Lewis adducts (generally depicted as **83**); several such adducts were prepared by Mikhailov and co-workers via reaction with amines.

In the 20 years following these studies by Mikhailov et al., the field of indenylborane chemistry received little attention. However, the potential utility of these complexes as transition metal ligands has prompted several research groups to take up the study of these molecules. In fact, the vast majority of reports pertaining to indenylboranes have appeared only in the last few years.

The use of pentafluorophenyl-containing indenylboranes as ligands in preparation of single-component zwitterionic [68] catalysts has been examined by Bochmann and co-workers [69]. The addition of bis(pentafluorophenyl)fluoro-borane to a solution of either $[C_9H_7]Li$ or $[C_9H_6SiMe_3]Li$ produced mixtures containing **84** and **85**, or **86** and **87**, respectively (Scheme 30). In the former reaction, fractional crystallization allowed for the isolation of the expected C(3) product (**85**) and the unusual C(2) species (**84**), which were generated in a 5:2 ratio. Although no mechanistic rationalization for the formation of **84** was provided by the authors, this result is intriguing since there is little precedent for the generation of such a main group complex via direct attack at the C(2) position of indenyl anions. An alternative route leading to **84** may involve addition of the $B(C_6F_5)_2$ unit to the indenyl C(1) position in the usual manner, followed by a [1,5]-boron shift (giving a C(2) boron-substituted isoindene) and subsequently a [1,5]-hydrogen migration (possibly base-catalyzed) in the isoindene. Treatment of crude mixtures of **84** and **85** with *tert*-butylamine yielded a single crystalline product, which was identified as

the Lewis adduct derived from **85**; analogous adducts of **84** were not identified. In contrast to **84** and **85**, crystalline material isolated from the reaction involving $[C_9H_6SiMe_3]Li$ was found to contain both of the silicon-substituted products, **86** and **87**, which were subsequently characterized as a mixture in solution by use of NMR spectroscopy. The authors provide no spectroscopic evidence for quasi-fluxional behavior in this system, though it is likely that **86** and **87** exist in solution as an equilibrium mixture, with interconversions occurring via [1,5]-silicon shifts. The **86**/**87** system, in which silicon continually occupies an sp^3-hybridized position, can be contrasted with the analogous non-fluorinated diarylboranes, **90** and **91**, reported by Lorberth and co-workers [70] (vide infra), in which boron apparently prefers to reside at an allylic locale.

The bis(indenyl)borate complex (**88**) has also been reported by Bochmann et al. [71]. Interestingly, the ^{1}H- and ^{13}C-NMR data reported for this species can be interpreted in terms of the presence of a single indenyl ring environment, suggesting the absence of diastereoisomerism. The alternative isomeric configuration (**89**), corresponding to the addition of indenyllithium to **85**, can be ruled out based on the observed 1:1:1 intensity ratio of the allylic (H(1)) and the two well-resolved vinylic (H(2), H(3)) resonances.

In 1997, Lorberth and coworkers [70] reported the synthesis and dynamic behavior of silicon- and boron-functionalized indenes. The disubstituted compounds (**90** and **91**) were generated in high yield as a 1:1 mixture, via quenching of $[C_9H_6SiMe_3]Li$ with Ph_2BBr at room temperature (Scheme 31). The analogous BX_2 compounds (X = Cl, Br) were also prepared by mixing $C_9H_6(SiMe_3)_2$ with an appropriate BX_3 precursor, albeit in lower yield and as a complicated mixture of isomers. The claim made by the authors that the mixture of **90** and **91** 'seems to be fluxional in solution', implies the interconversion of these species, though no dynamic NMR data were provided. The bis(η^1-indenyl) compounds (**92** and **93**), similarly prepared via anion quenching with the appropriate dichloroalkylborane, also appear to be quasi-fluxional. In the case of **92**, elementotropic rearrangements are proposed based solely on the complexity of the ^{1}H-NMR spectrum; for **93**, the authors claim that the observation of broadening in the H(1) region of the ^{1}H-NMR spectrum 'indicates some fluxionality of the $(Me_3Si)_3CB$ moiety'.

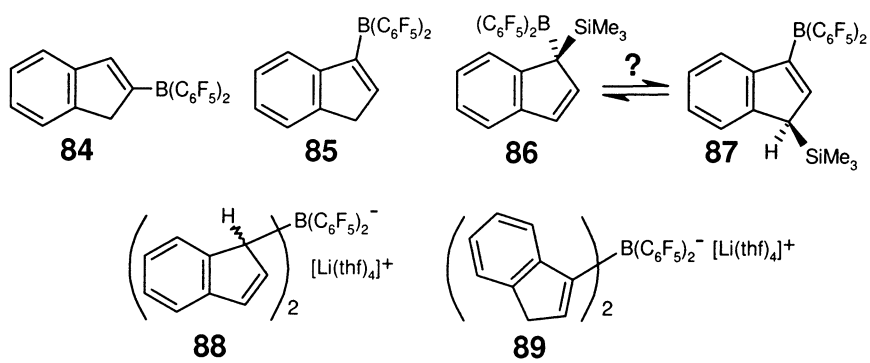

Scheme 30. Indenylboranes and borates containing pentafluorophenyl ligands.

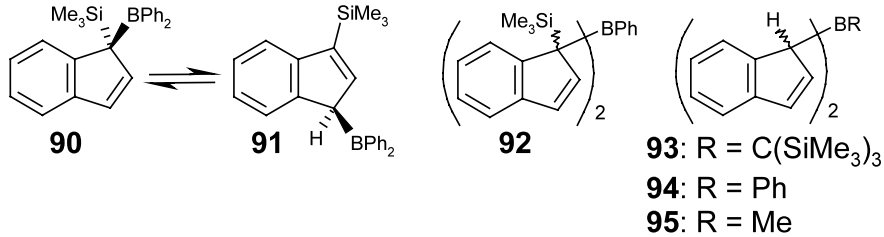

Scheme 31. A selection of mono(η^1-indenyl) and bis(η^1-indenyl)boranes.

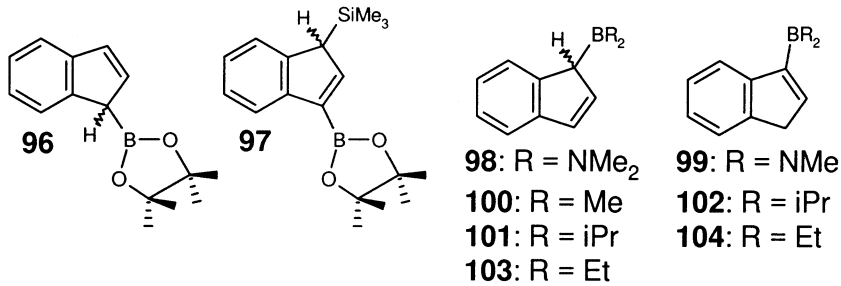

Scheme 32. Carbon, nitrogen, oxygen and silicon substituted indenylboranes.

In 1999, Reetz et al. [72] reported the synthesis of the bis(η^1-indenyl)borane, **94**, as a 1:1 mixture of *rac*- and *meso*-diastereoisomers in 75–85% yield from dichlorophenylborane and indenyllithium. Conversion of **94** into the thermodynamically favored bis(inden-3-yl) isomer (95% yield) was made possible by the addition of catalytic amounts of triisopropylphosphine.

Herberich and co-workers [73,74] have examined oxygen- and nitrogen-functionalized indenylboranes, and related transition metal derivatives (Scheme 32). The substituted indenes (**96** and **98**) were readily prepared via borylation of lithium indenide, while **97** was synthesized in ca. 80% yield by the reaction of the lithium indenide salt of **96** with chlorotrimethylsilane. In the case of **96**, only the allylic isomer was observed, even after distillative workup. In contrast, warming of **98** to temperatures above 0°C resulted in the rapid conversion of this kinetic product into the thermodynamically favored sp^2-isomer (**99**) in which the boron is attached to a vinylic site. These researchers accurately recognized that while the conversion of **98** to **99** could be rationalized in terms of [1,5]-hydrogen shifts, a base catalyzed process is more likely, given the apparently low barrier associated with isomerization in this system and the observed difference in behavior between the oxygen-functionalized borane (**96**) and the diamino compound (**98**).

Further studies by Herberich and co-workers involved an examination of the dialkylboranes (**100** and **101**). In keeping with the results detailed above, these sp^3-isomers were generated at low temperatures as the kinetic products, while treatment of **101** with triethylamine or pyridine gave rise to the sp^2-compound (**102**)

evinced by ^{1}H-, ^{11}B- and ^{13}C-NMR spectroscopic data. Interestingly, during the synthesis of **100**, the bis(indenyl)borane, **95**, was also identified as a minor component of the reaction mixture. The ^{1}H- and ^{13}C-NMR spectra of this minor product were assigned based on an approximate 1:1 mixture of C_2 and C_s isomers, with further support for this structural formulation coming from two-dimensional NMR experiments, as well as mass spectrometric studies.

More recently, Gridnev and Meller [75] synthesized the diethylborane (**103**) in 83% yield from indenyllithium and chlorodiethylborane. Based on 2D-EXSY NMR data obtained between 25 and 80°C, these workers provided an estimation of the activation energy associated with boron migrations in **103** ($E_a = 17.7 \pm 0.2$ kcal mol^{-1}). In consideration of the selectivity observed for sigmatropic rearrangements in related polyenyl-borane complexes, these workers propose a chemical exchange pathway involving [1,3]-boron shifts, which should proceed with inversion of configuration at the migrating boron center based on orbital symmetry considerations. Under ambient conditions, the transformation of **103** into **104** is rather slow, while at 100°C this isomerization process is rapid. After extended periods of time at elevated temperatures, **103** and **104** exist in equilibrium in a ratio of ca. 1:2.3; a small quantity of the corresponding C(2) isomer (analogous to **84** [69]) was also detected. Similarly, these authors noted that dissolution of **103** in perdeuteropyridine produced a 1:3.2:0.2 mixture of **103**, **104** and the aforementioned C(2) isomer, respectively.

In 1999, Braunschweig et al. [76] published a report pertaining to the synthesis and characterization of aminoborane derivatives of indene. Starting from the multiply bonded precursor, $(SiMe_3)_2NBCl_2$, the bis(η^1-indenyl)borane (**105**) was prepared as a mixture of diastereoisomers in 96% yield (Scheme 33). Interestingly, of the ^{1}H-, ^{11}B- and ^{13}C-NMR spectroscopic data obtained from samples of **105**, only the carbon data revealed the presence of the aforementioned isomeric mixture.

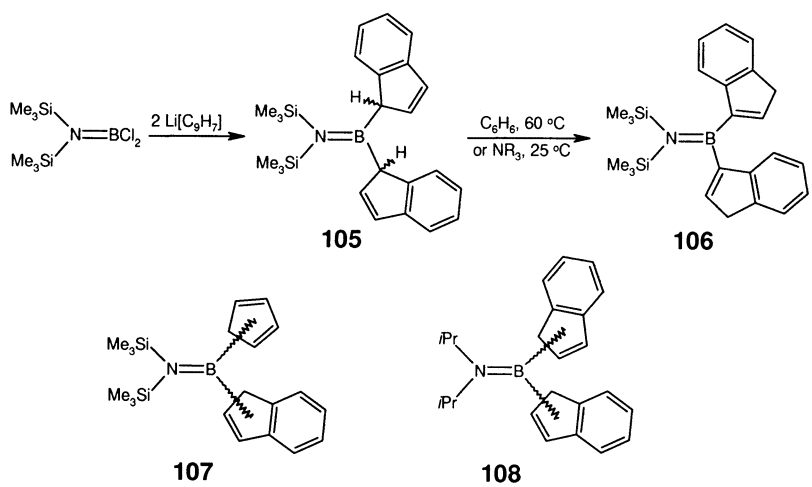

Scheme 33. Indenylboranes comprising amino functional groups.

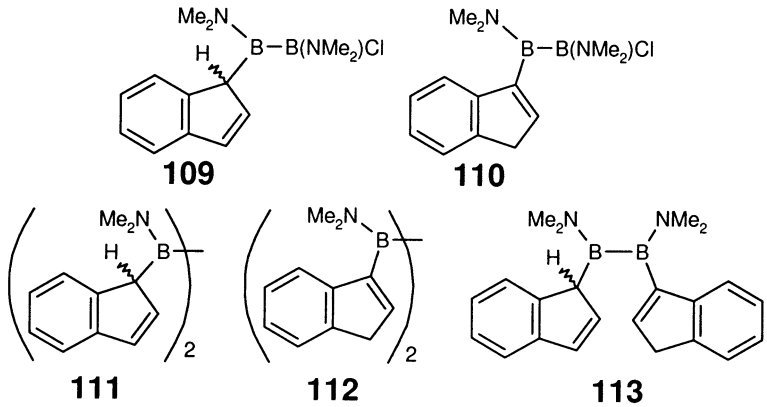

Scheme 34. Mono(η^1-indenyl) and bis(η^1-indenyl) diborane derivatives.

As is typical of 1*H*-inden-1-yl complexes of boron, conversion of **105** to the thermodynamically favored sp^2-bonded structure (**106**) was readily achieved in high yield by heating or via amine-catalysis. The structure of **106** was characterized by use of NMR spectroscopy and X-ray crystallography. In this report, Braunschweig et al. also detailed the in-situ generation of the mixed indenyl-cyclopentadienyl compound (**107**). Though not isolated, the formation of this species (possibly as a mixture of isomers) is inferred based on the subsequent generation of the corresponding zirconium and hafnium metallocene sandwich complexes.

In the same year, Ashe et al. [77] reported the use of the related boron-containing synthon, $(i\text{-Pr})_2NBCl_2$, in the high-yield preparation of the bis(indenyl)borane (**108**). This indenyl compound was generated as a mixture of double bond isomers, as evinced by the complexity of the ^{1}H-NMR spectrum obtained from samples of the isolated product.

Nöth and co-workers [78] examined the chemistry and molecular rearrangements of indenyldiboranes in 1998. The monoindenyl complex (**109**) was prepared in the usual manner via quenching of lithium indenide with the appropriate dichlorodiborane (Scheme 34). During distillative purification, this product was transformed into the sp^2-isomer (**110**). The corresponding bis(η^1-indenyl) complex (**111**) was prepared in an analogous manner by using half an equivalent of the dichlorodiborane. Although the B–C(1)indenyl connectivity in **111** is evident based on the ^{1}H- and ^{13}C-NMR spectral data provided, the authors fail to rationalize the complexity of these spectra, which are curiously assigned based on the presence of four unique indenyl ring environments in this product. In an attempt to interpret the multiple resonances present in these spectra, the authors allude to the possibility of hindered rotation about the boron–carbon bond in **111**, without acknowledging the potentially diastereomeric nature of the product. Indeed, the likely occurrence that **111** is actually generated as a mixture of C_s and C_2 isomers appears to have been overlooked, though the presence of such an isomeric mixture would not be expected to give rise to NMR spectra of such complexity. The X-ray crystallographic data

provided for **111** correspond to the homochiral diastereomer, which is presumably comprised of *RR* and *SS* enantiomers.

In the same report, Nöth and co-workers also discuss the thermal conversion of **111** into **112**, which proceeds via the spectroscopically and crystallographically characterized 'mixed' intermediate, **113**. Finally, in commenting on the viability of other synthetic routes to bis(η^1-indenyl)boranes, the authors state that the preparation of such complexes via substituent redistribution involving $B_2(NMe_2)_4$ is 'prevented simply by the access to tri(indenyl)borane, an as yet unknown triorganylborane', despite the fact that this precursor (**82**) had been described 25 years earlier by Mikhailov [67].

Following an early report by Zakharkin et al. [79] in which the reaction of $Ca(AlEt_4)_2$ and indene is described, Thiyagarajan et al. [80,81] provided what appears to be the only other examples of indenylalanes reported in the literature. These authors note that the addition of two equivalents of chlorodimethylalane to a solution containing $[Me_2Si(C_9H_6)_2]Li_2$ generates a mixture of air and moisture sensitive racemic diastereomeric products (**114**–**117**) (Scheme 35); recrystallization allowed for the isolation of **116**, which was characterized by X-ray crystallography. Based on temperature-dependent NMR data obtained from a mixture containing only **114** and **116**, Jordan and co-workers surmise that the interconversion of these products most likely occurs by way of sequential, suprafacial [1,5]-aluminum shifts, via the corresponding isoindene intermediate. At low temperatures (< -60°C), signals attributable to a 1:2 mixture of **114** and **116** were observed, and interconversion of these positional isomers was found to be slow on the NMR line-broadening time-scale; at room temperature, the isomerization process is rapid. After 3 days under ambient conditions, or after minutes at 70°C, solutions of **114** and **116** are transformed into a 1:1 mixture of *rac*- (**114** and **116**) and *meso*- (**115** and **117**) diastereomers. The generation of the *meso*-complexes is thought to occur by way of [1,5]-aluminum or [1,5]-silicon shifts, in combination with [1,5]-hydrogen shifts. In contrast, the interconversion of **116** and **117** may proceed by way of [1,5]-hydrogen shifts alone. Jordan and co-workers also observed that these complexes readily

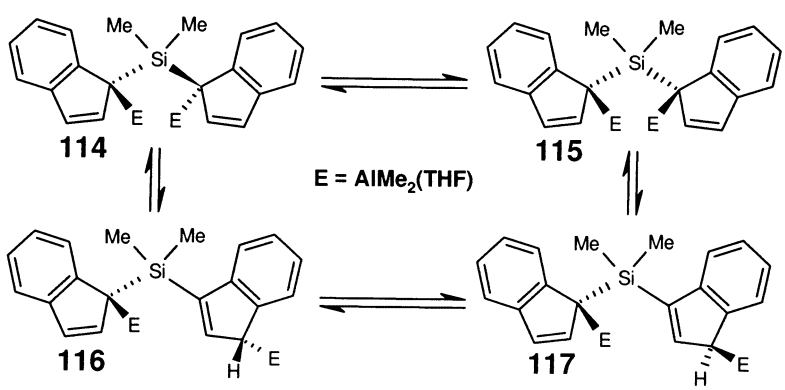

Scheme 35. An isomeric mixture of silicon- and aluminum-functionalized indenes.

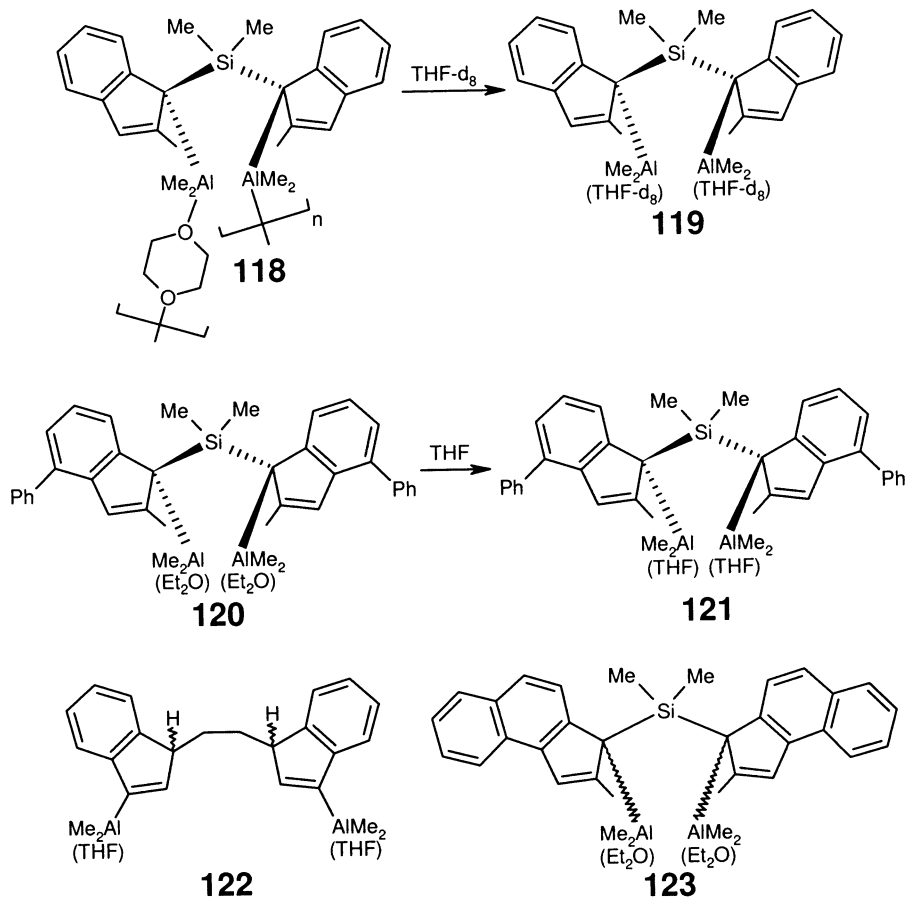

Scheme 36. Some structurally interesting aluminum-substituted indenes.

participate in aluminum-based ligand disproportionation reactions, under similar conditions for which diastereoisomerization is found. As a result, the *meso*/*rac* transformation depicted in Scheme 35 may be complicated by dissociative processes that make available intermolecular exchange pathways.

Jordan and co-workers [81] have synthesized other η^1-indenylalanes which are directly comparable to the aformentioned series. Starting from appropriately functionalized dianionic precursors, compounds **118** to **123** were prepared via addition of two equivalents of chlorodimethylalane in diethyl ether at 23°C (Scheme 36). The *rac*-polymeric product (**118**) was obtained in 41% yield following the addition of 1,4-dioxane, and was structurally characterized by use of single crystal X-ray diffraction techniques. This species rapidly undergoes ligand substitution with THF-d_8 at -90°C, resulting in the formation of **119** and the liberation of 1,4-dioxane. Unfortunately, **119** decomposes over the period of a day at ambient temperature, precluding an investigation of its rearrangement behavior.

In a similar manner, compound **120** is generated as a mixture of diastereomers in diethyl ether, though the corresponding tetrahydrofuran adduct, **121**, can be isolated in pure racemic form (62% yield) via solvent exchange. While no other isomers of this latter species can be detected below −90°C by use of NMR techniques, above room temperature **121** slowly isomerizes in the usual manner to a *rac*/*meso* mixture.

Compound **122** was also prepared in 54% yield by Jordan and co-workers [81] in diastereomerically pure form, though the stereochemistry of the product could not be ascertained by use of spectroscopic techniques. At 23°C in benzene-d_6, ca. 50% disproportionation/isomerization of **122** is observed after 2 days. The benzindene derivative (**123**) was prepared similarly as a colorless solid in 70% yield as a 2:1 mixture of *rac*- and *meso*-isomers. Recrystallization from a mixture of toluene and hexanes allowed for isolation of the pure racemic isomer, which was characterized by use of X-ray crystallography. In keeping with this η^1-indenylalane series, the low temperature ^{1}H-NMR spectrum of *rac*-**123** is entirely consistent with the solid state structure. As the sample is warmed, an equilibrium mixture of diastereomers is obtained, though isomerization is not accompanied by significant disproportionation.

Heavier Group 13 element indenyl derivatives have received only scant attention in the literature. In 1972, Poland and Tuck [82] reported on the preparation and spectroscopic characterization of $(C_9H_7)_3In{\cdot}Et_2O$, $Li[(C_9H_7)_4In]$ and $Li[(C_9H_7)_4In{\cdot}Et_2O]$. However, it is unclear whether these species exhibit averaged ^{1}H-NMR spectral features (reported at 35°C) owing to rapid structural rearrangements involving η^1-coordinated indenyl ligands, or as a result of static η^5-indenyl bonding configurations. Similarly, indenylthallium(I) has been reported by Garg and co-workers [83].

3.2. Group 14

Given the numerous carbon-functionalized indenes that have been reported to date, and that the free energies associated with sigmatropic shifts of the carbon fragments in these molecules are often too high to be detected by use of dynamic NMR techniques, a comprehensive summary of these molecules is beyond the scope of this review. As such, an overview of these compounds is restricted to a few noteworthy examples; Halterman [84] has recently published a detailed synopsis of indene functionalization.

In a series of papers spanning over 20 years, Jones and co-workers [85–87] examined the factors that affect the migration of alkyl groups in substituted indenes. As depicted in Scheme 37, the occurrence of a suprafacial [1,5]-alkyl group (R) shift in a substituted, optically active indene (**124**) yields the symmetrical isoindene (**125**). This phenomenon has been exploited by Jones and co-workers in examining two types of dynamic systems: For 'R' groups migrating more slowly than hydrogen, these alkyl shifts were monitored by the formation of C(2)-substituted indenes, as in **126**, while for 'R' substituents that undergo more rapid shifts, the loss of optical activity was used as a probe of the rearrangement process. In

addition to studying simple alkyl-substituted indene derivatives, the dibenz[e,g]indene system (**127**) has been employed by Jones and co-workers as a means of reducing the barrier to alkyl group shifts by enhancing the aromatic character of the migratory transition state species.

The capacity of the two fused benzo fragments in **127** to stabilize the corresponding isoindene is exemplified by the parent compound, cyclopenta[l]phenanthrene, **128**. A report by McGlinchey and co-workers [88] included the NMR spectroscopic and X-ray crystallographic characterization of the Diels–Alder adduct (**129**), a rare example of a thermally generated isoindene (**130**), trapped in situ by its progenitor (**128**) (Scheme 38).

The list of alkyl substituents that may be introduced into the indenyl framework appears to be limited only by the chemist's imagination; some intriguing examples

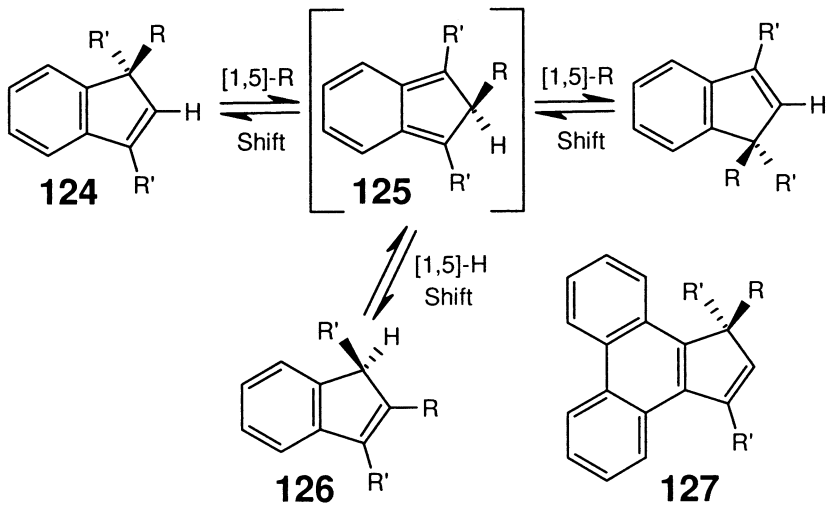

Scheme 37. Suprafacial, sigmatropic alkyl group and hydrogen atom shifts in substituted indenes, **124**; 'R'' is typically methyl or phenyl.

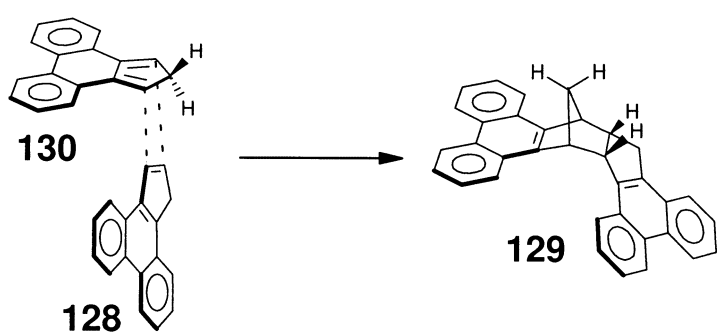

Scheme 38. Diels–Alder cycloaddition involving **128** and **130**, leading to the adduct, **129**.

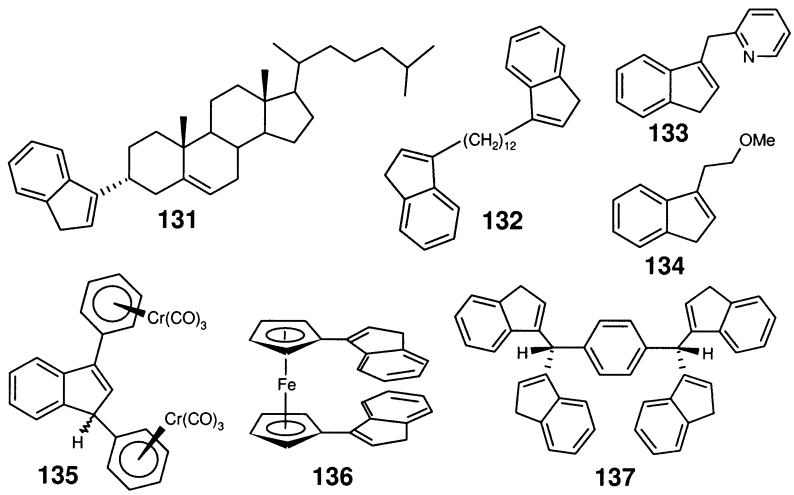

Scheme 39. A limited selection of interesting C(1) and C(3) substituted alkylindenes.

of such alkylindenes are presented in Scheme 39. Erker et al. [89,90] have prepared and crystallographically characterized the cholestenyl-substituted indene (**131**) and 1,12-bis(3-indenyl)dodecane (**132**) which were subsequently used in the preparation of zirconocene-based precatalysts. Similarly, the preparation of indenes bearing alkyl-tethered donor groups has attracted considerable attention because of their use in the preparation of 'constrained-geometry' catalysts [91]. Compounds **133** and **134** represent two of the growing number of indenyl derivatives containing pendant nitrogen [92] and oxygen [93] donors, respectively. Indenes containing pendant organometallic fragments are also known, including the binuclear chromium complex (**135**) [94,95] and the ferrocene derivative (**136**) [96]. A final compound worthy of mention is the crystallographically characterized tetra(indenyl)xylene (**137**) which was prepared by Mugnier and co-workers [97] by use of electrochemical methods.

The study of indenylsilanes dates back to 1951, when Sommer and Marans [11] reported the preparation and characterization of mono(η^1-indenyl)silanes, including **138**–**141**, and the bis(η^1-indenyl) complexes, **197**, **198** and **199** (Schemes 40 and 50, respectively). The synthetic methodology employed by these workers involved the quenching of sodium or lithium indenide with an appropriate alkylhalosilane; this general approach has proven to be the most efficient route to Group 14 derivatives of indene. In the case of the chlorosilanes (**140** and **141**), exchange of chloride for *n*-butoxide was realized by the addition of *n*-butanol, in the presence of pyridine.

The dynamics of indenylsilanes were first probed by Rakita and Davison [98] by use of variable-temperature NMR techniques. Based on the partial collapse of the H(1) and H(3) signals in the ^{1}H-NMR spectrum of **138** acquired at 180°C, and in light of the apparent quasi-fluxional behavior of the corresponding germanium and tin complexes (vide infra), the aforementioned indenylsilane was deemed stereochemically non-rigid.

In 1970, Larrabee and Dowden [42] reported their attempt to quantify the barrier to silicon migrations in **138**. Using the saturation transfer methodology developed by Forsén and Hoffman [99] Larrabee et al. noted that for experiments carried out at 150°C, saturation of the H(1) resonance of **138** resulted in a decrease in the intensity of the H(3) resonance, but not the H(2) signal. Since the relaxation processes in **138** were found to be fast in comparison to the exchange rate, these spectroscopic data allowed only for a maximum value of the activation energy of (ca. 29 kcal mol^{-1}) to be calculated. These workers also noted that silicon shifts must be significantly more rapid than hydrogen shifts in **138**, since the generation of vinylic isomers (**149** and **155**) was observed to be slow relative to the observed rate of chemical exchange between H(1) and H(3).

Larrabee and Dowden [42] also examined the mechanism of silicon migrations in **138** by use of Diels-Alder chemistry (Scheme 41). Given that the barrier to silicon shifts in this compound was considerably greater that that found for the cyclopentadienyl analogue, these workers postulated that isoindenes may mediate the observed interconversion of the H(1) and H(3) environments in **138**. In an attempt to probe for the presence of silicon-substituted isoindene intermediates in these migratory processes, an equimolar mixture of **138** and maleic anhydride was heated to 150°C. The product obtained from this reaction, following sulfuric acid methanolysis workup, yielded NMR spectroscopic data which implied the generation of the cycloadduct (**162**), and thus, the operation of a [1,5]-silicon shift process involving **138**. The role of orbital symmetry conservation in dynamic Group 14 η^1-indenyl systems was elegantly discussed in a subsequent report by Larrabee [100].

Related Diels–Alder adducts derived from dicyanomaleimide and TCNE were described by Ashe [43] in the same year. In addition to qualitatively alluding to the

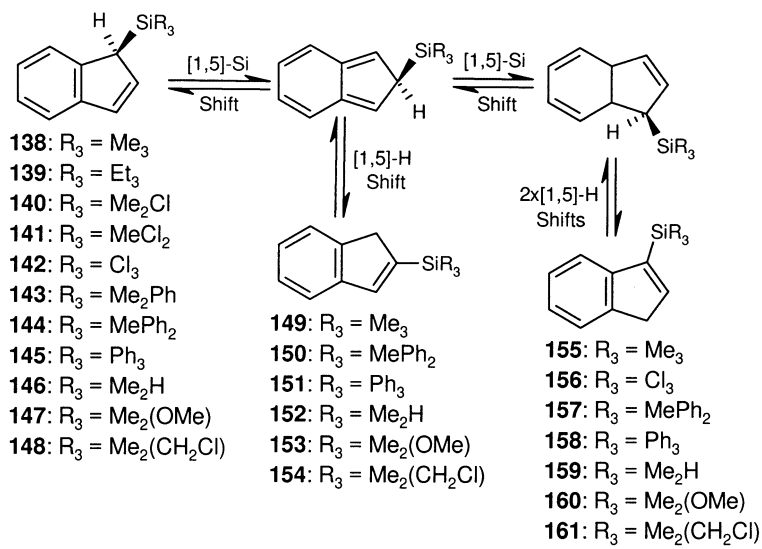

Scheme 40. Sigmatropic shift rearrangements involving simple indenylsilanes.

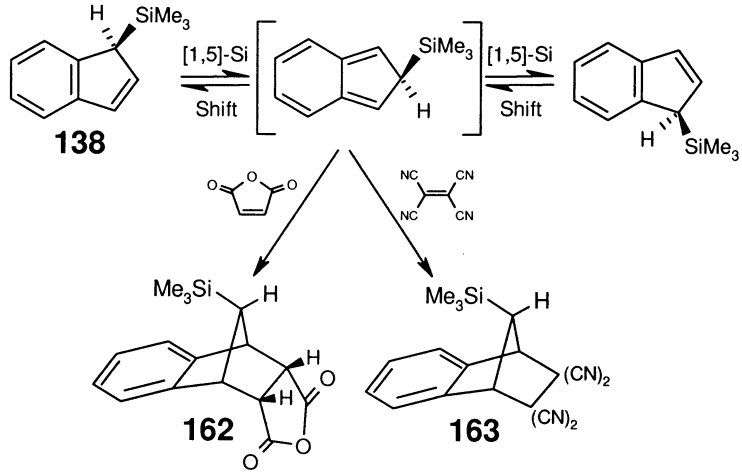

Scheme 41. Diels–Alder trapping of trimethylsilyl(isoindene) with maleic anhydride and tetracyanoethylene, yielding **162** and **163**, respectively.

intermediacy of isoindenes, treatment of **138** with a large excess of dienophile allowed the determination of temperature-dependent rate constants associated with [1,5]-silicon migrations in **138**, by use of dilatometric techniques. Analysis of these data permitted an estimation of the activation energy (E_a ca. 22.5 kcal mol^{-1}) for this migratory process. This value is in good agreement with the barrier (E_a ca. 22.4 kcal mol^{-1}) determined by Ustynyuk and co-workers [101] by use of variable-temperature ^{13}C-NMR techniques. Crystallographic evidence for the anti-orientation of the trimethylsilyl and dienophilic fragments in the TCNE derivative (**163**) was provided by Stradiotto et al. [102] in 1996.

In 1970, Davison and Rakita [103] published what is perhaps the most mechanistically insightful study pertaining to η^1-indenylsilane dynamics. These workers cleverly realized that while suprafacial [1,3]-silicon shifts in **164** would interconvert the *R* and *S* enantiomers of this compound (thus equilibrating the two halves of the indenyl framework), the trimethylsilyl groups in **164** would retain their magnetic non-equivalence. In contrast, a mechanism involving sequential [1,5]-silicon shifts would proceed via the symmetric isoindene intermediate (**165**) leading both to a permutation of the related indenyl environments and to chemical exchange of the trimethylsilyl groups. During the course of a variable-temperature NMR study, these authors noted that the silicon fragments in **164** were equilibrated on the NMR time-scale with the same barrier (E_a ca. 26 kcal mol^{-1}) as that associated with exchange between the H(1) and H(3) sites. This observation provided compelling evidence for a [1,5]-silicon shift mechanism in which both silicon groups reside temporarily at C(2) in the isoindene (**165**) as depicted in Scheme 42.

Davison and Rakita [103] provided a preliminary examination of silyl- and indenyl-based substituent effects on the rate of [1,5]-silicon migrations. Variable-temperature NMR data acquired for **143** (Scheme 40) clearly indicated chemical

exchange of the diastereotopic methyl groups at silicon. Comparison of these data to calculated spectra permitted an estimation of the activation energy for this process (E_a ca. 23 kcal mol^{-1}). The interconversion of the diastereotopic methyl groups in **143** is consistent with the generation of a symmetrical isoindene intermediate during the course of the suprafacial migratory process. Interestingly, the ^{1}H-NMR spectrum of the methyl-substituted compound (**169**) obtained at 160°C, was found to contain no significant amount of the related isomers, **170** and **171** (Scheme 43). The latter compound is the anticipated product of a sequential [1,5]-silicon shift process, and should be observable by use of NMR techniques, assuming that **169** and **171** are comparable in terms of thermodynamic stability. Attempts to study the molecular dynamics of the symmetrically substituted species,

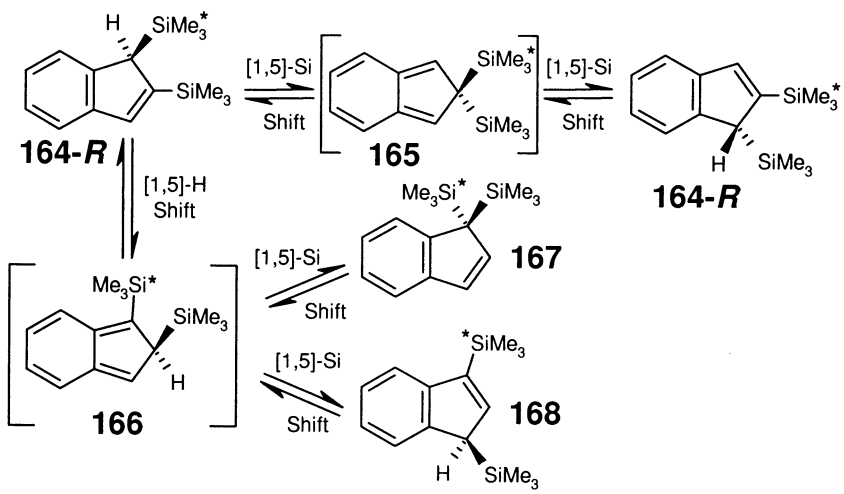

Scheme 42. Scrambling of the trimethylsilyl groups in **164**, due to [1,5]-silicon shifts; one silicon group is arbitrarily marked with an asterisk (*) to aid in monitoring its position throughout the various migratory processes.

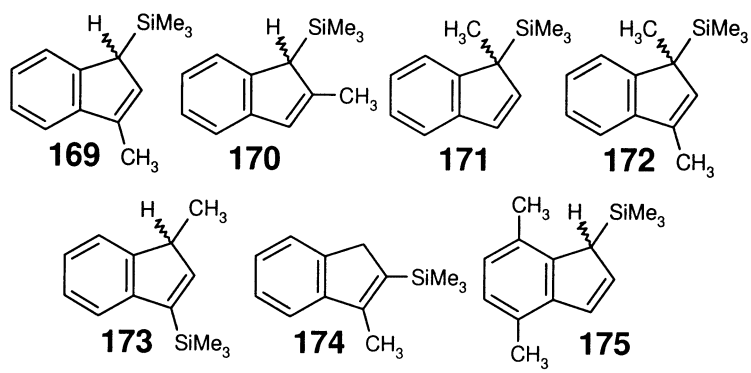

Scheme 43. Some η^1-indenylsilanes bearing methyl substituents.

172, were impeded due to difficulties in preparing this compound. However, the synthesis of **172** was eventually realized by Rausch and co-workers [104] in 1999, and studies pertaining to the molecular dynamics of this molecule were published by Stradiotto et al. [105] the following year (vide infra).

Andrews et al. [106,107] examined the effect of methyl substitution at the indenyl C(2), C(4) and C(7) positions on the rate of [1,5]-silicon shifts in η^1-indenylsilanes. Molecular orbital calculations conducted by these workers suggest that the smallest π-electron density occurs at C(4) and C(7) of the indenyl radical, while the electron density reaches a maximum at the C(2) position. As such, Rakita et al. proposed that alkyl substitution at C(4) and C(7) should stabilize the transition state species, whereas substitution at C(2) would have a destabilizing effect. In an attempt to test the validity of these computational results, the dynamics of **170** and **175** were studied by use of variable-temperature NMR spectroscopy. Indeed, using the coalescence temperature approximation method, the free energy of activation associated with [1,5]-silicon shifts in **170** ($\Delta G^{\ddagger}$ ca. 26.5 kcal mol^{-1}) was found to be larger than for the parent compound (**138**) ($\Delta G^{\ddagger}$ ca. 23.8 kcal mol^{-1}), while for **175** ($\Delta G^{\ddagger}$ ca. 21.8 kcal mol^{-1}) a lower barrier was calculated. Although there appears to be a real difference between the barriers associated with **170** and **175** ($\Delta G^{\ddagger}$ ca. 5 kcal mol^{-1}), it is unclear whether or not there is a statistically significant difference between **138** and either **170** or **175**. Moreover, the authors recognize that steric factors, in addition to electronic stabilization, may contribute to the observed free energy differential.

The thermal isomerization of η^1-indenylsilanes has been examined in considerable detail. Davison and Rakita [103] reported that prolonged heating (180°C) of solutions of **164** led to the formation of a mixture containing **164**, **167** and **168**, presumably via [1,5]-hydrogen shifts and the isoindene, **166** (Scheme 42). Spectroscopic identification of **167** and **168** was made possible by comparison with data obtained from a mixture ($\sim$ca. 1:1) of these compounds, rationally prepared via silylation of **138**. The synthesis of 1,1-bis(trimethylsilyl)indene (**167**) and 1,1-bis(triethylsilyl)indene, was originally described by Sommer and Marans [11]; however, in the absence of NMR data, these authors were unable to detect the existence of a 1,1- and 1,3-isomeric mixture.

The kinetics associated with this class of rearrangements were subsequently examined in a series of publications authored by Rakita and Taylor [108–110]. Throughout the course of their studies, these workers prepared and characterized numerous new indenylsilanes (**144**–**155**, **157**–**161**, **173** and **174**), and found that the equilibrium distribution of C(1), C(2) and C(3) isomers, but not the activation parameters, were sensitive to the nature of the substituents at silicon. This lack of substituent effect on [1,5]-silicon migrations in indenylsilanes is congruous with the corresponding cyclopentadienylsilanes [111].

In light of the seemingly insignificant effect that silicon substituents have on the rate of [1,5]-silicon migrations in indenylsilanes, McGlinchey and co-workers [112,113] endeavored to utilize the approach of Jones and co-workers [85–87] as a means of perturbing the indene-isoindene equilibrium. Computational studies carried out by these researchers at the semi-empirical level of theory suggested that the strategic incorporation of fused aromatic rings, as in **176**–**179**, should lead to a

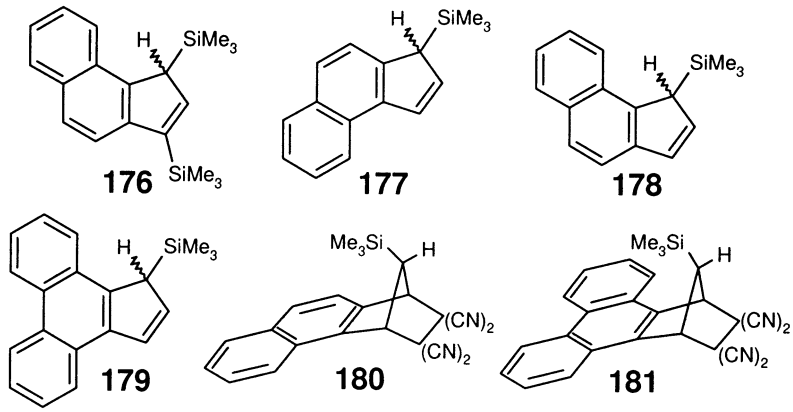

Scheme 44. Benzannulated indenylsilanes and the corresponding tetracyanoethylene cycloadducts.

reduced barrier for [1,5]-silicon shifts in these systems, presumably due to the enhanced aromatic character of the transition state species (Scheme 44). These predictions were validated by kinetic data obtained from 2D-EXSY and single selective inversion NMR experiments involving these compounds. The interconversion of **177** and **178** was found to proceed with a $\Delta G^{\ddagger}$ value of ca. 21.9 kcal mol^{-1}, while the incorporation of two fused benzo rings onto the indenyl framework, as in **179**, lowered the barrier even further ($\Delta G^{\ddagger}$ ca. 17.6 kcal mol^{-1}). In fact, the barrier to silatropic shifts in this latter molecule was reduced so significantly that the ^{1}H- and ^{13}C-NMR spectra obtained exhibited normal peak coalescence phenomena between 30 and 90°C. Further support for the occurrence of [1,5]-silicon shifts in these systems was provided through Diels–Alder trapping of the isoindene intermediates with TCNE, yielding **180** and **181**. Brintzinger and co-workers have also reported alkylated derivatives of **179** [114].

In 1998, Stradiotto, Brook and McGlinchey [115] examined the effect of introducing a dicobalt cluster adjacent to silicon, on the rate of silatropic shifts in η^{1}-indenylsilanes. These workers postulated that based on the conceptual model put forth by Epiotis and Shaik [116], it is plausible to envisage the development of positive charge at the migrating silicon center during the course of suprafacial [1,5]-silicon shifts in indenylsilanes, given the potential for the indenyl moiety to behave as an 'intrinsic acceptor' by generating a transition state with 10π aromatic character. It was therefore anticipated that the alleviation of positive charge by the neighboring dicobalt fragment [117] in **183** (Scheme 45) would be reflected in a somewhat reduced barrier for [1,5]-silicon shifts. The stereochemically non-rigid nature of both the alkynylsilane (**182**) and the corresponding dicobalt derivative (**183**) was ascertained by use of 2D-EXSY NMR techniques, while for **182**, single selective inversion ^{1}H-NMR experiments yielded $\Delta G^{\ddagger}$ ca. 24 kcal mol^{-1} for this rearrangement process. At the elevated temperatures required for the acquisition of rate data, compound **183** showed significant decomposition and so a reliable estimate of the migratory barrier could not be obtained. However, under similar

experimental conditions, these workers noted that the relative intensities of the cross-peaks in the $^1H-^1H$ EXSY spectra of **182** and **183** were qualitatively similar, suggesting only a marginal difference in the exchange rates in these two systems. Qualitative evidence for the intermediacy of isoindenes in the molecular rearrangements of **182** and **183** was obtained by conducting TCNE trapping experiments similar to those employed by Ashe [43]; cycloaddition products analogous to **163** [102] (Scheme 41) were obtained from reactions involving either **182** or **183**. The adduct derived from the latter was characterized by use of X-ray crystallography, which revealed that the dienophile (TCNE) attacked the face opposite to that occupied by the dinuclear cluster.

In continuation of their examination of the factors that influence the rate [1,5]-silicon shifts in η^1-indenylsilanes, Stradiotto et al. [105] endeavored to study the molecular dynamics of related η^6-$Cr(CO)_3$ derivatives. Treatment of **138** with hexacarbonylchromium at elevated temperatures led not to the formation of the desired complex (**184**), but rather to the corresponding 3-indenyl isomer (**185**), for which [1,5]-silicon migrations are not directly viable. The ^1H- and ^{13}C-NMR signals attributable to the methylene group and the single vinylic methine unit proved to be particularly diagnostic of the structure depicted in Scheme 46. The generation of **185**, that is formally the tricarbonylchromium complex of **155** (Scheme 40), can be rationalized in terms of two consecutive [1,5]-hydrogen shifts that become possible at the high temperatures employed in the synthesis. The authors were unable to comment as to whether this rearrangement occurs in the precursor (**138**) in the complex (**184**) or via some bimolecular chromium-mediated reaction pathway.

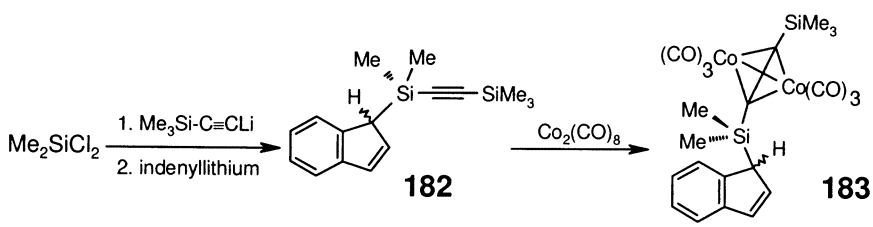

Scheme 45. The synthetic route to the alkynyl-substituted η^1-indenylsilanes (**182** and **183**).

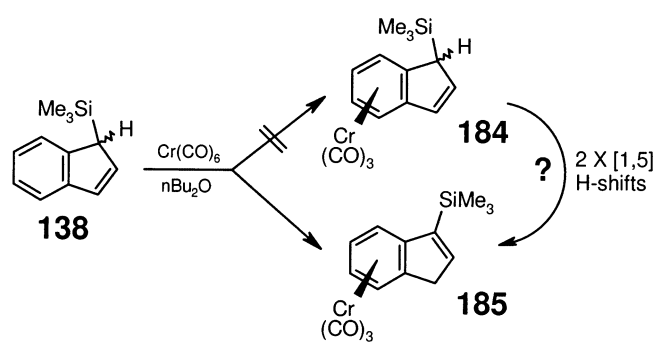

Scheme 46. Unexpected generation of the η^6-$Cr(CO)_3$ complexed indenylsilane (**185**).

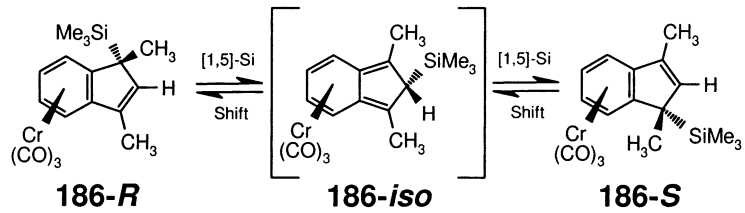

Scheme 47. Molecular rearrangements involving the chromium-complexed η^1-indenylsilane (**186**).

Alternatively, complexation of the dimethylindenylsilane (**172**) was selected by these researchers as a means of generating a chromium-containing η^1-inden-1-ylsilane, since the barrier to [1,5]-methyl shifts is considerably higher than that associated with hydrogen migrations. Using the aforementioned synthetic approach, **172** and excess $Cr(CO)_6$ were allowed to react at elevated temperatures, yielding a single chromium-containing complex (**186**) (Scheme 47). That the product contained the required C(1)-bonded trimethylsilyl unit was confirmed by use of NMR spectroscopy; the *exo*-geometry of **186** was ultimately demonstrated by use of X-ray crystallography. The molecular dynamics of **186** were qualitatively examined by these workers using 2D-EXSY NMR techniques, while an analysis of the temperature-dependent rate data obtained from single selective inversion ^{1}H-NMR experiments revealed the barrier to silicon shifts in **186** ($\Delta G^{\ddagger}$ ca. 24 kcal mol^{-1}) to be indistinguishable from the uncomplexed silane (**172**) ($\Delta G^{\ddagger}$ ca. 23 kcal mol^{-1}). The fact that the presence of the chromium fragment served neither to increase nor diminish the rate of [1,5]-silicon shifts was unexpected, and is a testament to the robust nature of the [1,5]-silicon shift process in η^1-indenylsilanes. Treatment of **172** with TCNE led to the formation of the anticipated cycloaddition product, whose crystallographically determined structure directly resembles that of the related cycloadduct (**163**) [102] (Scheme 41). No chromium-containing adduct was isolated from analogous TCNE trapping experiments involving **186**.

Indenylsilanes appearing as part of larger polycyclic molecular arrays have been reported in the literature (Scheme 48). Youngs and co-workers [118–120] demonstrated that the geometrically constrained bis(trimethylsilyl)dibenzo[a,f]-fulvalene (**188**) can be readily prepared via oxidative coupling of the dianion derived from **187**, by using Group 13 metal halides. Coupling of the monoanion obtained from **187** instead generated the helical dimeric species, **189**. In 1996, Olmstead et al. [121] discussed the unexpected generation of **190**, in their attempt to generate an *ansa*-titanocene compound. Four years later, McGlinchey and co-workers [105] reported the synthesis of the silicon-functionalized dibenzofulvalene, **192**, in 68% yield from a mixture of the *meso* and D,L isomers of **191**. Compounds **187**–**190** and **192** were all characterized by use of single crystal X-ray diffraction techniques.

The aforementioned utility of heavier Group 14 element η^1-indenyl derivatives in metallocene pre-catalyst development has brought about renewed interest in this field of study. Chart 1 depicts the exponential growth in the number of publications pertaining to indenylsilanes, related derivatives and corresponding metal complexes,

over the past decade[3]. Indeed, an attempt to exhaustively document each and every derivative from within this burgeoning field would be an onerous task, one that falls outside of the mandate of this survey. Some intriguing silicon-based examples from the recent literature include both aminoalkyl- and methoxy-substituted η^1-indenylsilanes, such as **193** (Scheme 49), that were prepared by Rausch and coworkers [122,123] for use in the generation of trichlorotitanium-based catalyst precursors. Similarly, Okuda and co-workers [124,125] have employed successfully nitrogen-functionalized silicon complexes, including **194** and **195**, in the preparation of 'constrained-geometry' metal catalyst precursors. Equally interesting is the carborane-containing η^1-indenylsilane (**196**) reported by Xie and co-workers [126,127].

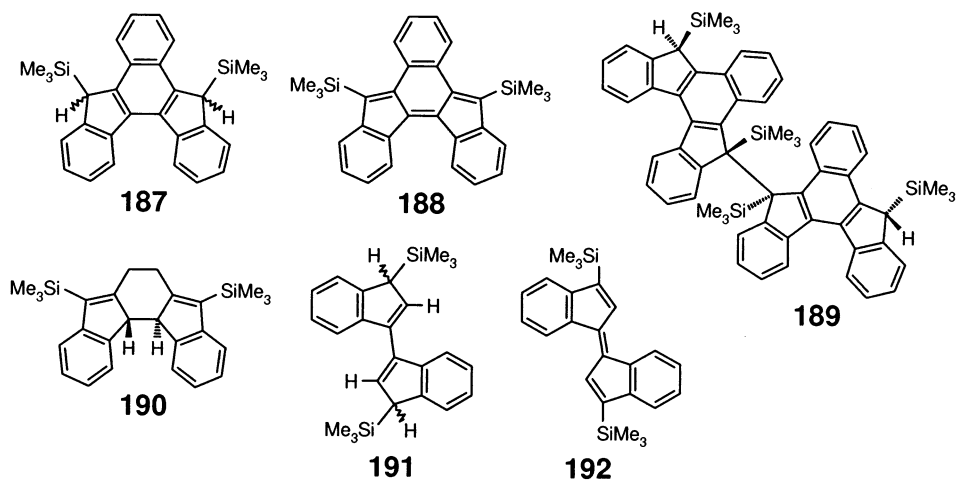

Scheme 48. Indenylsilanes comprising a portion of larger polycyclic molecules.

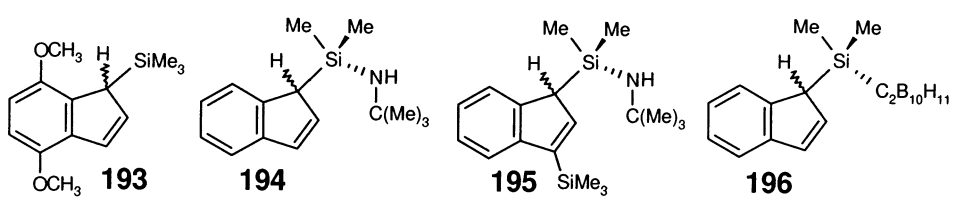

Scheme 49. η^1-lndenylsilanes bearing alkoxy, amido and carboranyl groups.

[3] Publications include academic, patent or otherwise.

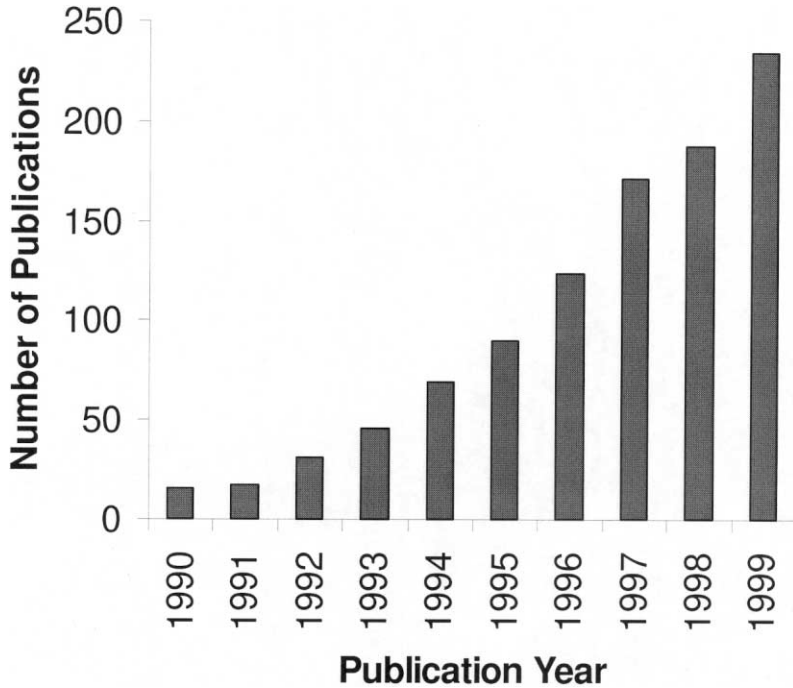

Chart 1. Growth in the number of publications pertaining to indenylsilanes, related compounds and their metal derivatives over the past decade.

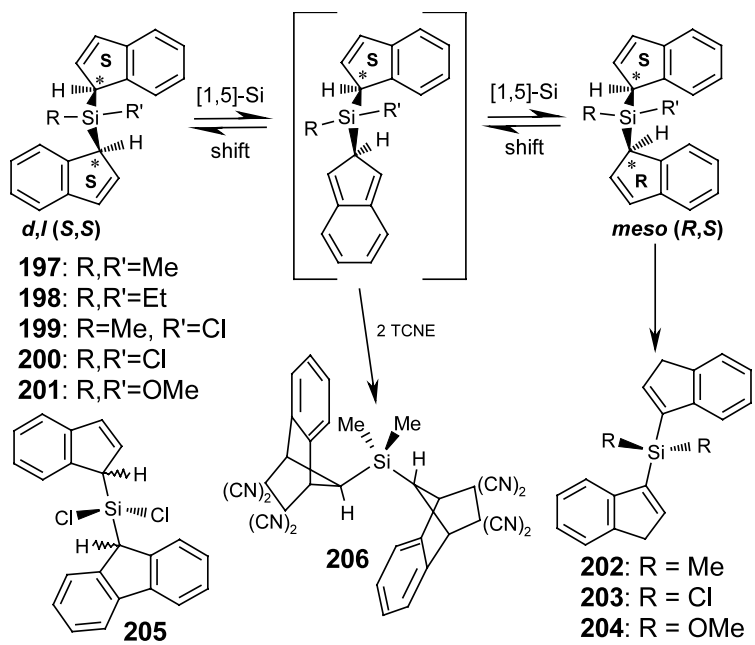

Scheme 50. Sigmatropic shifts and cycloaddition chemistry, involving bis(η^1-indenyl)silanes.

More than 40 years after Sommer and Marans [11] first reported on the preparation of poly(η^1-indenyl)silanes, Rausch and co-workers [128] published the synthesis and characterization of the indenylsilanes (**142**, **156** (Scheme 40) and **205**) and the bis(η^1-indenyl)silanes (**200**–**204**) (Scheme 50). An important facet of this study involved an examination of the molecular dynamics of bis(η^1-indenyl)silanes, by use of variable-temperature NMR spectroscopy. In the case of **197**, the *meso*-isomer (C_s symmetry) contains two magnetically non-equivalent silyl–methyl groups, while the C_2 symmetry of the racemic compound renders these methyl groups magnetically equivalent. Additionally, though the pairs of indenyl ligands within each of these C_s and C_2 isomers are equivalent, each diastereomer exhibits unique indenyl ^{1}H- and ^{13}C-NMR chemical shifts.

The molecular dynamics of **197** (and similarly **200** and **201**) were studied by Rausch and co-workers [128] by monitoring the conversion of a pure sample of the D,L (racemic) isomer (isolated by crystallization) into a mixture containing both diastereomers. At temperatures above 110°C, the authors noted that the ^{1}H-NMR methyl resonances attributable to the two diastereomers began to broaden; coalescence phenomena at higher temperatures were not explored due to instrumental limitations. In an attempt to extract additional kinetic data below this temperature, an alternative methodology was employed in which a pure sample of the *rac*-isomer was maintained at a given temperature for ca. 15 min, and the measured intensity ratio of the *rac* to *meso* methyl resonances was taken as the equilibrium constant (K_{eq}) at that temperature. Based on the temperature-dependent K_{eq} data obtained from these experiments, Rausch and co-workers proposed that the isomerization of **197** occurs by way of a concerted, intramolecular [1,3]-silicon shift pathway below 110°C, with some other 'fluxional process' (presumably [1,5]-silicon shifts) being operative at higher temperatures.

Troubled by the claim of Rausch and co-workers that the aforementioned bis(η^1-indenyl)silanes are 'not fluxional up to 110°C' [128], and concerned by the proposal of [1,3]-silicon shifts involving **197** at low temperatures, McGlinchey and co-workers [129] reinvestigated the dynamics of this system in 1995, by use of 2D-EXSY and single selective inversion NMR techniques. Using these methods, McGlinchey and coworkers were able to monitor and obtain temperature-dependent rate constants, rather than equilibrium constants, for the interconversion of the *rac*- and *meso*-isomers of **197**, even at temperatures below which this dynamic process is too slow to induce significant NMR line broadening. Moreover, these workers demonstrated successfully that kinetic data obtained between 47 and 107°C are fit by a single dynamic process, and yield $\Delta G^{\ddagger}$ ca. 24 kcal mol^{-1}. Using the TCNE trapping methodology of Ashe [43], McGlinchey and co-workers were successful in generating the double Diels–Alder adduct (**206**) (Scheme 50), via treatment of **197** with two equivalents of TCNE.

Additional evidence for the intermediacy of isoindenes in dynamic processes involving **197** was subsequently provided by Jordan and co-workers [130], who described the synthesis and X-ray structure of a novel C_1-symmetric *ansa*-hafnocene [$Me_2Si(\eta^5$-1-indenyl)(η^3-2-indenyl)]$Hf(NMe_2)_2$ (**209**) in which one of the indenyl

moieties is bridged to the silicon center through the indenyl C(2) position (Scheme 51). Jordan rationalized the formation of **209** as resulting from the intramolecular elimination of dimethylamine from the isoindene **208**, which is formed as a result of a single [1,5]-silicon shift of the $Me_2Si(\eta^5$-1-indenyl)$Hf(NMe_2)_3$ unit about the periphery of the uncoordinated indenyl ring in **207**. The intramolecular 'trapping' of the isoindene fragment in **208** strongly supports the viability of intermolecular [4 + 2] cycloadditions involving thermally generated isoindenes and electron-deficient dienophiles.

The industrial relevance of silicon-bridged ansa-metallocene has led to an explosive growth in this field of chemistry; the parent compound, bis(η^1-indenyl)dimethylsilane (**197**) and related species have even become commercially available reagents. Given the ease with which one can modify the indenyl framework, it is not surprising that a myriad of bis(η^1-indenyl)silanes exist [84]. Some unique examples are highlighted in the following sections.

Brintzinger and co-workers [131,132] have synthesized a series of interesting fused-ring derivatives of bis(η^1-indenyl)dimethylsilane (**197**) for use as ligands in the development of metallocene pre-catalysts. Starting from the appropriate benz[e]indene precursors, the silanes (**210** and **211**) were prepared in 36 and 49% yield, respectively. Compound **212**, a saturated derivative of **211**, was also generated successfully from 2-methyltetrahydrobenz[e]indene, while **213** was synthesized in 22% yield from a mixture of 1H- and 3H-cyclopenta[c]phenanthrene. It is interesting to note that although the expected statistical mixture of *meso*- and *rac*-isomers is observed for each of compounds **210**–**213**, only species possessing the 'outside' geometric configuration depicted in Scheme 52 are observed. Perhaps heightened steric constraints in these compounds prevent isomerization phenomena

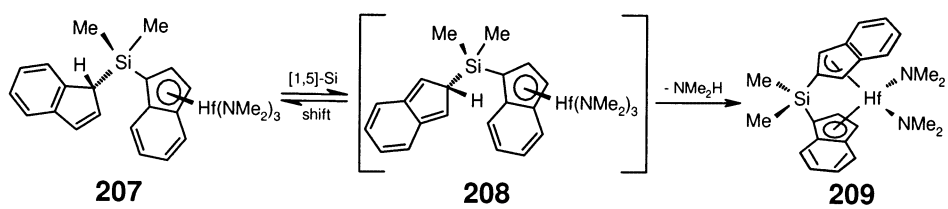

Scheme 51. Intramolecular trapping of an isoindene at a hafnium center.

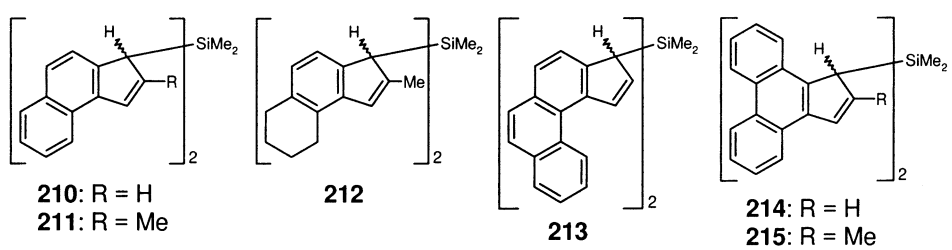

Scheme 52. Some benzannulated bis(η^1-indenyl)silanes.

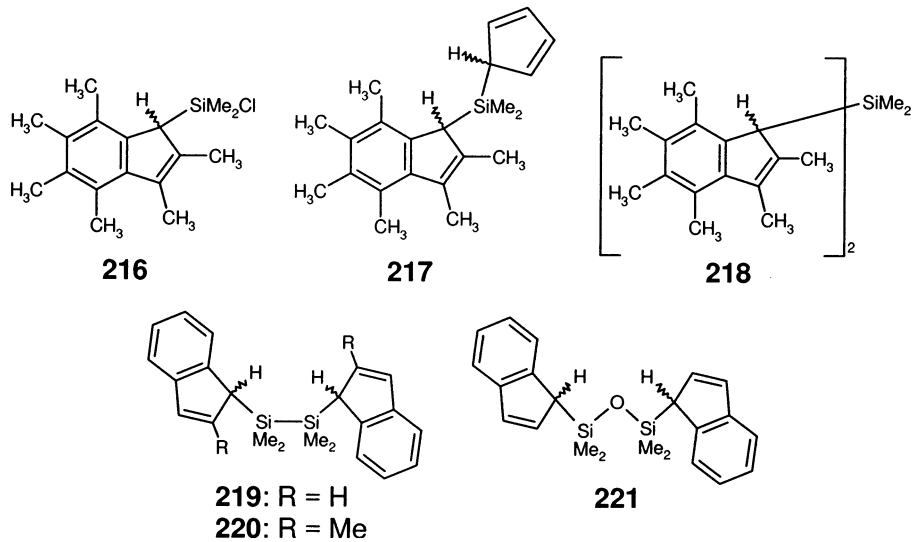

Scheme 53. A selection of structurally interesting η^1-indenylsilanes.

analogous to those that have been studied by McGlinchey and coworkers [112,113] in the related mono(η^1-indenyl)silane system, **177**/**178** (Scheme 44). Brintzinger and co-workers have also synthesized the cyclopentalphenanthrenyl complexes, **214** and **215**, the former of which is the bis(η^1-indenyl)silane analogue of **179** (Scheme 44).

O'Hare and co-workers [133,134] have prepared silanes derived from C_9Me_6H, a close analogue of the ubiquitous 'Cp*' ligand. With the ultimate goal of making benzannulated [1]-ferrocenophanes, these workers initially combined [$C_9Me_6H^-$] with one equivalent of dichlorodimethylsilane, generating the chlorosilane (**216**) in 66% yield (Scheme 53). Reaction of this compound with sodium cyclopentadienide in the usual manner led to the cyclopentadienyl derivative (**217**), though higher yields were realized when magnesocene was used as the source of [$C_5H_5^-$] (91 vs. 60%). The bis(η^1-indenyl)silane (**218**) was prepared in an alternative manner, via addition of $SiCl_4$ to two equivalents of lithium hexamethylindenide, followed by quenching with MeLi. Compound **218** is generated as a mixture of diastereomers, which differ with respect to solubility and capacity for lithiation. The *meso*-isomer of **218** is markedly more soluble than *rac*-**218**, and is readily converted to the corresponding dilithio species via treatment with *n*-butyllithium in the presence of tetramethylethylenediamine. In contrast, these workers were unable to cleanly generate the doubly deprotonated salt of *rac*-**218**.

Disilane η^1-indenyl compounds were reported by Spaleck et al. [135] in 1990, and later by Knjazhanski and co-workers [136]. Alkylation of dichlorotetramethyldisilane with an appropriately functionalized indenyllithium reagent yielded either **219** or **220** (82 and 68%, respectively) as crystalline solids (Scheme 53). Synthetic routes to the disilane (**219**) and the disiloxane (**221**) were also provided by Jin et al. [137].

Soga and co-workers [138–141] have demonstrated that bis(indenyl)silanes can even be incorporated into the backbone of polymeric materials, which subsequently can be utilized as supports for metallocene pre-catalysts.

The molecular dynamics and reactivity of tris(η^1-indenyl)silanes have been detailed in a series of reports by Stradiotto et al. [102,142,143]. Compounds **222**–**224** were prepared by quenching of an appropriate trichlorosilane with excess of indenyllithium, while the hexylsilane (**225**) was generated via hydrosilylation of 1-hexene with **224** (Scheme 54). In solution, these species exist as a statistical (1:3:3:1) mixture of interconverting isomers, as evinced by NMR spectroscopic data. The ^{1}H- and ^{13}C-NMR spectra of these species contain four equally intense resonances in each of the C(1)–H(1), C(2)–H(2) and C(3)–H(3) regions; two silicon peaks (1:3) are observed in the ^{29}Si-NMR spectra of these compounds. The connectivity between the various ^{1}H-, ^{13}C- and ^{29}Si-NMR signals within each of the four individual indenyl ring environments was ascertained by use of ^{1}H-, ^{13}C- and ^{29}Si one- and two-dimensional NMR spectroscopic techniques. Moreover, the assertion that all three of the indenyl ligands in these molecules bond to the silicon center through the indenyl C(1) carbon was validated by X-ray crystallographic data obtained for **224** [143].

These researchers qualitatively probed the molecular dynamics of compounds **222**–**224** by use of 2D-EXSY NMR; the development of off-diagonal cross-peaks between both the Si–R and indenyl ring environments clearly indicated the operation of a dynamic process. McGlinchey et al. also noted that the observed

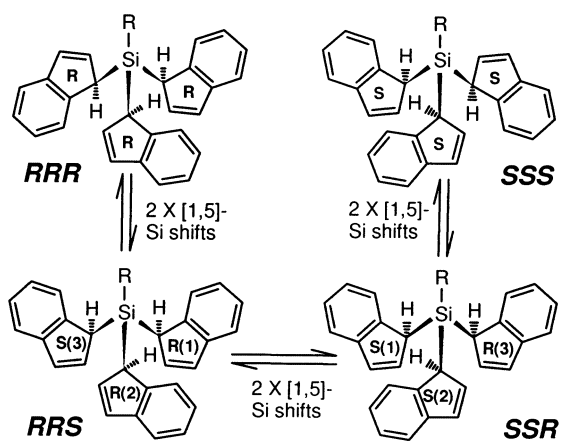

222: R = Me
223: R = $CH_2CH{=}CH_2$
224: R = H
225: R = $(CH_2)_5CH_3$

Scheme 54. Interconversion of the eight different indenyl ring environments in the *RRR*, *RRS*, *SSR* and *SSS* isomers of tris(η^1-indenyl)silanes. The '*R*' or '*S*' designations refer to the absolute configuration at C(1) in each indenyl ring environment.

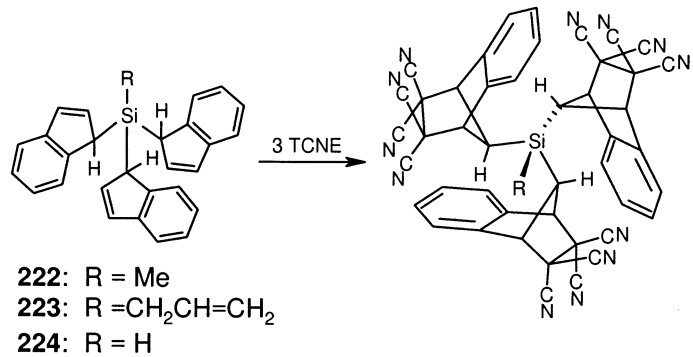

Scheme 55. Triple Diels–Alder cycloaddition reactions involving tris(η^1-indenyl)silanes.

chemical exchange routes linking both indenyl sites (H(1) and H(3)) and ring environments (*RRR*/*SSS* and *RRS*/*SSR*) were congruent with the stereochemical consequences associated with the operation of a sequential, suprafacial [1,5]-silicon shift process. Indeed, it was demonstrated that the allowed indenyl environment exchange pathways in tris(η^1-indenyl)silanes are readily mapped onto a hypercube [102]. Temperature-dependent single selective inversion NMR experiments yielded quantitative rate data, and ultimately a $\Delta G^{\ddagger}$ value of ca. 24 kcal mol^{-1} for silatropic shifts in molecules **222**–**224**.

In an attempt to gain further support for the operation successive [1,5]-silicon shifts in tris(η^1-indenyl)silanes, Stradiotto et al. [102,142,143] explored the cycloaddition chemistry of these molecules (Scheme 55). The products obtained after allowing either **222**, **223** or **224** to react with three equivalents of TCNE yielded NMR spectroscopic, mass spectrometric, and in some cases, X-ray crystallographic data consistent with the formation of the corresponding triple [4 + 2] Diels–Alder adducts.

Indenyl complexes of the heavier Group 14 elements have also been prepared and their dynamics examined. In 1969, Davison and Rakita [98] studied the behavior of trimethylgermyl- and trimethylstannylindene, **226** and **228**, respectively, by use of variable-temperature NMR (Scheme 56). As alluded to in the foregoing discussion of indenylsilane dynamics, these germanium and tin complexes are stereochemically non-rigid, as evidenced by the collapse of the H(1) and H(3) signals in the ^{1}H-NMR spectra of these compounds at elevated temperatures; NMR line-shape changes in the aromatic region are also indicative of an overall C(1) to C(3) migratory process. In keeping with the trend of diminishing migratory barriers upon descending the p-block [111], the ^{1}H-NMR spectral features observed for **138** at 180°C are evident for **226** between 134°C and 149°C, while for the tin complex (**228**), Davison and Rakita were able to observe the complete range of limiting low- to limiting high-temperature spectra. At temperatures below −37°C, the ^{1}H-NMR spectrum of **228** is consistent with a 'static' η^1-indenyl structure, as depicted in Scheme 56. As the sample is warmed, the H(1) and H(3) protons broaden in the usual manner, with complete collapse observed at 49°C. Above 140°C, the averaged 'dynamic'

^{1}H-NMR spectrum is observed for **228**. The persistence of tin-hydrogen coupling between the methyl hydrogen atoms and the tin center in **228** over the entire temperature range points to an intramolecular rearrangement process.

An additional facet of the aforementioned study published by Ustynyuk and co-workers [101], involved an examination of the dynamics of **226** and **228** by use of variable-temperature ^{1}H- and ^{13}C-NMR techniques. In the case of the η^{1}-indenylgermane (**226**), spectroscopic information obtained from ^{13}C-NMR experiments yielded a barrier to germanium shifts (E_a ca. 18.4 kcal mol^{-1}; $\Delta G^{\ddagger}_{300}$ ca. 21.8 kcal mol^{-1}) which is comparable to an earlier estimate of the activation energy (E_a ca. 22 kcal mol^{-1}) reported by Larrabee and Dowden [42]. Similarly, ^{13}C-NMR data were utilized by Ustynyuk and co-workers [101,144] in determining the barrier to tin migrations in the indenylstannane (**228**) (E_a ca. 12.7 kcal mol^{-1}; $\Delta G^{\ddagger}_{300}$ ca. 15.2 kcal mol^{-1}). The increased barrier to metallotropic shifts in these heavier Group 14 indenyl complexes, in comparison to their cyclopentadienyl analogues, was rationalized by Ustynyuk and co-workers in terms of the formation of an energetically unfavorable, short-lived isoindene intermediate during the migratory process. In an effort to fortify this proposal, **226** was reacted with TCNE, maleic anhydride and dimethyl acetylenedicarboxylate, yielding the Diels–Alder cycloadducts, **233**, **234** and **237**, respectively (Scheme 56). In contrast, these workers found that analogous reactions involving the indenylstannane (**228**) resulted in tin–indenyl bond cleavage, accompanied by the generation of ill-defined products containing both the dienophile and the trimethyltin fragment. These latter results

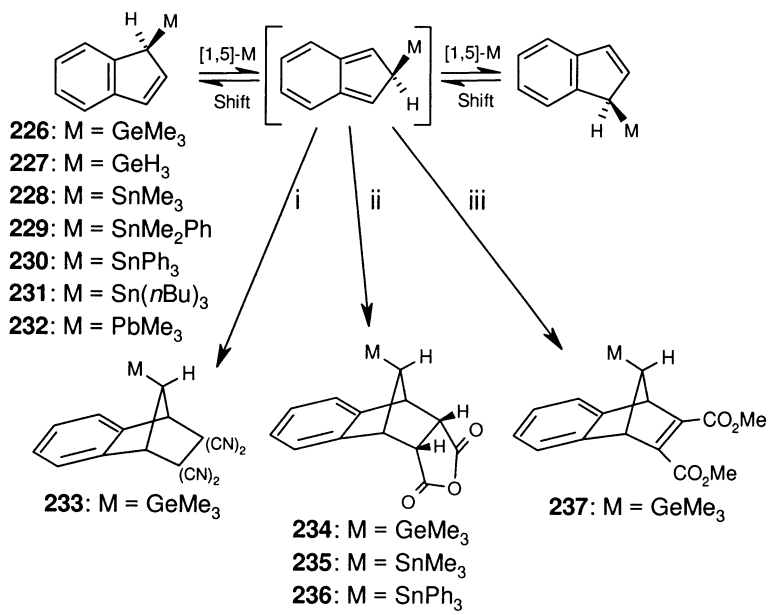

Scheme 56. Sigmatropic migrations and Diels–Alder cycloaddition chemistry of germanium- and tin-substituted indenes (i, tetracyanoethylene; ii, maleic anhydride; iii, dimethyl acetylenedicarboxylate).

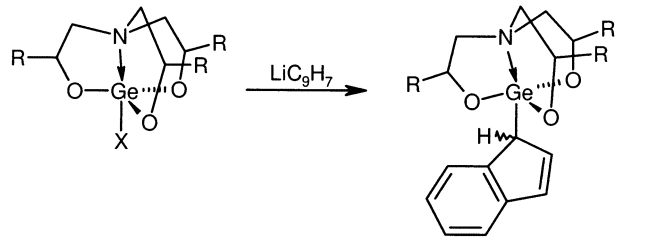

Scheme 57. Synthesis of the η^1-indenylgermatranes (**238** and **239**).

contradict findings published a year earlier by Rakita and Taylor [109], who provided NMR spectroscopic and mass spectrometric evidence in support of the [4 + 2] cycloadduct (**235**) and who referred to a report [145] in which the generation of **236** (presumably derived from **230**) is claimed. The isolation of such Diels–Alder adducts of germanium and tin qualitatively supports the proposal of a [1,5]-metalloid shift mechanism involving these heavier Group 14 compounds. Ustynyuk and co-workers [146] have also examined the dynamic behavior of the η^1-indenyl lead species, **232** (Scheme 56); the barrier to lead shifts in this compound was calculated based on variable-temperature NMR data ($\Delta G^{\ddagger}$ ca. 13.9 kcal mol^{-1}).

The synthesis, structure and dynamic behavior of the η^1-indenylgermane (**227**) were examined by Angus and Stobart [147] in 1973. These authors noted that between 175 and 195°C, ^{1}H-NMR signals attributable to the indenyl C_5 hydrogen atoms in **227** partially coalesce, corresponding to the onset of chemical exchange on the ^{1}H-NMR time-scale. Further measurements at higher temperatures proved impossible due to instrumental limitations, and so quantitative kinetic data were not provided. In addition to these variable-temperature NMR studies, vibrational spectroscopic as well as mass spectrometric studies involving **227** were carried out; ν[Ge–C(1)indenyl] was found to be near 370 cm^{-1}. More recently, Lorberth and co-workers [148] reported the synthesis and spectroscopic characterization of the η^1-indenylgermatranes (**238** and **239**) (Scheme 57).

As a complement to investigations pertaining to substituent effects in η^1-indenylsilanes, Davison and Rakita [103] probed some of the factors that influence the rate of [1,5]-tin shifts in the analogous stannyl complexes. Permutation of the magnetically non-equivalent diastereotopic methyl environments in **229** was evidenced by a series of ^{1}H-NMR spectra obtained between −23 and 52°C. Kinetic data obtained from these spectroscopic studies provided an estimate of the barrier to this fluxional process (ca. 14 kcal mol^{-1}). As observed for the asymmetrically substituted indenylsilane, **169**, the related methylindenyl tin complex (**240**) (Scheme 58), showed no sign of isomerization to the corresponding *gem*-disubstituted isomer. Although Davison and Rakita were unable to prepare the dimethylindenylsilane (**172**), the analogous tin compound (**242**) was synthesized successfully and studied by use of dynamic NMR techniques. This tin compound exhibits ^{1}H-NMR spectral features

at −41°C which are readily attributable to an η^1-dimethylindenyl group. As the temperature is raised, spectral changes typically associated with quasi-degenerate dynamic behavior ensue, which include broadening and coalescence of the indenyl methyl resonances. The fast-exchange limiting spectrum for **242** was obtained at 84°C, and includes a single sharp singlet in the indenyl methyl region, with accompanying tin satellites. The activation energy associated with tin migrations in this system (ca. 14 kcal mol^{-1}) cannot be distinguished from the barriers obtained for unsubstituted η^1-indenylstannanes, suggesting that the incorporation of methyl groups at C(1) and C(3) does little to perturb the indene–isoindene equilibrium in this system.

The effect of substituents on the rate of metallotropic shifts in η^1-indenylstannanes has been examined by Andrews et al. [106,107]. These workers noted that the behavior both of the C(2) and the C(4)/C(7) substituted η^1-indenylstannanes (**241** and **243**) is qualitatively similar to that observed for the corresponding silanes (**170** and **175**) (Scheme 43). Variable-temperature NMR data obtained from samples of these η^1-indenylstannanes show that methyl substitution at C(2), as in **241**, results in a heightened barrier to metallotropic shifts ($\Delta G^{\ddagger}$ ca. 18.6 kcal mol^{-1}), while the introduction of C(4) and C(7) methyl groups, as in **243**, has no statistically significant effect on this barrier ($\Delta G^{\ddagger}$ ca. 14.0 kcal mol^{-1}), relative to the unsubstituted compound (**228**).

In 1997, Morris et al. [149] reported the preparation and variable-temperature study of (η^1-C_9H_7)Sn(*n*-Bu)$_3$ (**231**) (Scheme 56). These authors attribute the apparent signal averaging in the NMR spectra of **231** at 40°C to 'a rapid 1,3 shift', rather than the successive [1,5]-tin shifts predicted by the Woodward–Hoffmann rules. Moreover, whereas it is claimed by these workers that the broadening of the methylene ^{1}H-NMR signals of the butyl chains in **231** indicates slowed rotation about the C(1)–Sn axis, it is perhaps more resonable to assume that this phenomenon arises simply as a result of the diastereotopic character of these methylene protons when the Bu_3Sn group is attached to the stereogenic indenyl C(1) center.

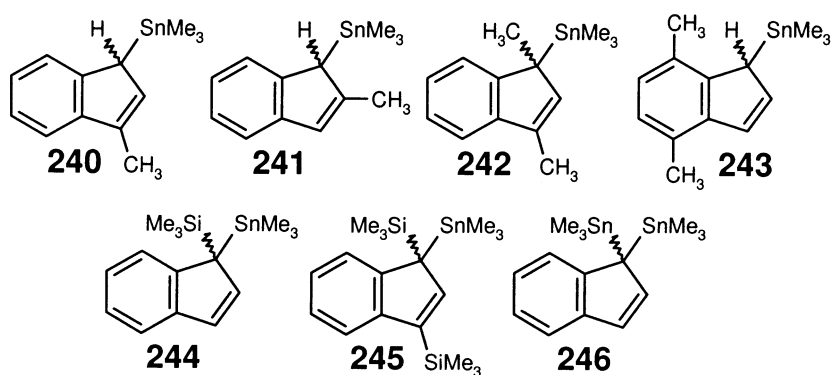

Scheme 58. Some alkyl- and silyl-substituted indenylstannanes.

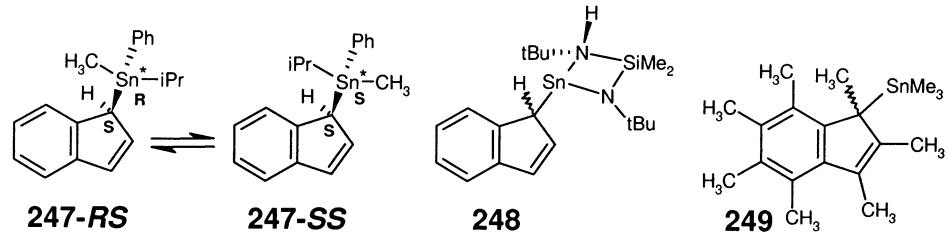

Scheme 59. The dynamics of the chiral-at-tin indenylstannanes (**247**) and the structures of the bis(amino)stannylene complex (**248**) and the heptamethylindenylstannane (**249**).

In 1975, Orrell et al. [150] reported the synthesis and dynamic behavior of the polymetallated indenes (**244**–**246**) (Scheme 58). Variable-temperature ^{1}H-NMR studies conducted between 0 and 170°C revealed that these molecules exhibit dynamic behavior typical of this class of compounds. Based on a comparison of experimentally derived and computed spectral data, the Arrhenius parameters for the metallotropic shift of the trimethylstannyl fragments in **244** (E_a ca. 13.4 kcal mol^{-1}), **245** (E_a ca. 16.1 kcal mol^{-1}) and **246** (E_a ca. 16.4 kcal mol^{-1}) were determined. Interestingly, the 1,1-isomer of **246**, depicted in Scheme 58, was found to predominate in solution over the corresponding 1,3-isomer (ratio > 20:1), an observation which is counterintuitive based on steric considerations alone, and which contrasts the approximate 1:1 ratio observed for the bis(trimethylsilyl)indene isomers, **167** and **168** (Scheme 42) [103]. It is possible that electronic factors strongly favor sp^3-bonded tin fragments in these indenyl complexes. In discussing these kinetic results, Orrell et al. noted that while the observed ^{1}H-NMR line shape changes can be rationalized in terms of a direct [1,3]-metalloid shift pathway, a sequential [1,5]-metalloid shift mechanism involving a short-lived isoindene intermediate cannot be ruled out.

Following reports by Kashin et al. [151,152] on the synthesis and reactivity of optically active indenyl compounds of tin, McMaster and Stobart [153] published an important study regarding the dynamics of η^1-indenylstannanes bearing chiral tin fragments. Compound **247** was prepared as a four-component mixture via quenching of indenyllithium with (*i*-Pr)(Me)(Ph)SnBr; the generation of these isomers is a result of the racemic nature of the tin bromide precursor and the presence of the chiral C(1) center on indene. The two compounds possessing indenyl sp^3 carbon atoms with 'S' absolute configurations are depicted in Scheme 59; enantiomers exist for each of these two molecules, but are not shown. This interesting molecular system provided these researchers with a direct means of probing the effect of suprafacial metallotropic shifts on the stereochemistry at the migrating tin center. For example, the occurrence of such migrations involving **247**-*RS*, in which the configuration at tin is retained, results in the formation of the enantiomer of **247**-*SS* (i.e. **247**-*RR*). In contrast, if migrations were to proceed with inversion of configuration at the metal center, then diastereomeric interconversion would not occur; instead, **247**-*RS* would simply interconvert with its enantiomer

247-*SR*, a process which cannot be detected by use of NMR spectroscopy. At low temperature (-60°C) the ^{1}H- and ^{13}C-NMR spectra of **247** were interpreted by these workers in terms of an unequal population (ca. 60:40) of diastereomers; unique sp^3-hydrogen atoms on the indenyl and $Sn-CH_3$ groups were readily discernible. Upon warming to 60°C, coalescence of the distinguishable NMR sub-spectra for the diastereomers was observed. Moreover, the hydrogen atoms of the isopropyl groups in the isomers of **247** initially appeared as a complex multiplet at -60°C, but collapsed to an A_3B_3X pattern in the fast exchange regime (>60°C). This latter result is especially significant as it demonstrates that even in the fast exchange limit, the isopropyl methyl groups remain magnetically non-equivalent, an observation which is consistent with a process involving retention of configuration at tin.

In 1996, Veith et al. [154] demonstrated that nitrogen-functionalized stannylenes react with indene to give η^1-bonded 'adducts', such as **248**, via attack by tin at the indene C(1), followed by migration of the hydrogen onto one of the nitrogen atoms (Scheme 59). In contrast to the analogous π-cyclopentadienyl adduct, the indenyl complex (**248**) was shown to contain a metal–indenyl σ-bond based on X-ray crystallographic data. Variable-temperature ^{1}H- and ^{13}C-NMR studies revealed that **248** is stereochemically non-rigid, yielding a value of ca. 14 kcal mol^{-1} for the activation enthalpy associated with this dynamic process.

The synthesis and dynamics of the heptamethylindenylstannane (**249**) was presented by Herrmann et al. [155] in 1997. This compound was prepared in 65% yield via alkylation of chlorotrimethyltin with $[C_9(CH_3)_7]Li$, and subsequently characterized by use of X-ray crystallographic and NMR spectroscopic techniques. Although no kinetic data were provided, it appears that **249** is quasi-fluxional, based on the comments made by these authors that warming causes a 'hapticity change' that is observable by NMR spectroscopy. In the same year, Nifant'ev and Ivchenko [156] also reported the preparation of some interesting indenylstannanes, which were subsequently used in the preparation of metallocene complexes.

Twenty-five years after Gilman and Gist [157] first reported the synthesis of the mono(η^1-indenyl) complex (**230**) and the bis(η^1-indenyl)stannane (**250**), McMaster and Stobart [158] examined qualitatively the dynamic behavior of the latter molecule and other poly(η^1-indenyl) complexes of germanium and tin (**251**–**254** in Scheme 60). The tris(η^1-indenyl)tin species were prepared in the usual manner from lithium indenide and the appropriate trichloroalkylstannane, in approximately 50% yield. Proton NMR spectroscopic data obtained at -60°C from samples of these compounds consisted of signals attributable to the alkyl substituent (*n*-Bu in **251**; Ph in **252**), a complex multiplet due to the aromatic and olefinic hydrogen atoms, and four distinct diastereotopic H(1) signals between 3.7 and 3.5 ppm. Warming to 60°C caused these latter signals to merge into a single broad resonance which eventually collapsed, accompanied by the growing in of a well-resolved triplet near 6.2 ppm. Spectral data obtained from ^{13}C-NMR studies coincided with these ^{1}H-NMR experiments; at low temperature, four unique indenyl C(1) resonances were found for **251**, while for **252**, three signals of approximate intensity ratio 1:2:1 were observed. Upon warming, these and the other geometrically related indenyl

signals coalesced, which is in keeping with the operation of a metallotropic shift process that is rapid on the NMR time-scale. Diastereotopic effects and coalescence behavior were also detected for the tetra(η^1-indenyl) complexes (**253** and **254**). Interestingly, such effects were not found for bis(η^1-indenyl)diphenylstannane (**250**) paralleling the situation described by Cotton and Marks for the mercury analogue (**78**) (Scheme 28) [62]. Single crystal X-ray diffraction data for the S_4-symmetric isomers of both **253** and **254** were provided in a subsequent publication by Atwood et al. [159].

Although the vast majority of studies regarding quasi-degenerate rearrangements in η^1-indenyl main group compounds have involved the Group 14 elements, these are certainly not unique in this regard, as evidenced by the Group 13 examples provided in Section 3.1. In fact, the dominance of Group 14 species in this field of study is likely more a result of the ease with which these molecules are prepared and purified, in addition to the inherent thermodynamic stability of the allylic isomers of these Group 14 compounds.

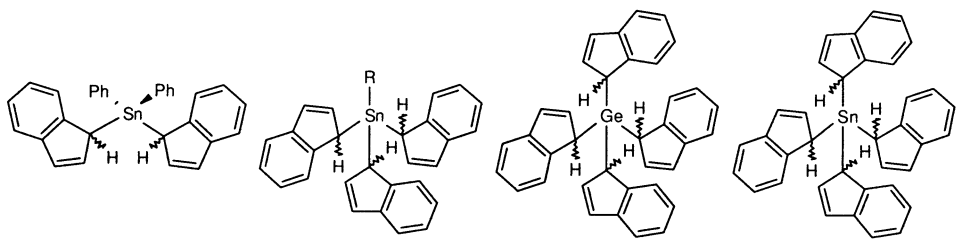

250 **251**: R = *n*Bu **252**: R = Ph **253** **254**

Scheme 60. Poly(η^1-indenyl) complexes of germanium and tin.

3.3. Group 15

In 1955, Woodstock and co-workers [160] reported the synthesis of $(C_9H_7)PCl_2$ (**255**) via reduction of the complex derived from indene and PCl_5 with red phosphorus in the presence of catalytic amounts of iodine. In a subsequent report, Babkina et al. [161] demonstrated that this compound could also be prepared in low yield by γ-irradiation of indene and trichlorophosphine (Scheme 61). These latter workers determined the composition of **255** based upon elemental analysis and mass spectrometric results; however, in the absence of NMR data, the structure of **255** remains ambiguous.

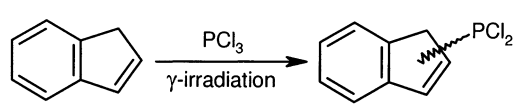

255

Scheme 61. Generation of the η^1-indenylphosphine (**255**) from indene and PCl_3.

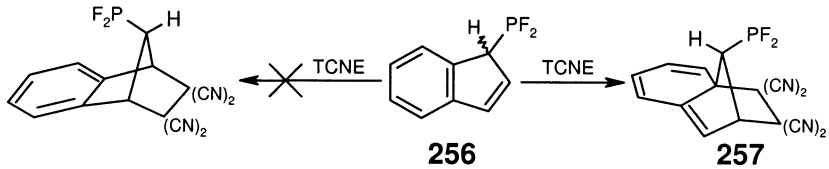

Scheme 62. Reaction of the η^1-indenylphosphine (**256**) with tetracyanoethylene, leading to the proposed 1:1 adduct (**257**).

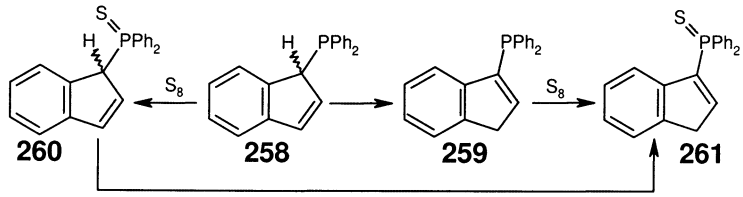

Scheme 63. Chemical transformations involving the η^1-indenylphosphines (**258**–**261**).

The synthesis and characterization of $(\eta^1\text{-}C_9H_7)PF_2$ (**256**) was examined by Schmutzler and co-workers [162] in 1989. Multi-NMR spectroscopic data revealed the P–C(1) connectivity depicted for this compound in Scheme 62. Although no kinetic data were provided, the authors noted that upon reacting **256** with TCNE, a 1:1 adduct is obtained. The product proposed by Schmutzler and co-workers (**257**), formally corresponds to the [4 + 2] cycloadduct derived directly from the 1*H*-inden-1-yl species (**256**). While the non-equivalence of the fluorine atoms in the ^{19}F-NMR spectrum of **257** does concur with such a structural formulation, in the absence of crystallographic data, products of ene or [2 + 2] additions involving **256** remain viable alternatives.

In 1992, Anderson and co-workers [163] examined the isomerization behavior and reactivity of η^1-indenylphosphines bearing phenyl substituents. These workers noted that treatment of indenyllithium with chlorodiphenylphosphine yielded the sp^3-bonded kinetic product (**258**), which was characterized fully by use of standard spectroscopic and physical techniques (Scheme 63). The phenyl groups attached to phosphorus atom in **258** were found to exhibit diastereotopism, resulting from the stereogenic C(1) center on the indenyl moiety. On standing in solution at ambient temperature for several days, **258** was quantitatively converted into the thermodynamically favored C(3) isomer (**259**), which in turn was characterized by use of ^{1}H-, ^{13}C- and ^{31}P-NMR spectroscopy and X-ray crystallography. Based on the fact that passing solutions of **258** over alumina accelerated this isomerization process, the authors invoked an acid- or base-catalyzed protonation/deprotonation mechanism to account for the rapid conversion of **258** into **259**. Indeed, such a proposal seems tenable, as the rate of uncatalyzed [1,5]-hydrogen migrations in indenes is rather low under ambient conditions. The corresponding phosphine sulfides, **260** and **261** were subsequently prepared from **258** and **259,** respectively; a similar transformation of **260** into **261** was noted.

Despite the tendency of **258** to isomerize into **259**, Anderson and co-workers demonstrated that freshly prepared samples of each of these compounds could be used as ligands in the preparation of platinum complexes. Reactions involving $PtCl_2$(COD), PtMeCl(COD) and $PtMe_2$(COD) all yielded products in which the stereochemical integrity of the indenylphosphine ligand was maintained. For example, the reaction of **258** with $PtCl_2$(COD) resulted in the formation of *cis*-[$PtCl_2(PPh_2(1\text{-}C_9H_7))_2$], which was readily identified as a mixture of C_2 and C_s diastereomers based on ^{1}H-, ^{13}C-, and ^{31}P-NMR spectral data. In a more recent report, Starzewski et al. [164] demonstrated that indenylphosphines can be used in combination with indenylboranes in the development of novel ligands for donor/acceptor *ansa*-metallocene systems.

As an extension of the work of Anderson et al., Stradiotto et al. [165] reported on the preparation, characterization and reactivity of indenyldiphosphines. Lithiation of **258**, followed by quenching with chlorodiphenylphosphine and subsequent oxidation with an oxygen or sulfur source led to the formation of **263** and **264** (Scheme 64). The following year, Curnow and coworkers [166] provided characterization data for **262**, as well as the selenium derivative (**265**). Interestingly, 1,3-disubstituted compounds were formed exclusively in all of these reactions. The solution molecular structures of compounds **263**–**265** were elucidated based upon NMR spectroscopic data, while single crystal X-ray diffraction studies confirmed these geometries in the solid state.

In 1967, Crofts and Williamson [167] detailed the synthesis of 1-indenylidenetriphenylphosphorane (**266**) in 36% yield from 1-bromoindene and triphenylphosphine (Scheme 65). These workers noted that **266** couples with diazonium salts to give arylazo-substituted methylenephosphoranes; aspects of this reactivity were examined in a subsequent report by Ford [168]. More recently, Romão and co-workers [169] invoked the generation of free $[(C_9H_7)PR_3]^+$ species resulting from the nucleophilic addition of phosphines to the indenyl ring in $[(\eta^5\text{-}C_5H_5)Mo(CO)_2(\eta^5\text{-}C_9H_7)]^{2+}$.

The transformation of the sterically encumbered η^1-indenylphosphine (**267**) into the novel benzophosphapentafulvene (**268**) was realized by Märkl and Raab [170] in 1989. Treatment of (2,4,6-tBu$_3$C$_6$H$_2$)PCl_2 with one equivalent of indenyllithium led

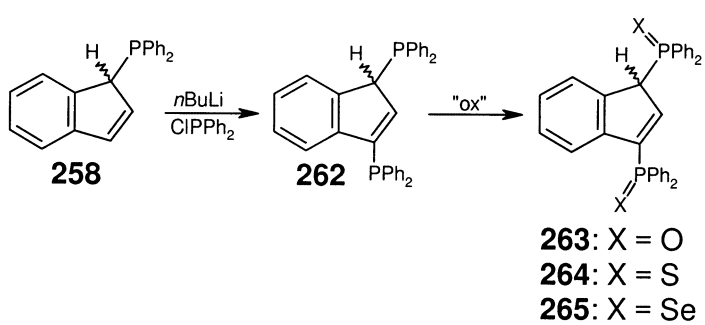

Scheme 64. Synthesis and oxidation of 1,3-bis(diphenylphosphino)indene (**262**).

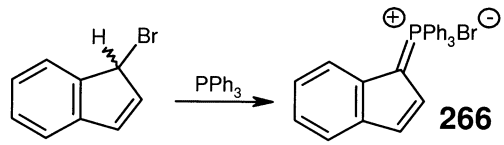

Scheme 65. Conversion of 1-bromoindene into 1-indenylidenetriphenylphosphorane (**266**).

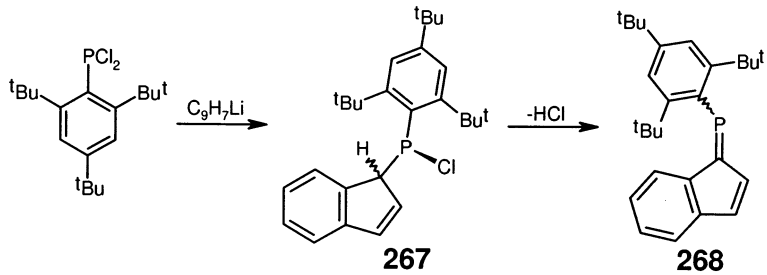

Scheme 66. Transformation of the sterically encumbered η^1-indenylphosphine (**267**) into the benzophosphapentafulvene (**268**) via extrusion of hydrogen chloride.

to the formation of **267** in 71% yield (Scheme 66). The spatial demands of the aryl substituent in **267** are manifested in the observation of restricted rotation phenomena on the NMR time-scale under ambient conditions. Compound **268** is subsequently produced in 76% yield (ca. 70:30 mixture of *E* and *Z* isomers) upon loss of hydrogen chloride from **267**; **268** is also preparable directly from (2,4,6-*t*-$Bu_3C_6H_2$)PCl_2 and the lithio salt of trimethylsilylindene (**138**) (Scheme 40). Noteworthy are the considerable downfield positions of the ^{31}P-NMR resonances ($\delta = +280.6$, *E*-**268**; $\delta = +272.9$, *Z*-**268**) associated with **268**.

Regitz and co-workers [171,172] have demonstrated that η^1-indenylphosphines can be generated from diazo precursors. Irradiation in benzene of an appropriately designed phosphorylvinyl-diazomethane produced the corresponding carbene via extrusion of dinitrogen; ring closure followed by a [1,5]-hydrogen shift generated the η^1-indenylphosphine (**269**) albeit in only 5% yield (Scheme 67). The intermolecular addition of a related phosphorus-functionalized carbene to propyne also led to **269**, but in 38% yield. In the latter reaction, compound **270** is the actual photolysis product, which is converted to **269** upon chromatographic purification. This silica-promoted C(3) to C(1) isomerization process contrasts the conversion of **258** to **259** (Scheme 63), observed by Anderson and co-workers [163].

In 1983, Dötz et al. [173] noted that arylcarbene chromium compounds react with bis(diphenylphosphino)acetylene (DPPA) by way of carbonyl substitution to give the bis(phosphino)indene complexes (**271**–**273**) in up to 85% yield (Scheme 68). These compounds were thoroughly characterized by use of standard analytical techniques, and in the case of **273**, X-ray crystallography.

Aumann et al. [174] have also observed the intramolecular cyclization of arylcarbene–Group 6 precursors, yielding η^1-indenylphosphines. According to these re-

searchers, the transformation of such a metal carbene into the corresponding phosphine, such as **276**, proceeds sequentially via the isolable intermediates (**274** and **275**) (Scheme 69). These observations are in keeping with those of Dötz et al. [173], and represent further examples of sp^2-bonded η^1-indenylphosphines rearranging into sp^3-bonded complexes. All of the compounds **274**–**276** were characterized fully by use of NMR spectroscopy and other analytical techniques, and in the case of **275** (R = *t*-Bu; M = Cr), by use of X-ray crystallographic techniques. The η^1-indenylphosphines (**276**) readily react with air to form the corresponding phosphine oxides (**277**) behavior which appears to be typical of this class of molecules.

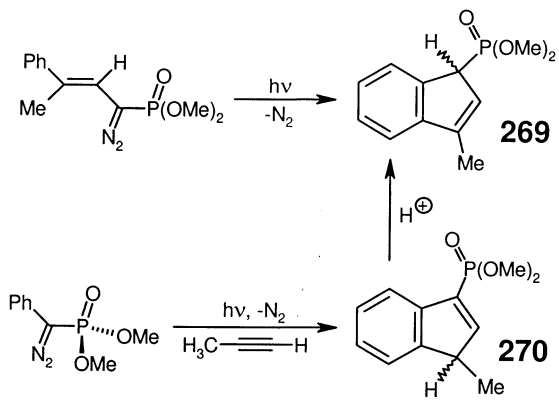

Scheme 67. Carbene reactions leading to the phosphorus-functionalized indenes (**269** and **270**).

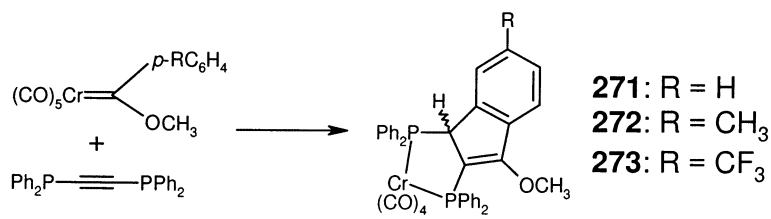

Scheme 68. Generation of chromium complexes containing functionalized 1,2-bis(diphenylphosphino)indene moieties.

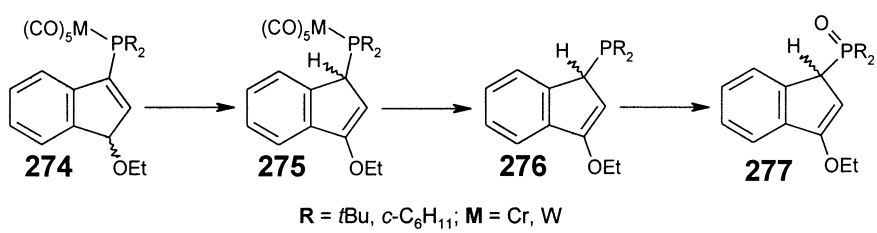

Scheme 69. Chemical transformations of Group 6 complexes bearing η^1-indenylphosphine ligands.

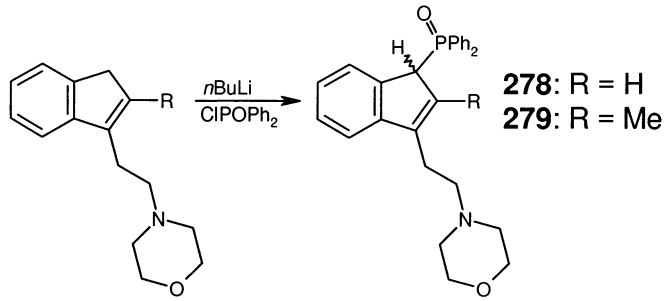

Scheme 70. Functionalization of (morpholinoethyl)indenes, leading to the phosphinoyl compounds (**278** and **279**).

Unfortunately, no experimental data pertaining to the molecular dynamics of these interesting metal-complexed indenylphosphines were provided.

Reggio et al. [175] have exploited indenylphosphines in the synthesis of model compounds used to examine the bioactive conformation of aminoalkylindoles at the cannabinoid CB1 and CB2 receptors. The Horner-Wittig reagents, **278** and **279** were prepared in 75 and 72% yield, respectively, via lithiation of an appropriate (morpholinoethyl)indene, followed by quenching with diphenylphosphinic chloride (Scheme 70). These compounds were characterized primarily by use of ^{1}H-NMR spectroscopy and mass spectrometry.

In 1999, Majoral and co-workers [176] reported on the stepwise conversion of an α-phosphinozirconacene to a series of C(2) functionalized indenes. Treatment of the zirconaindene (**280**) with one equivalent of isonitrile led to the formation of the chelating imino complexes (**281** and **282**) (Scheme 71) in nearly quantitative yield, based on ^{1}H-, ^{13}C- and ^{31}P-NMR spectroscopic data. In contrast to the stability of **281**, the xylyl isocyanide derivative (**282**) slowly rearranges in solution to give what is reported to be the first β-phosphino indenoimine (**283**); this latter compound was isolated in 67% yield and fully characterized by use of standard analytical techniques. Further support for the proposed structural connectivity in **283** was obtained from X-ray crystallographic studies conducted on the corresponding sulfide derivative (**284**). Interesting reactivity was also observed between **281** and **282** and HCl·Et_2O; in both cases, the corresponding β-aminophosphine (**285** or **286**) was isolated in 60 and 73% yield, respectively. Oxidation of **286** with elemental sulfur produced the crystallographically characterized indene (**287**).

Poly(η^1-indenyl)phosphines, including the bis(η^1-indenyl)phosphine (**288**) and the tris(η^1-indenyl) compound (**289**) have been prepared by Schmutzler and co-workers [162] The tris(η^1-indenyl)phosphine (**289**) was prepared from lithium indenide and triphenylphosphite, and isolated as an analytically pure solid in 37% yield (Scheme 72). The simplicity of the NMR spectra obtained from samples of **289** is indicative of the tris(1*H*-inden-3-yl) structure depicted in Scheme 72, as no diastereotopic behavior is possible for this isomer. Similarly, the generation of **288**, and isomers of this compound, was identified based on ^{1}H-, ^{13}C-, ^{19}F- and ^{31}P-NMR data. From

a reaction which included (η^1-C_9H_7)PF_2 (**256**) and isomers of **288**, the platinum compound (**290**) was isolated and characterized by use of X-ray crystallographic techniques. In spite of the fact that the quality of these diffraction data is rather low, the connectivity in the sp^2-bonded (C_9H_7)PF_2 ligand in **290**, and the presence of both C(1)- and C(3)-bonded indenyl groups in the unexpected tris(indenyl)phosphine fragment is unmistakable.

In 1998, the research groups of Alt and Jung [177], Schaverien et al. [178] and Lensink and Gainsford [179] each independently reported the synthesis of the bis(η^1-indenyl)phosphine (**292**). Alt and Jung [177] generated this compound in 80% yield as a mixture of isomers, by the addition of dichlorophenylphosphine to two

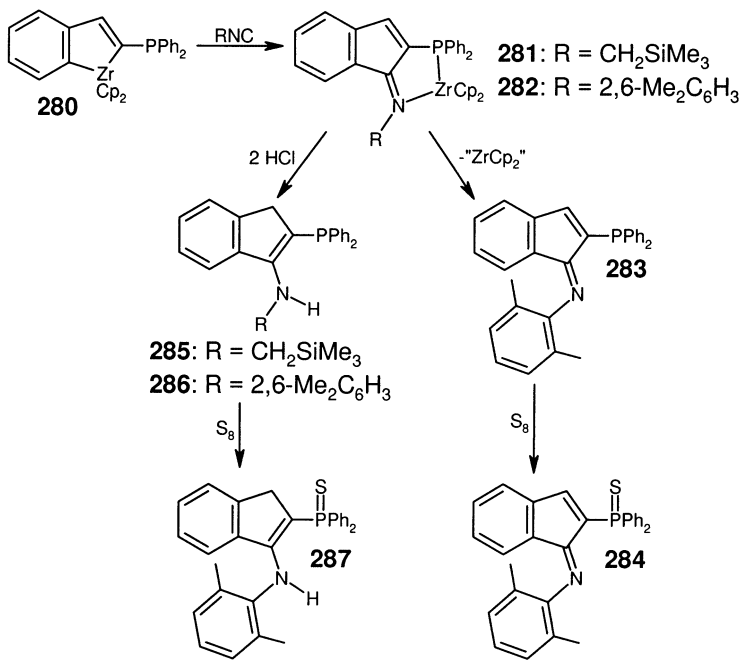

Scheme 71. Reactions involving the α-phosphinozirconaindene (**280**), leading to the nitrogen- and phosphorus-containing indenyl compounds (**281**–**287**).

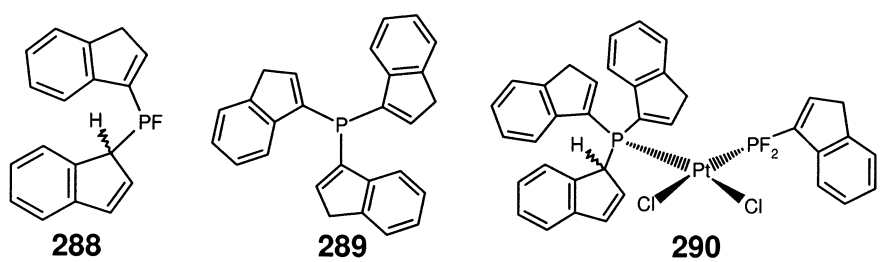

Scheme 72. The poly(η^1-indenyl)phosphines (**288** and **289**) and the platinum complex (**290**).

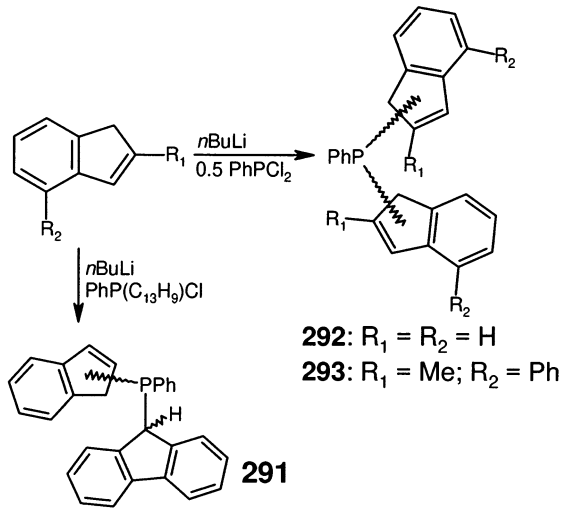

Scheme 73. Synthesis of the mixed phosphine ligand (**291**) and the poly(η^1-indenyl)phosphines (**292** and **293**).

equivalents of indenyllithium in diethylether (Scheme 73). This mixture was characterized by use of ^{1}H-, ^{13}C- and ^{31}P-NMR spectroscopic techniques; the observation of a methylene carbon resonance indicates the existence of a vinyl-substituted indenyl isomer. Alt and co-workers also reported the preparation of the mixed phosphine (**291**) which was similarly generated as a mixture of isomers. In addition to reporting on the synthesis of **292** in tetrahydrofuran, Schaverien et al. [178] prepared the functionalized bis(η^1-indenyl)phosphine (**293**) and provided ^{1}H-NMR spectroscopic data for this compound.

A more thorough examination of the synthesis and isomerization behavior of bis(η^1-indenyl)phenylphosphines has been provided by Lensink and Gainsford [179]. These workers noted that while salt elimination is an effective method for preparing **292**, the structure of the phosphine product obtained is influenced by the solvent employed in the reaction. When tetrahydrofuran was used, the symmetrical isomer (**294**) was generated and subsequently characterized by use of NMR spectroscopy; a single ^{31}P-NMR revealed the presence of only one isomer, while ^{1}H- and ^{13}C-NMR spectral data indicated the bis(1*H*-inden-3-yl) configuration depicted in Scheme 74. Owing to the instability of **294**, this compound was further purified by conversion to the sulfide, **295**. The structure of this latter molecule was confirmed by use of X-ray diffraction techniques.

When the analogous reaction sequence was conducted using toluene in place of tetrahydrofuran, the bis(1*H*-inden-1-yl)phosphine sulfide (**296**) was generated. No attempt was made to isolate or identify the unoxidized phosphine intermediate(s). The asymmetry at the phosphorus center in the heterochiral configuration of **296** results in the observation of two non-equivalent *meso*-isomers for this compound. Indeed, the ^{31}P-NMR spectrum of the crude reaction mixture was found to contain

three signals, which is consistent with the formation of one *rac*-isomer and two *meso*-isomers. In an attempt to probe for dynamic behavior in this system, a pure sample of the crystallographically characterized racemic isomer of **296** was heated in $CDCl_3$. After several hours at 60°C, only minute quantities of the *meso*-isomers were detected, suggesting that under these conditions, molecular rearrangements leading to stereochemical scrambling in **296** are rather slow. However, after extended periods of time an intermediate species assigned as **297** was observed. The intermediacy of **297** was also noted during the pyridine-catalyzed conversion of **296** into **295**. In light of these results, the authors suggest that the observed solvent effect discussed above is a result of an indenyllithium promoted (1*H*-inden-1-yl)phosphine to (1*H*-inden-3-yl)phosphine isomerization process, which is enhanced in the more polar tetrahydrofuran reaction medium.

The list of indenyl complexes of the heavier Group 15 elements that have been prepared and characterized is rather short. In addition to work published by Rastogi and co-workers [180–182] it is possible that a report published by Lorberth et al. [70] contains the few known examples of such compounds. The indenylarsanes (**298**–**303**) were prepared in greater than 43% yield from arsenic halides and indenyllithium (Scheme 75). The structure of the simplest of these (**298**) was

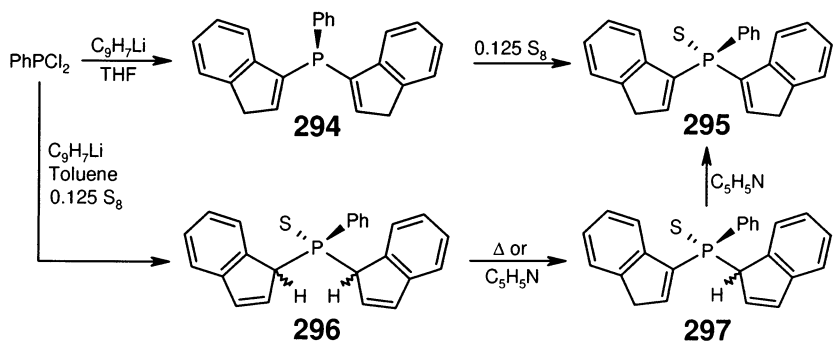

Scheme 74. The bis(η^1-indenyl)phosphine (**294**) and related sulfido isomers (**295**–**297**).

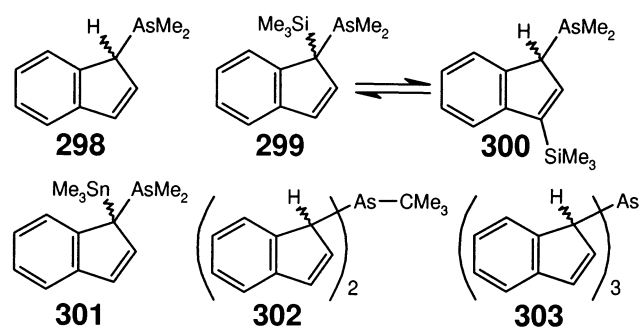

Scheme 75. Indenylarsane and poly(η^1-indenyl)arsane complexes.

assigned based on solution ^{1}H- and ^{13}C-NMR data; resonances attributable to the sp^3-bonded η^1-indenyl framework were observed, as were signals assignable to the diastereotopic methyl groups. This compound served effectively as a precursor to the silane, **299** and the stannane, **301**. While upon warming **299** was converted into a mixture (ca. 1:1) of this compound and the 1,3-substituted compound (**300**), a similar rearrangement was not observed for **301**.

The spectroscopic characterization of poly(η^1-indenyl)arsanes was also detailed in this report [70]. The NMR spectra of the product mixture derived from the quenching of lithium indenide with dichloro(*tert*-butyl)arsane indicated the presence of *meso*- and *rac*-isomers; owing to the asymmetry at the arsenic center, two *meso*-isomers exist for **302**, leading to a three component mixture. Fractional crystallization allowed for a sample containing about 85% of the *racemic* compound and 15% of one of the *meso*-isomers to be isolated. The latter compound was characterized by use of X-ray diffraction techniques, which revealed sp^3-bonded indenyl groups consistent with both the solution NMR data, and with the depiction of the molecule presented in Scheme 75.

The description provided by these authors of the tris(η^1-indenyl)arsane system (**303**) is considerably more convoluted. Based on the observation of four unique indenyl environments in the ^{1}H- and ^{13}C-NMR spectra of the purified product mixture, Lorberth et al. [70] propose that **303** exists as a mixture of four isomers in solution, the identities of which can supposedly be determined based on the introduction of a third indenyl group to the isomers of **302**. It is evident, though, that this rationale is seriously flawed. When one instead employs the group theory approach of McMaster and Stobart [158], four unique indenyl environments are predicted for the tris(η^1-indenyl)arsane system (**303**). However, these arise due to the existence of an isomer of C_1 symmetry, in which all three indenyl ring environments are magnetically non-equivalent, and a C_3-symmetric compound, which is one-third less abundant than the C_1 isomer, but for which all three indenyl environments are equivalent. This scenario has been examined in detail by Stradiotto et al. [102,142,143] for tris(η^1-indenyl)silanes (Section 3.2). The claim by Lorberth and co-workers that four isomers are present is correct, but not in the sense implied by these authors; each of the C_1 and C_3 isomers of **303** has an enantiomeric partner, the pairs of which cannot be distinguished by use of NMR techniques.

4. Concluding remarks

Transition metal and main group η^1-indenyl compounds represent a unique class of organometallic molecules, the historical relevance of which has been delineated in the preceding sections. Studies pertaining to the dynamics of these species have advanced our understanding of circumambulations in functionalized polyenes, and in some cases have served as important probes of orbital symmetry control in such intramolecular rearrangements. Upon evaluation of the molecular dynamics studies detailed herein, a common mechanistic pathway involving suprafacial [1,5]-elemen-

Table 1
Experimentally determined activation parameters for C(1) to C(3) metalloid shifts in transition metal and main group η^1-indenyl complexes

Migrating element	Compound number	E_a (kcal mol^{-1})	$\Delta G^{\ddagger}$ (kcal mol^{-1})	Reference
Zr	**1**	–	14.4	[12]
Re	**17**	–	12.0 ± 0.1	[19]
Fe	**31**	–	20 ± 2	[34]
Ir	**59**	–	12–13 [a]	[52]
Ir	**66**	–	12–13 [a]	[54]
Hg	**78**	12.9 ± 0.6	–	[62]
B	**82**	13 ± 1	–	[67]
B	**103**	17.7 ± 0.2	–	[75]
Si	**138**	<29	–	[42]
Si	**138**	22.5	–	[43]
Si	**138**	22.4 ± 1.0	23.8 ± 0.1	[101]
Si	**138**	–	23.8	[106,107]
Si	**143**	23.0 ± 1.6	–	[103]
Si	**164**	26.1 ± 1.4	–	[103]
Si	**170**	–	26.5	[106,107]
Si	**172**	–	23 ± 1	[105]
Si	**175**	–	21.8	[106,107]
Si	**177/178**	–	21.9 ± 0.5	[112,113]
Si	**179**	–	17.6 ± 0.2	[112,113]
Si	**182**	–	24 ± 2	[115]
Si	**186**	–	24 ± 1	[105]
Si	**197**	–	24.2 ± 0.5	[129]
Si	**222**	–	24.0 ± 0.5	[102]
Si	**223**	–	25 ± 2	[142]
Si	**224**	–	24 ± 1	[143]
Ge	**226**	22	–	[42]
Ge	**226**	18.2 ± 0.5	21.6 ± 0.1	[101]
Ge	**226**	18.4 ± 0.4	21.8 ± 0.1	[101]
Sn	**228**	–	15.0	[106]
Sn	**228**	12.0 ± 0.3	15.3 ± 0.1	[101,144]
Sn	**228**	12.1 ± 0.2	15.1 ± 0.1	[101,144]
Sn	**228**	12.7 ± 0.4	15.2 ± 0.1	[101,144]
Sn	**228**	13.8 ± 0.8	–	[144]
Sn	**229**	14.1 ± 0.4	–	[103]
Sn	**231**	–	15.4	[149]
Sn	**241**	–	18.6	[106,107]
Sn	**242**	14.2 ± 0.7	–	[103]
Sn	**243**	–	14.0	[106,107]
Sn	**244**	13.4 ± 0.1	17.1	[150]
Sn	**245**	16.1 ± 0.3	17.6 ± 0.3	[150]
Sn	**246**	16.4 ± 0.2	17.1	[150]
Pb	**232**	–	13.9	[146]

[a] Barrier estimated from ^{1}H-NMR spectroscopic data provided within the cited reference.

totropic shifts emerges; partitions between transition metal and main group η^1-indenyl systems in this context appear to be superficial. Empirically determined activation parameters for metal(loid) shifts in η^1-indenyl complexes are collected in Table 1.

Despite the long history of η^1-indenyl chemistry, this field is by no means antiquated; the number and variety of derivatives continues to grow at an astounding rate. Numerous transition metal derivatives generated from precursors of higher hapticity have recently been reported, underscoring the relevance of the η^1-binding mode, especially in systems that are capable of ligand substitution chemistry. More prominent in the last decade has been the development of main group η^1-indenyl compounds, particularly those of the Group 14 elements. The utility of these species in the preparation of chiral *ansa*-metallocene pre-catalysts has inspired remarkable ingenuity with respect to the design and synthesis of novel main group η^1-indenyl compounds. The interesting properties conferred by these ligands upon the associated metal center, coupled with demand for indenyl-based ligand architectures of increasing complexity, will most certainly promote continued innovation in this area.

Acknowledgements

Financial support from the Natural Sciences and Engineering Research Council (NSERC) of Canada is gratefully acknowledged. We thank our colleague Dr M.A. Brook for his interest and encouragement.

References

[1] F.A. Cotton, Acc. Chem. Res. 1 (1968) 257.
[2] M.J. Calhorda, L.F. Veiros, Coord. Chem. Res. 185-186 (1999) 37.
[3] For an example, see: R.C. Kerber, B. Waldbaum, Organometallics 14 (1995) 4742.
[4] I.A. Lobanova, V.I. Zdanovich, Russ. Chem. Rev. 57 (1988) 967.
[5] For a recent example, see: C.A. Gamelas, E. Herdtweck, J.P. Lopes, C.C. Romão, Organometallics 18 (1999) 506.
[6] For an example, see: H. Chen, M. Fajardo, B.F.G. Johnson, J. Lewis, P.R. Raithby, J. Organomet. Chem. 389 (1990) C16.
[7] J.M. O'Connor, C.P. Casey, Chem. Rev. 87 (1987) 307.
[8] M.E. Rerek, L.-N. Ji, F. Basolo, J. Chem. Soc. Chem. Commun. (1983) 1208.
[9] F. Basolo, New J. Chem. 16 (1994) 19.
[10] R.L. Halterman, Chem. Rev. 92 (1992) 965.
[11] L.H. Sommer, N.S. Marans, J. Am. Chem. Soc. 73 (1951) 5135.
[12] C. Schmid, H.G. Alt, W. Milius, J. Organomet. Chem. 544 (1997) 139.
[13] E.L. Muetterties, Inorg. Chem. 4 (1965) 769.
[14] E.H. Licht, H.G. Alt, W. Milius, S. Abu-Orabi, J. Organomet. Chem. 560 (1998) 69.
[15] M.L.H. Green, N.H. Popham, J. Chem. Soc. Dalton Trans. (1999) 1049.
[16] M.G. Thorn, P.E. Fanwick, R.W. Chesnut, I.P. Rothwell, Chem. Commun. (1999) 2543.
[17] H.G. Alt, J.S. Han, R.D. Rogers, J. Organomet. Chem. 454 (1993) 165.

[18] O.I. Trifonova, A.A. Borisenko, Yu.A. Ustynyuk, N.A. Ustynyuk, Russ. Chem. Bull. 42 (1993) 1222.
[19] C.P. Casey, J.M. O'Connor, Organometallics 4 (1985) 384.
[20] C.P. Casey, J.M. O'Connor, W.D. Jones, K.J. Haller, Organometallics 2 (1983) 535.
[21] R. Hoffmann, R.B. Woodward, Acc. Chem. Res. 1 (1968) 17.
[22] R.B. Woodward, R. Hoffmann, The Conservation of Orbital Symmetry, Academic Press, New York, 1970.
[23] J. Dalton, C.A. McAuliffe, J. Organomet. Chem. 39 (1972) 251.
[24] M.A. McKinney, D.T. Haworth, J. Chem. Ed. 57 (1980) 110.
[25] F.A. Cotton, A. Musco, G. Yagupsky, J. Am. Chem. Soc. 89 (1967) 6136.
[26] H. Bang, T.J. Lynch, F. Basolo, Organometallics 11 (1992) 40.
[27] W.A. Herrmann, F.E. Kuhn, C.C. Romão, J. Organomet. Chem. 489 (1995) C56.
[28] Y. Zhou, M.A. Dewey, J.A. Gladysz, Organometallics 12 (1993) 3918.
[29] S.W. Lee, M.G. Richmond, Inorg. Chem. 30 (1991) 2237.
[30] A.J. Arce, R. Muchado, Y. De Sanctis, R. Isea, R. Atencio, A.J. Deeming, J. Organomet. Chem. 580 (1999) 339.
[31] P.A. Deck, F.R. Fronczek, Organometallics 19 (2000) 327.
[32] F.A. Cotton, J. Organomet. Chem. 100 (1975) 29.
[33] M.J. Bennett, F.A. Cotton, A. Davison, J.W. Faller, S.J. Lippard, S.M. Morehouse, J. Am. Chem. Soc. 88 (1966) 4371.
[34] M. Stradiotto, D.W. Hughes, A.D. Bain, M.A. Brook, M.J. McGlinchey, Organometallics 16 (1997) 5563.
[35] C.L. Perrin, T.J. Dwyer, Chem. Rev. 90 (1990) 935.
[36] A.D. Bain, J.A. Cramer, J. Magn. Reson. A103 (1993) 217.
[37] A.D. Bain, J.A. Cramer, J. Phys. Chem. 97 (1993) 2884.
[38] F.A. Cotton, T.J. Marks, J. Am. Chem. Soc. 91 (1969) 7523.
[39] C.H. Campbell, M.L.H. Green, J. Chem. Soc. A (1970) 1318.
[40] D.J. Ciappenelli, F.A. Cotton, L. Kruczynski, J. Organomet. Chem. 42 (1972) 159.
[41] R.C. Kerber, R. Garcia, A.L. Nobre, Organometallics 15 (1996) 5756.
[42] R.B. Larrabee, B.F. Dowden, Tetrahedron Lett. 12 (1970) 915.
[43] A.J. Ashe III, Tetrahedron. Lett. 24 (1970) 2105.
[44] J.A. Belmont, M.S. Wrighton, Organometallics 5 (1986) 1421.
[45] B.R. Waldbaum, R.C. Kerber, Inorg. Chim. Acta 291 (1999) 109.
[46] P. Blenkiron, G.D. Enright, N.J. Taylor, A.J. Carty, Organometallics 15 (1996) 2855.
[47] M.I. Bruce, B.W. Skelton, A.H. White, N.N. Zaitseva, Inorg. Chem. Commun. 2 (1999) 17.
[48] P. Caddy, M. Green, E. O'Brien, L.E. Smart, P. Woodward, Angew. Chem. Int. Ed. Engl. 16 (1977) 648.
[49] J.S. Merola, R.T. Kacmarcik, Organometallics 8 (1989) 778.
[50] A. Habib, R.S. Tanke, E.M. Holt, R.H. Crabtree, Organometallics 8 (1989) 1225.
[51] T. Foo, R.G. Bergman, Organometallics 11 (1992) 1811.
[52] S. Bellomo, A. Ceccon, A. Gambaro, S. Santi, A. Venzo, J. Organomet. Chem. 453 (1993) C4.
[53] C. Bonifaci, G. Carta, A. Ceccon, A. Gambaro, S. Santi, A. Venzo, Organometallics 16 (1996) 1630.
[54] P. Cecchetto, A. Ceccon, A. Gambaro, S. Santi, P. Ganis, R. Gobetto, G. Valle, A. Venzo, Organometallics 17 (1998) 752.
[55] T.A. Huber, F. Bélanger-Gariépy, D. Zargarian, Organometallics 14 (1995) 4997.
[56] T.A. Huber, M. Bayrakdarian, S. Dion, I. Dubuc, F. Bélanger-Gariépy, D. Zargarian, Organometallics 16 (1997) 5811.
[57] F.M. Alías, T.R. Belderraín, M. Paneque, M.L. Poveda, E. Carmona, P. Valerga, Organometallics 17 (1998) 5620.
[58] D. O'Hare, Organometallics 6 (1987) 1766.
[59] M.N. Ackermann, R.K. Ajmera, H.E. Barnes, J.C. Gallucci, A. Wojcicki, Organometallics 18 (1999) 787.

[60] T. Saegusa, Y. Ito, S. Tomita, J. Am. Chem. Soc. 93 (1971) 5656.
[61] B. Fischer, J. Boersma, G. van Koten, W.J.J. Smeets, A.L. Spek, Organometallics 8 (1989) 667.
[62] F.A. Cotton, T.J. Marks, J. Am. Chem. Soc. 91 (1969) 3178.
[63] W. Kitching, B.F. Hegarty, J. Organomet. Chem. 16 (1969) 39.
[64] W. Kitching, B.F. Hegarty, D. Doddrell, J. Organomet. Chem. 21 (1970) 29.
[65] F.A. Cotton, D.L. Hunter, J.D. Jamerson, Inorg. Chim. Acta 15 (1975) 245.
[66] B.M. Mikhailov, T.K. Baryshnikova, V.S. Bogdanov, V.V. Negrebetskii, Dokl. Akad. Nauk. SSSR 207 (1972) 613.
[67] B.M. Mikhailov, T.K. Baryshnikova, V.S. Bogdanov, Zh. Obshch. Khim. 43 (1972) 1949.
[68] W.E. Piers, Chem. Eur. J. 4 (1998) 13.
[69] R. Duchateau, S.J. Lancaster, M. Thornton-Pett, M. Bochmann, Organometallics 16 (1997) 4995.
[70] K. Rufanov, E. Avtomonov, N. Kazennova, V. Kotov, A. Khvorost, D. Lemenovskii, J. Lorberth, J. Organomet. Chem. 536-537 (1997) 361.
[71] M. Bochmann, S.J. Lancaster, O.B. Robinson, J. Chem. Soc. Chem. Commun. (1995) 2081.
[72] M.T. Reetz, M. Willuhn, C. Psiorz, R. Goddard, Chem. Commun. (1999) 1105.
[73] G.E. Herberich, E. Barday, A. Fischer, J. Organomet. Chem. 567 (1998) 127.
[74] E. Barday, B. Frange, B. Hanquet, G.E. Herberich, J. Organomet. Chem. 572 (1999) 225.
[75] I.D. Gridnev, A. Meller, Main Group Met. Chem. 21 (1998) 271.
[76] H. Braunschweig, C. von Koblinski, M. Mamuti, U. Englert, R. Wang, Eur. J. Inorg. Chem. (1999) 1899.
[77] A.J. Ashe III, X. Fang, J.W. Kampf, Organometallics 18 (1999) 2288.
[78] J. Knizek, I. Krossing, H. Nöth, W. Ponikwar, Eur. J. Inorg. Chem. (1998) 505.
[79] L.I. Zakharkin, S. Ya. Zavizion, L.L. Ivanov, Zh. Obshch. Khim. 45 (1975) 1900.
[80] B. Thiyagarajan, R.F. Jordan, V.G. Young, Organometallics 17 (1998) 281.
[81] B. Thiyagarajan, R.F. Jordan, V.G. Young, Organometallics 18 (1999) 5347.
[82] J.S. Poland, D.G. Tuck, J. Organomet. Chem. 42 (1972) 307.
[83] K. Chandra, R.K. Sharma, A.K. Garg, B.S. Garg, Chem. Ind. (1980) 537.
[84] R.L. Halterman, in: A. Togni, R.L. Halterman (Eds.), Metallocenes: Synthesis, Reactivity and Applications, Ch. 8, Wiley–VCH, Toronto, 1998, pp. 455–544.
[85] D.W. Jones, J. Chem. Soc. C (1969) 1729.
[86] M.J. Collett, D.W. Jones, S.J. Renyard, J. Chem. Soc. Perkin Trans. I (1986) 1471.
[87] D.W. Jones, R.J. Marmon, J. Chem. Soc. Perkin Trans. I (1993) 681.
[88] S.S. Rigby, M. Stradiotto, S. Brydges, D.L. Pole, S. Top, A.D. Bain, M.J. McGlinchey, J. Org. Chem. 63 (1998) 3735.
[89] G. Erker, M. Aulbach, D. Wingbermuhle, C. Kruger, S. Werner, Chem. Ber. 126 (1992) 755.
[90] G. Erker, C. Mollenkopf, M. Grehl, R. Fröhlich, C. Krüger, R. Noe, M. Riedel, Organometallics 13 (1994) 1950.
[91] J. Haggin, Chem. Eng. News (1996) 26.
[92] Z. Ziniuk, I. Goldberg, M. Kol, J. Organomet. Chem. 545–546 (1997) 441.
[93] C. Qian, G. Zou, J. Sun, J. Organomet. Chem. 566 (1998) 21.
[94] C. Qian, J. Guo, J. Sun, J. Chen, P. Zheng, Inorg. Chem. 36 (1997) 1286.
[95] F.-E. Hong, S.-Y. Sun, S.-L. Wang, F.-L. Liao, Polyhedron 17 (1998) 1643.
[96] P. Scott, U. Rief, J. Diebold, H.-H. Brintzinger, Organometallics 12 (1993) 3094.
[97] J.C. Gard, F. Williot, M. Bernard, P. Richard, M. Kubicki, D. Lucas, Y. Mugnier, J. Lessard, New J. Chem. 21 (1997) 929.
[98] P.E. Rakita, A. Davison, Inorg. Chem. 8 (1969) 1164.
[99] S. Forsén, R.A. Hoffman, J. Chem. Phys. 39 (1963) 2892.
[100] R.B. Larrabee, J. Organomet. Chem. 74 (1974) 313.
[101] Yu.N. Luzikov, N.M. Sergeyev, Yu.A. Ustynyuk, J. Organomet. Chem. 65 (1974) 303.
[102] M. Stradiotto, S.S. Rigby, D.W. Hughes, M.A. Brook, A.D. Bain, M.J. McGlinchey, Organometallics 15 (1996) 5645.
[103] A. Davison, P.E. Rakita, J. Organomet. Chem. 23 (1970) 407.
[104] T.E. Ready, J.C.W. Chien, M.D. Rausch, J. Organomet. Chem. 583 (1999) 11.

[105] M. Stradiotto, P. Hazendonk, A.D. Bain, M.A. Brook, M.J. McGlinchey, Organometallics 19 (2000) 590.
[106] M.N. Andrews, P.E. Rakita, G.A. Taylor, Tetrahedron Lett. 21 (1973) 1851.
[107] M.N. Andrews, P.E. Rakita, G.A. Taylor, Inorg. Chim. Acta 13 (1975) 191.
[108] P.E. Rakita, G.A. Taylor, Inorg. Chem. 11 (1972) 2136.
[109] P.E. Rakita, G.A. Taylor, J. Organomet. Chem. 61 (1973) 71.
[110] G.A. Taylor, P.E. Rakita, J. Organomet. Chem. 78 (1974) 281.
[111] P. Jutzi, Chem. Rev. 86 (1986) 983.
[112] S.S. Rigby, H.K. Gupta, N.H. Werstiuk, A.D. Bain, M.J. McGlinchey, Polyhedron 14 (1995) 2787.
[113] S.S. Rigby, H.K. Gupta, N.H. Werstiuk, A.D. Bain, M.J. McGlinchey, Inorg. Chim. Acta 251 (1996) 355.
[114] N. Schneider, M.-H. Prosenc, H.-H. Brintzinger, J. Organomet. Chem. 545-546 (1997) 291.
[115] M. Stradiotto, M.A. Brook, M.J. McGlinchey, Inorg. Chem. Commun. 1 (1998) 105.
[116] N.D. Epiotis, S. Shaik, J. Am. Chem. Soc. 99 (1977) 4936.
[117] M.J. McGlinchey, L. Girard, R. Ruffolo, Coord. Chem. Rev. 143 (1995) 331.
[118] D. Malaba, L. Chen, C.A. Tessier, W.J. Youngs, Organometallics 11 (1992) 1007.
[119] D. Malaba, A. Djebli, L. Chen, E.A. Zarate, C.A. Tessier, W.J. Youngs, Organometallics 12 (1993) 1266.
[120] D. Malaba, C.A. Tessier, W.J. Youngs, Organometallics 15 (1996) 2918.
[121] M.M. Olmstead, S.R. Hitchcock, M.H. Nantz, Acta Crystallogr. Sect. C 52 (1996) 1523.
[122] P. Foster, M.D. Rausch, J.C.W. Chien, J. Organomet. Chem. 527 (1997) 71.
[123] M.S. Blais, J.C.W. Chien, M.D. Rausch, Organometallics 17 (1998) 3775.
[124] F. Amor, J. Okuda, J. Organomet. Chem. 520 (1996) 245.
[125] K.C. Hultzsch, P. Voth, K. Beckerle, T.P. Spaniol, J. Okuda, Organometallics 19 (2000) 228.
[126] Z. Xie, S. Wang, Q. Yang, T.C.W. Mak, Organometallics 18 (1999) 2420.
[127] S. Wang, Q. Yang, T.C.W. Mak, Z. Xie, Organometallics 18 (1999) 4478.
[128] Y. Chen, M.D. Rausch, J.C.W. Chien, Organometallics 12 (1993) 4607.
[129] S.S. Rigby, L. Girard, A.D. Bain, M.J. McGlinchey, Organometallics 14 (1995) 3798.
[130] J.N. Christopher, R.F. Jordan, J.L. Petersen, V.G. Young, Organometallics 16 (1997) 3044.
[131] U. Stehling, J. Diebold, R. Kirsten, W. Röll, H.-H. Brintzinger, Organometallics 13 (1994) 964.
[132] N. Schneider, M.E. Huttenloch, U. Stehling, R. Kirsten, F. Schaper, H.-H. Brintzinger, Organometallics 16 (1997) 3413.
[133] F.M. Alías, S. Barlow, J.S. Tudor, D. O'Hare, R.T. Perry, J.M. Nelson, I. Manners, J. Organomet. Chem. 528 (1997) 47.
[134] J. Tudor, S. Barlow, B.R. Payne, D. O'Hare, P. Nguyen, C.E.B. Evans, I. Manners, Organometallics 18 (1999) 2281.
[135] W. Spaleck, M. Antberg, V. Dolle, R. Klein, J. Rohrmann, A. Winter, New J. Chem. 14 (1990) 499.
[136] O. Pérez-Camacho, S.Ya. Knjazhanski, G. Cadenas, M.J. Rosales-Hoz, M.A. Leyva, J. Organomet. Chem. 585 (1999) 18.
[137] R. Jin, B. Wang, X. Zhou, R. Wang, H. Wang, Youji Huaxue 13 (1993) 35; Chem. Abstr. 118 (1993) 234133c.
[138] K. Soga, T. Arai, H.T. Ban, T. Uozumi, Macromol. Rapid Commun. 16 (1995) 905.
[139] T. Arai, H.T. Ban, T. Uozumi, K. Soga, Macromol. Chem. Phys. 198 (1997) 229.
[140] T. Arai, H.T. Ban, T. Uozumi, K. Soga, J. Polym. Sci. A Polym. Chem. 36 (1998) 421.
[141] H.T. Ban, T. Uozumi, T. Sano, K. Soga, Macromol. Chem. Phys. 200 (1999) 1897.
[142] M. Stradiotto, M.A. Brook, M.J. McGlinchey, New J. Chem. 4 (1999) 317.
[143] M. Stradiotto, M.A. Brook, M.J. McGlinchey, J. Chem. Soc. Perkin 2 (2000) 611.
[144] N.M. Sergeyev, Yu.K. Grishin, Yu.N. Luzikov, Yu.A. Ustynyuk, J. Organomet. Chem. 38 (1972) C1.
[145] J.C. Hogan, PhD Thesis, Boston College, 1969.
[146] Yu.K. Grishin, M. Bakhbukh, Yu.A. Ustynyuk, N.N. Zemlyanskii, N.D. Kolosova, Kocheshkov Dokl. Akad. Nauk SSSR 237 (1977) 594.

[147] P.C. Angus, S.R. Stobart, J. Chem. Soc. Dalton Trans. (1973) 2374.
[148] S.S. Karlov, P.L. Shutov, N.G. Akhmedov, M.A. Seip, J. Lorberth, G.S. Zaitseva, J. Organomet. Chem. 598 (2000) 387.
[149] R.J. Morris, P.L. Bock, J.M. Jefferis, D.M. Goedde, Polyhedron 16 (1997) 3699.
[150] K.G. Orrell, V. Šik, M.O. Dunster, E.W. Abel, J. Chem. Soc. Faraday Trans II 71 (1975) 631.
[151] A.N. Kashin, V.A. Khutoryanskii, V.N. Bakunin, I.P. Beletskaya, O.A. Reutov, J. Organomet. Chem. 128 (1977) 359.
[152] A.N. Kashin, V.N. Bakunin, V.A. Khutoryanskii, I.P. Beletskaya, O.A. Reutov, J. Organomet. Chem. 171 (1979) 309.
[153] A.D. McMaster, S.R. Stobart, J. Chem. Soc. Dalton Trans. (1982) 2275.
[154] M. Veith, M. Olbrich, W. Shihua, V. Huch, J. Chem. Soc. Dalton Trans. (1996) 161.
[155] W.A. Herrmann, M.R. Geisberger, F.E. Kühn, G.R.J. Artus, E. Herdtweck, Z. Anorg. Allg. Chem. 623 (1997) 1229.
[156] I.E. Nifant'ev, P.V. Ivchenko, Organometallics 16 (1997) 713.
[157] H. Gilman, L.A. Gist, J. Org. Chem. 22 (1957) 250.
[158] A.D. McMaster, S.R. Stobart, J. Am. Chem. Soc. 104 (1982) 2109.
[159] J.L. Atwood, A.D. McMaster, R.D. Rogers, S.R. Stobart, Organometallics 3 (1984) 1500.
[160] E.N. Walsh, T.M. Beck, W.H. Woodstock, J. Am. Chem. Soc. 77 (1955) 929.
[161] É.I. Babkina, L.S. Vinogradskaya, E.I. Dobrova, N.A. Gur'eva, Zh. Obshch. Khim. 43 (1973) 2084.
[162] L. Heuer, U.K. Bode, P.G. Jones, R. Schmutzler, Z. Naturforsch. 44b (1989) 1082.
[163] K.A. Fallis, G.K. Anderson, N.P. Rath, Organometallics 11 (1992) 885.
[164] K.A.O. Starzewski, W.M. Kelly, A. Stumpf, D. Freitag, Angew. Chem. Int. Ed. Engl. 38 (1999) 2439.
[165] M. Stradiotto, C.M. Kozak, M.J. McGlinchey, J. Organomet. Chem. 564 (1998) 101.
[166] J.J. Adams, D.E. Berry, J. Browning, D. Burth, O.J. Curnow, J. Organomet. Chem. 580 (1999) 245.
[167] P.C. Crofts, M.P. Williamson, J. Chem. Soc (C) (1967) 1093.
[168] J.A. Ford Jr, Tetrahedron Lett. 7 (1968) 815.
[169] C.A. Gamelas, E. Herdtweck, J.P. Lopes, C.C. Romão, Organometallics 18 (1999) 506.
[170] G. Märkl, K.M. Raab, Tetrahedron Lett. 30 (1989) 1077.
[171] A. Hartmann, W. Welter, M. Regitz, Tetrahedron Lett. 20 (1974) 1825.
[172] W. Welter, A. Hartmann, M. Regitz, Chem. Ber. 111 (1978) 3068.
[173] K.H. Dötz, I. Pruskil, U. Schubert, K. Ackermann, Chem. Ber. 116 (1983) 2337.
[174] R. Aumann, B. Jasper, R. Fröhlich, Organometallics 14 (1995) 231.
[175] P.H. Reggio, S. Basu-Dutt, J. Barnett-Norris, M.T. Castro, D.P. Hurst, H.H. Seltzman, M.J. Roche, A.F. Gilliam, B.F. Thomas, L.A. Stevenson, R.G. Pertwee, M.E. Abood, J. Med. Chem. 41 (1998) 5177.
[176] V. Cadierno, M. Zablocka, B. Donnadieu, A. Igau, J.-P. Majoral, A. Skowronska, J. Am. Chem. Soc. 121 (1999) 11086.
[177] H.G. Alt, M. Jung, J. Organomet. Chem. 568 (1998) 127.
[178] C.J. Schaverien, R. Ernst, W. Terlouw, P. Schut, O. Sudmeijer, P.H.M. Budzelaar, J. Mol. Catal. A 128 (1998) 245.
[179] C. Lensink, G.J. Gainsford, Aust. J. Chem. 51 (1998) 667.
[180] R.C. Sharma, M.K. Rastogi, Curr. Sci. 52 (1983) 862.
[181] M.K. Rastogi, Indian J. Chem. A 25A (1986) 689.
[182] P. Dabas, M.K. Rastogi, Asian J. Chem. 9 (1997) 645.